REVERSAL OF PHENOTYPE AND PLASTICITY OF MYOFIBROBLASTS TO TARGET PERI-IMPLANTATION FIBROSIS

TAN Bing-Shi Ariel

(B. Eng.(Hons.) & BSc. UWA)

A THESIS SUBMITTED FOR THE DEGREE OF DOCTOR OF PHILOSOPHY

NUS Graduate School for Integrative Sciences and Engineering

NATIONAL UNIVERSITY OF SINGAPORE

2012

<u>Declaration Page</u>

Declaration

I hereby declare that the thesis is my original work and it has been written by me in its entirety. I have duly acknowledge all the sources of information which have been used in the thesis.

This thesis has also not been submitted for any degree in any university previously.

Tan Bing-Shi Ariel

7th December 2012

Acknowledgements

Table of Contents

Summary

Peri-implant fibrosis poses a substantial setback in regenerative medicine and effective fibrosis treatment remains an unmet clinical need. Our group has firstly described the potential anti-fibrotic effects of suberoylanilide hydroxamic acid (SAHA). When administered in the presence of profibrotic factor transforming growth factor (TGF)-β, SAHA abrogated TGFβ1-effects by preventing fibroblast transition into collagen I overproducing and α-SMA expressing myofibroblasts. However, SAHA no longer exerted anti-fibrotic effects when myofibroblasts were treated with TGFβ1 24h prior to SAHA. Many hormones and growth factors impact cells in pulses, yet current protocols employ continuous TGFβ1 exposure to cells. We therefore evaluated the effects of pulsatile TGFβ1 treatment in the creation and maintenance of the myofibroblast phenotype to better assess SAHA's anti-fibrotic potential in a physiologically relevant setting. We demonstrated that a single 0.5h TGFβ1 pulse was sufficient to effect long-term changes towards the myofibroblast phenotype, potentiated by a second pulse 24h later. We further established that decellularized ECM deposited under TGFβ1 pulses induced myofibroblast features in previously untreated fibroblasts. Revisiting SAHA's effects in TGFβ1 pulses we demonstrated, for the first time the normalization of TGFβ1-effects and thereby reconfirmed SAHA's anti-fibrotic potential. As SAHA leads to the hyperacetylation of α-tubulin, a cytoskeletal component in fibroblasts, we therefore investigated mechanical and locomotional properties of SAHA-treated myofibroblasts as this may reveal an additional therapeutic facet. We presented novel evidence of compromised motility, but not contractility, in SAHA-treated myofibroblasts. Our findings contribute to the current understanding of fibroblast induction, maintenance and the use of an FDA-approved agent to curb fibrosis. Because SAHA is already in clinical use, the findings derived from this thesis can be faster translated towards clinical therapy.

List of Tables

List of Figures

List of Abbreviations

α-SMA: alpha – smooth muscle actin

ACTA2: alpha – smooth muscle actin (gene)

ADAM: disintegrin and metalloproteinase

COL1A1: collagen I alpha-I (gene)

CTGF: connective tissue growth factor

CpG: cytosine-guanine (rich region of DNA)

DNMT: DNA methyltransferase

ECM: extracellular ECM

ELISA: enzyme-linked immunosorbent assay

EMT: epithelial – mesenchymal transition

FBS: fetal bovine serum

Fc: Ficoll

FGF: fibroblast growth factor

FZD8: frizzled 8

H3: histone-3

HAT: histone acetyltransferase

HDAC(i): histone deacetylase (inhibitor)

HPB/C: hepatitis B/C

HSC: hepatic stellate cells

HSF: hypertrophic scar fibrosis

IPF: idiopathic pulmonary fibrosis

LAP: latency associated peptide

LTBP: latent TGFβ1-binding protein

LLC: large latent complex

MALDI-TOF: ECM-assisted laser desorption time of flight mass spectrometry

MMC: macromolecular crowding

MMP: ECM metalloproteinase

miRNA: micro-RNA

MeCP2: methyl CpG binding protein 2

NOX4: NADPH oxidase 4

PDGF: platelet derived growth factor

PMN: polymorphonuclear neutrophils

RT-PCR: reverse transcription-polymerase chain reaction

SAHA: suberoylanilide hydroxamic acid

SDS-PAGE: SDS-polyacrylamide gel electrophoresis

siRNA: small interfering-RNA

SLC: small latent complex

SMAD: mother against decapentaplegic homolog

SSc: systemic sclerosis

TCP: tissue culture plastic

TIMP: tissue inhibitor of metalloproteinases

TNF-α: tumor necrosis factor-alpha

TGFβ1: transforming growth factor-beta

TGIF: 5'-TG-3'-interacting factor

TSPAN2: tetraspanin 2

TβRI, II: TGFβ1 transmembrane receptors I, II

TSA: trichostatin A

VEGF: vascular endothelial growth factor

Chapter 1

Overview of research project

This chapter introduces the rationale and core hypotheses of the project. Aims and objectives are outlined, along with the strategy and methods to achieve them.

1.1 Background

Wound healing is a physiological response of tissue upon injury. However, when this response is perpetuated with events such as chronic inflammation, fibrosis ensues. Fibrosis comes in many forms, ranging from simple cosmetics scars, disfiguring impairments and peri-implant fibrosis – a bottleneck in tissue engineering that often leads to implant failure and/or loss of organ function, a consequence of the host's natural response in an attempt to destroy or phagocytose the implant. Hence, there is an urgent clinical need to: **i)** understand the regulation of fibrosis induction and maintenance; and **ii)** utilize modulators to reverse or curb fibrosis.

The hypotheses behind this project are based on the following observations:

- In an indication discovery approach, Wang et al. firstly observed the anti-fibrotic effects of the epigenetic drug – suberoylanilide hydroxamic acid (SAHA). SAHA is a FDA-approved, broadband histone deacetylase (HDAC) inhibitor currently in clinical use for T cell lymphoma. When administered in conjunction with profibrotic cytokine transforming growth factor beta-1 (TGFβ1), SAHA abrogated TGFβ1-effects in normal and pathological fibroblasts lines by preventing differentiation into alpha-smooth muscle actin (α-SMA) positive myofibroblasts and normalized collagen deposition back to normal or subnormal levels [Wang et al. 2009].

However, when fibroblasts were treated with TGFβ1 24h before SAHA, SAHA was no longer able to exert anti-fibrotic effects (*own observations*).

- We therefore, were forced to relook current *in vitro* fibrosis setups. Current *in vitro* fibrotic studies traditionally employ TGFβ1 as a culture media additive for four days to generate myofibroblasts [Hinz et al. 2001]. However, a time course study of active TGFβ1 generation in an incisional wound repair animal model reported pulsatile *in vivo* TGFβ1 regulation [Yang et al. 1999].

- Intrigued by the findings of the newly developed *in vitro* model, a study into the mechanistic events of TGFβ1 pulsatile regulation was conducted.

The hypothesis behind this project was:

Simulating prevailing *in vivo* cytokine regulation will lead to the development of physiologically relevant *in vitro* model, better suited for (SAHA-based) anti-fibrotic agent characterization

1.2   Aims and Objectives

In order to address the hypothesis, this project was divided into the following aims:

Aim #1: Characterize the effects of TGFβ1 pulses to develop a physiologically relevant *in vitro* fibrotic model

For effective anti-fibrotic compound screening, an *in vitro* model that accurately recapitulated physiological *in vivo* cytokine regulation was required. An in-depth characterization of two wound healing models: a single-pulse model – which reflects a normal wound healing situation; and the multiple pulses model – simulating a wound healing situation leading to fibrosis, was presented.

Aim #2: To investigate "memory" in TGFβ1 pulses

Epigenetics and cell – ECM communication play a key role in fibrogenesis. We therefore, investigated autocrine TGFβ1 production, epigenetics mechanisms and the influence of TGFβ1-pulsed ECM on the fibroblast phenotype. Further, we investigated the effects of the normal fibroblast ECM on the myofibroblast phenotype.

Aim #3: To study the potential of SAHA as an anti-fibrotic drug

SAHA has recently demonstrated anti-fibrotic potential. However, there was still the need to better understand SAHA's effects in curbing fibrosis before moving into animal studies. As SAHA is an FDA-approved cancer drug in clinical use, data obtained from this study can be moved into the preclinical animal models with good reasons and data from *in vivo* studies can be faster translated towards clinical therapy.

a) Assess SAHA's effects on TGFβ1-pulsed myofibroblast formation

Prior treatment with TGFβ1 before SAHA treatment sets a boundary for SAHA's anti-fibrotic potential. Several permutations of SAHA treatment in conjunction with TGFβ1 pulsing were assessed.

b) Elucidate SAHA's effects on locomotion, contractility and apoptosis in myofibroblasts

SAHA hyperacetylated α-tubulin, a cytoskeletal component in fibroblasts and suggested that HDAC6, a microtubule associated deacetylase was inhibited. However, SAHA's effects on the mechanical properties of myofibroblasts remains unknown, and results derived from studying mechanical properties in SAHA-treated myofibroblasts may reveal an additional therapeutic facet towards anti-fibrosis treatment.

1.3 Research Strategy

Aim #1: Development of a physiologically relevant *in vitro* fibrotic model

To recapitulate and assess *in vivo* TGFβ1 regulation *in vitro,* the following models were studied:

- Single TGFβ1 pulse: 3 time-points were assessed – 0.5h, 4h and 48h of TGFβ1 treatment, with cytokine removal thereafter

- Multiple TGFβ1 pulse(s): We assessed the effects of 0.5h (2 x 0.5h) and 4h (2 x 4h) pulses, with cytokine removal in between, over 2 consecutive days

- Conventional TGFβ1 pulse: Current protocols expose cells to 4 days of TGFβ1 treatment and this timeframe was chosen to simulate current *in vitro* experimental setups

Cultures were maintained for a further 14 days in 0.5% FBS DMEM, with endpoint analysis at days 1, 7 and 14 post-treatment. Readout parameters included the classic markers of myofibroblasts: α-SMA; collagen I production; and the transcription of selected fibrogenic genes – α-SMA (ACTA2), Frizzled 8 (FZD8), NADPH-oxidase 4 (NOX4) and Tetraspanin 2 (TSPAN2).

Aim #2: To investigate "memory" in TGFβ1 pulses

Mechanistic studies to explain the long-term effects of TGFβ1 pulse(s) were conducted. Briefly, TGFβ1 levels in the supernatant were measured using an enzyme-linked immunosorbent assay (ELISA). Acetylation and DNA methylation investigations were performed. To investigating cell – ECM communication, the effect of TGFβ1-pulsed decellularized ECM on the phenotype of untreated fibroblasts was assessed. The influence of fibroblast ECM on myofibroblasts phenotype was studied.

<u>Aim #3: To study the potential of SAHA as an anti-fibrotic drug</u>

a) <u>Assess SAHA treatment on TGFβ1-pulsed myofibroblast formation</u>

Focusing on the 4h and 2 x 4h TGFβ1 pulse(s), the efficacy of SAHA on reducing and/or curbing TGFβ1-pulsed myofibroblast formation was studied thus:

- SAHA pre-treatment on TGFβ1 pulse(s): Cells were treated with SAHA for 24h before exposure to either 4h or 2 x 4h TGFβ1 pulse(s), with cytokine removal thereafter.

- SAHA post-treatment on TGFβ1 pulse(s): Cells were treated with either 4h or 2 x 4h TGFβ1 pulse(s), followed by 24h of SAHA treatment and removal thereafter.

- SAHA pre-treatment – TGFβ1 pulse(s) – SAHA post-treatment: Cells were exposed to 24h of SAHA treatment followed by TGFβ1 pulse(s). Cells were immediately treated with SAHA for 24h and removed thereafter.

Cultures were maintained for a further 7 days in 0.5% FBS DMEM with endpoint analysis at days 1 and 7 post-treatment. Readout parameters included the classic markers of myofibroblasts: α-SMA and collagen I production.

b) <u>Elucidate SAHA's effects on locomotion, contractility and apoptosis in myofibroblasts</u>

- Motility of the cells using a scratch assay: Cultures were treated with or without TGFβ1 to induce myofibroblast formation. Thereafter, cytokine-containing media was removed and cells were treated with or without SAHA and maintained for a further 3 days. Readout parameters at selected time-points included live cell analysis of migration into scratch area.

- Assessment of the contractile ability of cells in a collagen gel: Using a commercial collagen contraction assay, cultures were treated with or without TGFβ1 treatment to induce myofibroblast formation. Thereafter, cytokine containing media was removed and cultures

treated with or without SAHA and maintained for a further 3 days. Readout parameters at various time-points included live cell analysis of contraction.

- Apoptosis induction in SAHA-treated cells: Cultures were treated with or without 4 days of TGFβ1. Cytokine containing media was removed and replaced with or without SAHA. Cultures were maintained for a further 4 days with endpoint analysis at days 1, 2 and 4. Fluorometric assays were used to measure apoptosis induction.

Chapter 2

Literature Review: The etiology of fibrosis

This chapter contains an in-depth review of fibrogenesis, its progression and the clinical burden fibrosis poses today and describes the rationale behind the project. Cell – ECM interactions and epigenetic modifications focusing on fibrogenesis are discussed.

2.1   Overview of Fibrosis

Wound healing can take place in every part of the body and consists of a cascade of tightly-regulated events to enable the body to repair and regain function. Upon healing, the original wound is replaced by connective tissue. This is commonly known as a scar.

A scar is, in general, not harmful to the body and represents a quick repair system to regain function. However, when there is an imbalance in the wound healing process, such as the perpetuation of tissue injury, chronic inflammation, excessive consumption of alcohol, chemo- or radiotherapy, and/or other toxins, fibrosis ensues. Histopathologically, fibrosis is characterized by the excessive accumulation and reduced remodeling of the ECM. It involves the misregulation of collagen I and the hyperproliferation of fibroblasts / myofibroblasts. The response to tissue insult commences at the point of injury, and the initiation of fibrosis ranges from weeks to months.

2.1.1 The global burden of fibrosis

Fibrosis poses a substantial disease burden, in South-East Asia as well as globally. Fibroproliferative diseases affect almost every organ. For example, there are at least 5 million cases worldwide of idiopathic lung fibrosis (IPF). The mortality rate for IPF is 50% after 2 to 3 years post diagnosis and at least 45,000 individuals in the US die from this disease every year [Meltzer et al. 2008, Mason 1999]. Scleroderma/systemic sclerosis (Ssc) displays much variation in severity between patients, ranging from cutaneous regions to internal organs. Patients with severe, rapidly progressive SSc have been estimated to have only a 50% chance of five-year survival [Furst et al. 2012]. Viral hepatitis B and C (HPB/C) are rampant and continue to pose significant clinical risks. For hepatitis C alone, the global prevalence is estimated at 170 million [Pol et al. 2012]. End stage liver disease leading to liver transplantation, complications of chronic infections and liver fibrosis/cirrhosis are similarly common [WHO, 2004]. Keloid and hypertrophic (less severe) complications are common within scar tissue. Other occurrences of fibrosis include endomyocardial / old myocardial fibrosis (heart), myelofibrosis (bone marrow) and Crohn's disease (intestine), all pathological conditions which highlight the unmet clinical need for an effective anti-fibrotic therapy.

2.1.2 Peri-implant fibrosis: A bottleneck in regenerative medicine

The objective of tissue engineering is the successful incorporation of implanted biomaterials, cells or whole organs into the body [Ratner B.D 2002]. An unaddressed bottleneck in this discipline is foreign body reaction or peri-implant fibrosis, a consequence of the host's natural response to destroy or phagocytose the implant [Anderson et al. 2008]. Host responses to an implant follow a cascade of events similar to, but ultimately divergent from wound healing. If the host is unable to break down the implant, the implant will eventually be encapsulated within fibrous tissue with minimal vascularisation, effectively isolating it from surrounding tissues. Evidence of fibrous encapsulation around implanted biomedical devices [Tang et al. 1995],

biosensors [Henninger et al. 2007], aortic valve replacements [O'Keefe et al, 2011; Cicha et al. 2011], synthetic prosthetics [Harrell et al. 2006, Dolce et al. 2010] and breast implants [Zeplin et al. 2010; Bartsich et al. 2011] have been well documented. In summary, peri-implant fibrosis impairs the function of biomaterials and biomedical devices, rendering many unsuccessful preliminary efforts to engineer biomaterials safe for implantation.

2.2 Wound healing and fibrosis: Focus on foreign body reaction

Wound healing is a highly conserved physiological process designed to be nature's "quick fix" for the repair of injured tissue. It has not evolved to serve aesthetics, but rather to rapidly replace tissue without regard for the restoration of normal morphology and functionality. This mechanism has evolved to reduce the duration of exposure to the environment and the risks of subsequent bacterial infections. The process often compromises tissue architectural integrity, resulting in inadequate restoration. An overview of fibrous encapsulation after foreign body reaction is illustrated in Figure 1.
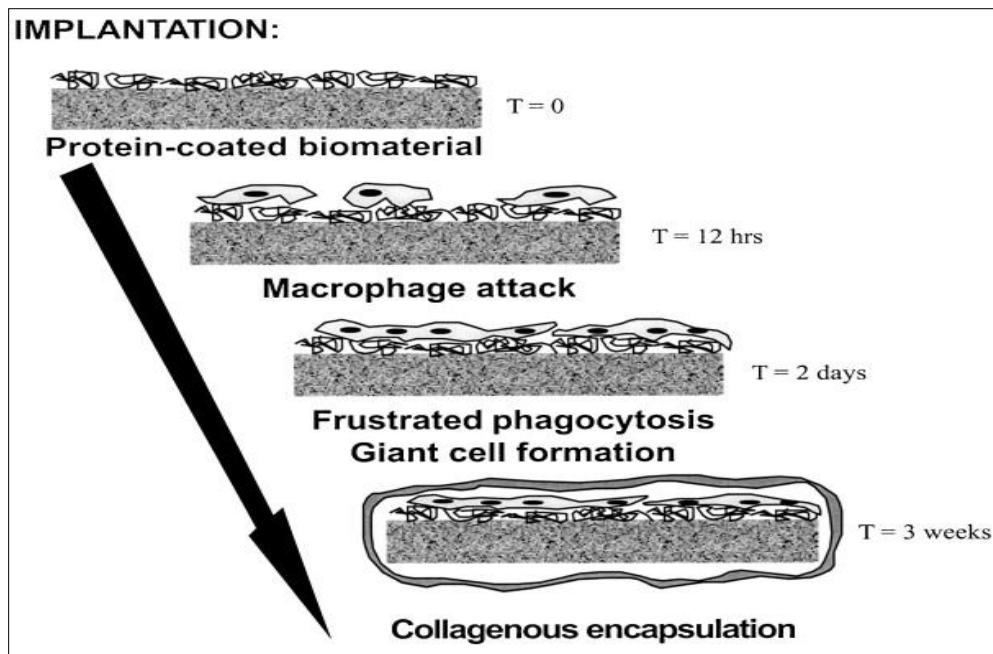
Figure 1. Different stages of foreign body reaction leading to collagenous encapsulation surrounding the implant. Adapted from [Ratner B.D 2002].

Host reactions upon implantation can be classically divided into hemostasis, acute and chronic inflammatory, proliferative and remodeling phases leading to fibrous capsule formation. In this thesis however, an alternative model by Nguyen et al. will be used as a reference [Nguyen et al. 2009]. This model describes a clearer, more delineated process, where wound healing is divided into two major phases: the early and cellular phase (Table 1).

Stage	Duration post-implant	Phase Classification	Description
1	Within minutes – 24h	Early	• Platelet activation and aggregation • Initiation of inflammation • Endothelial cell migration
2	Day 1 - 2	Cellular	• Infiltration of macrophages and inflammatory components
3	Within hours – day 1 – 2	Cellular	• Re-epithelization • Damaged ECM breakdown
4	Day 4 – 14	Cellular	• Fibroblast – myofibroblast differentiation
5	Day 4 – 14	Cellular	• Endothelial cell migration and angiogenesis
6	Day 4 – months/years	Cellular	• Remodeling of scar tissue • Maturation of tissue

Table 1. Duration of fibrosis formation and progression surrounding an implant. In this model, wound healing is delineated into the early and cellular phases. Summarized from [Nguyen et al. 2009].

2.2.1 Early phase: Hemostasis and formation of the fibrin clot

The immediate response (within minutes) of a host to a foreign object is a barrage of chemical and mechanical signals, resulting in the formation of a provisional ECM (the hemostatic plug). The damage to surrounding blood vessels triggers a response activating several "stress signals" for platelet activation and aggregation, which in turn establish hemostasis. Platelets (thrombocytes) are the most abundant cell source recruited as they release a reservoir of molecules that become involved in the coagulation cascade. Activated platelets initiate inflammation by releasing chemotactic agents such as metalloproteinases, tissue factor,

serotonin, bradykinin, histamine, prostaglandins, prostacyclin and thromboxane, all of which are involved in the formation of hemostatic plug. Platelets also release a panoply of growth factors, including platelet-derived growth factor (PDGF) and TGFβ1, which in turn initiate the chemotaxis of neutrophils, fibroblasts, macrophages and endothelial cells from surrounding regions [Nurden et al. 2011]. Platelets also express glycoproteins that allow the conversion and collective accumulation of fibrinogen-to-fibrin at the implant site. This forms a fibrin clot of provisional ECM which then serves as a "scaffold" to provide support for subsequent epithelial migration and cellular infiltration. Thus, the provisional ECM forms the structural and mechanical basis for subsequent cellular activity by providing a source of cues that controls the complex process of wound healing.

2.2.2 Cellular phase

In the cellular phase, different cell types work in synergy to restore a rudimentary degree of structural integrity to the implant region. The various components that are individually addressed here do not occur in series, but instead partially overlap in time.

2.2.2.1 Inflammation and macrophages infiltration

After formation of the provisional ECM, immune cells infiltrate the injury site and mount an inflammatory response within minutes to days. Short-lived, blood-derived polymorphonuclear neutrophils (PMNs) and monocytes, the latter subsequently activated to become macrophages, rapidly migrate into injured area. Together, macrophages and neutrophils remove foreign microorganisms, bacteria, damaged ECM components and other non-essential materials [Mahdavian-Delavary et al. 2011]. It is also interesting to note that multiple aspects of the inflammatory response are in part governed by the biomaterial-dependent behavior of PMNs. Various responses of PMNs have been observed on several biomaterials [Gemell et al. 1996, Chang et al. 1999, Rosenson-Schloss et al. 2002, Tan et al. 2002] and it has been established

that surface material chemistry, size and shape greatly influences the behavior of PMNs in response to an implant. Mononuclear leukocytes such as monocyte-derived macrophages and lymphocytes are also involved in this phase of wound healing. These cells play a role in neovascularization and the development of connective tissue. Recently, a unique population of monoculear leukocytes known as fibrocytes, or bone-marrow derived progenitors has been described. Circulating fibrocytes make up less than 1% of the circulating leukocyte population and have been documented to assist in the coordination of the inflammatory and reparative stages of wound healing [Keeley et al. 2010]. Fibrocytes are recruited early in the wound healing phase, and have the ability to take on an antigen-presenting role, thereby producing a barrage of signaling molecules. Furthermore, fibrocytes have the ability to secrete collagen I and ECM metalloproteinases (MMPs), proteins which greatly contribute to ECM remodeling [Grieb et al. 2011]. Although not fully elucidated, there is speculation that fibrocytes may be precursors to fibroblasts and myofibroblasts [Abe R. 2001, Schmidt et al. 2003, Ekert et al. 2011].

Macrophages also play a critical role by releasing pro-fibrotic cytokines – PDGF, vascular endothelial growth factor (VEGF), fibroblast growth factors (FGFs) and TGFβ1 in bid to promote the migration, proliferation and differentiation of fibroblasts and endothelial cells. Macrophages are essential for the wound healing process, and the inhibition of macrophage function may lead to compromised inflammatory response, markedly impaired vascularization and defective wound healing [van Amerongen et al. 2007, Sakurai et al. 2003].

2.2.2.2 Re-epithelization

The process of re-epithelization (that occurs within hours and lasts for a few days) commences with the migration of epidermal cells. Basal keratinocytes from surrounding areas (wound edge and surrounding dermal appendages) are the main cell type responsible for re-epithelization.

12

Keratinocytes first migrate without proliferating, and when at the injury site, proliferate, a process which continues until the integrity of the epidermis has been attained. There are several reports that migration over the wound site is stimulated by such factors as lack of contact inhibition, hypoxia [O'Toole et al. 1987], chymase (chymotrypsin-like serine protease predominantly produced by mast cells) [Firth et al. 2008] and nitric oxide [Witte et al. 2002]. This process is mediated by cytokines such as epidermal growth factor (EGF), secreted by platelets [Wells et al. 1999], and TGFβ1, secreted by keratinocytes, macrophages and platelets. EGF and TGFβ1 permit cell detachment and subsequent migration towards the injury site. Epidermal cells also express several forms of the transmembrane receptor protein, integrin, which relocate over actin filaments within the cytoskeleton to serve as attachment anchors to the ECM during migration. Integrins allow cells to interact with a variety of ECM proteins, including fibronectin (FN), and binds to other ECM components such as collagens, heparan sulfate, fibrin [Pankov et al. 2002], and vitronectin (which promotes cell adhesion and spreading) [Preissner et al. 1998]. This process is also mediated by the secretion of zymogens and enzymes which assist in the removal of fibrin clots and damaged ECM proteins through the secretion serine protease, plasmin and collagenases. Plasminogen (zymogen) is activated by tissue plasminogen activator and urokinase upon binding to clots [Silverstein et al. 1984].

The re-epithelization process is also characterized by the gradual shift from the generalized secretion of pro-inflammatory mediators towards formation of a basement membrane and synthesis of granulation tissue.

2.2.2.3 Fibroblast – myofibroblast differentiation

Approximately 4 days post-implantation (when the inflammatory period is ending), fibroblasts invade the wound site and proliferate rapidly. A fibroblast's chief duty is to secrete collagen, and the large increase in the fibroblast population results in the abundant production and

accumulation of collagen in the ECM, a process mediated by TGFβ1 [Desmoulière et al. 1993, Kottler et al. 2004] and PDGF in the microenvironment. There are two major aspects of the wound healing in this phase – collagen deposition and contraction. Collagen fibrils are the main component of connective tissues, and form the basis of structural integrity in the wound bed. As the provisional ECM does not confer much resistance to the wound bed, it becomes essential that collagen is laid down to provide strength and support as the wound closes. Also, collageneous ECM allows the attachment of cells involved in the processes of angiogenesis, inflammation and tissue reconstruction to attach, grow and differentiate [Ruszczak et al. 2003]. To date, 28 members of the collagen family have been identified [Gelse et al. 2003], with collagens type I, III and IV being the most essential ones for wound healing. Immediately post-injury, collagens type III and IV (together with FN) are the proteins providing the predominant tensile strength until the stronger type I collagens replace them at later stages. The other aspect of wound healing is wound contraction, regulated by a specific cell type known as the myofibroblast. Upon stimulation by TGFβ1, fibroblasts differentiate into myofibroblasts. Besides fibroblasts, myofibroblasts can also originate from other sources, including hepatic stellate cells (HSCs) [Sato et al. 2003], epithelial or endothelial cells which undergo epithelial or endothelial – mesenchymal transition (EMT) as in renal fibrosis [Hertig et al. 2010, Fragiadaki et al. 2011], and fibrocytes [Ogawa et al. 2006]. Classic markers of the myofibroblasts include elevated collagen I production, the expression of the contractile cytoskeletal protein α-SMA, and filamentous actin (F-actin) [Hinz et al. 2001]. Myofibroblasts however, are distinct from smooth muscle cells, despite both cell types expressing α-SMA as a key marker. Recent evidence has demonstrated distinct transcriptional control mechanisms regulating the expression of α-SMA [Gan et al. 2007], and these two cell types can be considered as distinct. The population of myofibroblasts in the wound area increases at approximately one week post-wounding and lasts for several weeks, even after the wound is completely re-epithelized [Stadelmann et al. 1998]. Contraction is mediated by several cellular elements, including integrins, which enable cells to

sense mechanical perturbations and transmit intracellular stress to their environment [Wipff et al. 2008]. Other mediators of contraction include integrin ligand proteins such as FN, vitronectin and collagen cross-linking enzyme lysyl oxidase [Harrison et al. 2006]. The buildup of collagen, together with contractile forces, allows closure of the wound. In a normal wound healing process, upon restoration of tissue integrity, myofibroblasts stop contracting and undergo apoptosis [Desmoulière A. 1995, Kis et al. 2011].

Even as the myofibroblasts produce new collagen, collagenases degrade it, and during a normal wound healing process, a balance between collagen production and degradation will be attained. However, fibrosis occurs when there is an imbalance between production and degradation, or when the myofibroblasts do not undergo apoptosis, resulting in the formation of a scar [Rieder et al. 2007].

2.2.2.4 Angiogenesis (Neovascularization)

Along with the fibroblast – myofibroblast differentiation phase, there is a concurrent process of from day 4 onwards. Angiogenesis is imperative for wound healing as it provides oxygen and nutritional support for the new tissue. Macrophages are the first cell types to enter the wound bed and they release tumor necrosis factor (TNF-α), which in turn stimulates VEGF production by fibroblasts and keratinocytes [Frank et al. 1995]. In response, endothelial cells migrate into the wound bed, a process largely mediated by the FN within provisional ECM and the cytokines VEGF, FGF, angiopoietins and TGFβ1 released by macrophages, fibroblasts, epithelial cells and endothelial cells in response to either hypoxia [Brahimi-Horn et al. 2011] or high concentrations of lactate pyruvate [Draoui et al. 2011]. This process is accompanied by the degradation of the fibrin clot to facilitate migration (mediated by MMPs and serine proteases). The most critical pro-angiogenic factor is VEGF, which stimulates multiple components of the angiogenic cascade. VEGF stimulates the proliferation of endothelial cells [Tie et al. 2012] and

increases ECM permeability in the provisional ECM, a process necessary for angiogenesis [Dvorak et al. 1995]. The increase in the endothelial cell population leads to tubular formation, which is further driven by nitric oxide, a potent vasodilator which protects tissues from hypoxia and ischemia [Blantz et al. 2002].

When the tissue is adequately perfused, often in configurations that do not conform to those in the uninjured dermis, the migration and proliferation of endothelial cells slows and eventually, blood vessels that are no longer required undergo apoptosis [Tie et al. 2012].

2.2.2.5 Remodeling and maturation of tissue

Remodeling commences 4 days post-injury, but can last up to months or even years depending on the size of the wound. In response to TGFβ1, remodeling of the ECM begins when collagen deposits are in abundance. Similar to the angiogenic process of ECM degradation, MMPs and collagenases (secreted by fibroblasts, epidermal cells and macrophages) act to breakdown the early type III collagen. Fibroblasts and myofibroblasts are the key effector cells responsible for collagen I secretion into the surrounding extracellular space [Harrison et al. 2006], and excess ancillary collagen fibres are removed or replaced by the stronger type I collagen. The remaining fibres are subsequently reorganized to add stability and provide a suitable microenvironment to re-attain cellular metabolism. As remodeling takes place, the tensile strength of the wound eventually increases, ultimately regaining up to 80% of that of normal tissue [Lindstedt et al. 1975].

Wound healing progresses in a predictable, highly regulated manner, with each stage characterized by a well-orchestrated cascade of factors and ECM proteins. If any of these steps go awry, the healing process becomes inappropriate, leading to either a chronic wound or a pathological condition known as scarring or fibrosis.

2.3 TGFβ1: A cytokine with many facets

There are a plethora of growth factors which regulate fibrogenesis, the most prominent being members of the TGFβ1 family. Mammalian TGFβ1 exists in three isoforms – TGFβ1, 2 and 3. Despite being structurally similar, they exert diverse effects *in vivo* [Pelton et al. 1991]. TGFβ2 plays a vital role in embryonic development [Roberts et al. 1992] while TGFβ3 regulates molecules involved in cellular adhesion and ECM formation in the cleft palate and lung [Kaartinen et al. 1995]. With regard to wound healing, TGFβ3 promotes scarless wound healing [Kohama et al. 2002, Shah et al. 1994, Ferguson et al.1996] while TGFβ1 is a well known factor in fibrosis. TGFβ1 is a growth factor with pleiotropic effects necessary for the maintainence of homeostasis in the body [Liu et al. 2011, Ruscetti et al. 2003]. A strongly regulated molecule during physiological events, TGFβ1 deploys both positive and negative feedback mechanisms [Heldin et al. 1997] and exerts its effects on hundreds of genes, resulting in dramatic geno- and phenotype changes [Ranganathan et al. 2007]. The focus of this thesis is on TGFβ1-induced fibroblast – myofibroblast differentiation.

2.3.1 Mechanisms of TGFβ1 activation

All mammalian TGFβ1 molecules are first synthesized as precursor molecules containing both a propeptide region and an inactive TGFβ1 homodimer (Figure 2). There is significant amount of the large latent complex (LLC) in the ECM, and, because different cellular mechanisms require precise levels of TGFβ1 signaling, activation of the inactive precursors allows appropriate mediation of TGFβ1 signaling *in vivo* [Annes et al. 2003]. Activation of latent TGFβ1 involves the liberation of TGFβ1 from the LLC from the ECM. Release of active TGFβ1 involves the disruption of the bonds attaching it to the latency associated peptide (LAP). Current literature suggests that the mechanism of TGFβ1 activation is varied and context dependent, but it is generally suggested that conformational changes in the LAP structure releases bioactive TGFβ1

and exposes TGFβ1 receptor binding sites [Khalil N et al. 1999, Biernacka et al. 2011]. This process is mediated by proteases, integrins, MMPs (specifically MMP-2 and MMP-9) [Wipff et al. 2008], thrombospondin-1 [Sweetwyne et al. 2012], hydroxyl radicals from reactive oxygen species [Barcellos-Hoff et al. 1994] and pH [Annes et al. 2003], a mechanisms which denatures the LAP thereby inducing the activation of TGFβ1 [Lyons et al. 1988].
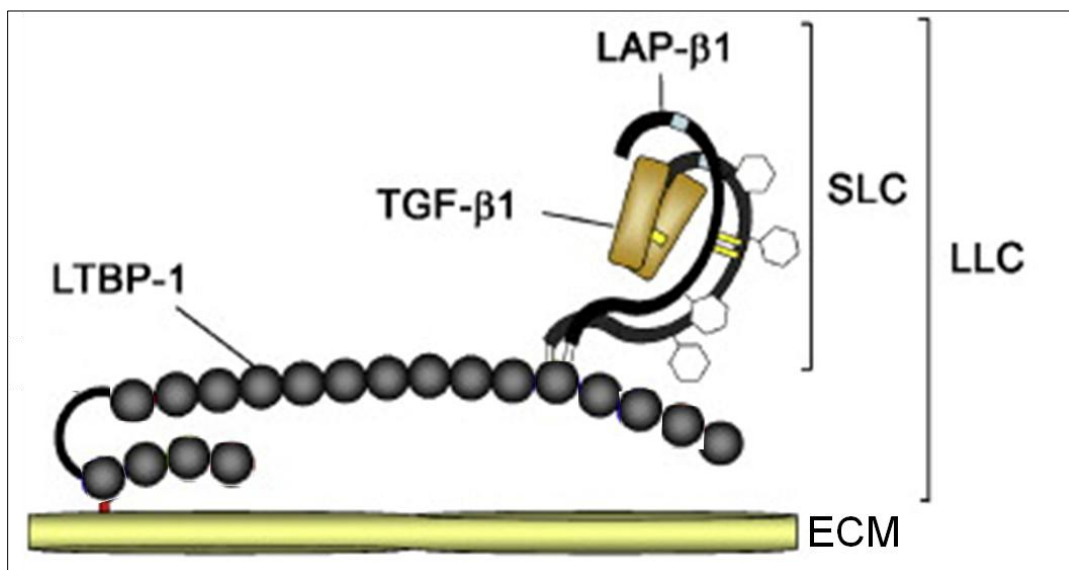
Figure 2. TGFβ1 is secreted as an inactive complex. The TGFβ1 homodimer interacts with an N-terminal latency associated peptide (LAP) to form the small latent complex (SLC), which is unable to associate with its receptors. The SLC remains in the cell until it is bound by another protein known as the latent TGFβ1-binding protein (LTBP1) by disulfide bonds, forming a larger complex known as the large latent complex (LLC). The LLC is secreted and binds to ECM components such as elastin fibrils and FN rich fibres [Todorovic et al. 2005]. Adapted from [Wipff et al. 2008].

2.3.2 TGFβ1 regulation and effects in fibrosis

Members of the TGFβ1 family initiate signaling pathways through binding transmembrane type I and II receptors (TβRI, TβRII). TGFβ1 – TβRI/II interaction involves the formation of a stable complex that activates type I receptor kinases, triggering a cascade of signaling events that allows TGFβ1 to exert its biological effects. The TGFβ1 signaling pathway consists of SMADs. SMADs are intracellular proteins which transduce extracellular signals from TGFβ1 ligands to the nucleus for transcriptional activation. TGFβ1 – TβRI/II interaction phosphorylates and activates of R-SMADs, which bind to SMAD4 for nuclear translocation and subsequent cell-

related transcription. Combinatorial R-SMAD activation is mediated by inhibitory SMADs (I-SMADs), SMAD6 and SMAD7. SMAD6/7 inhibits TGFβ1 signaling through binding of their MH2 domains to TβRI, thereby preventing the recruitment of R-SMADs [Shi et al. 2003]. TGFβ1 is a crucial regulator of fibroblast phenotype and function. Upon TGFβ1 stimulation, fibroblasts differentiate to become myofibroblasts, key effector cells in fibrotic processes. Although myofibroblasts are essential for tissue repair, there is still substantial controversy regarding the true classic markers of myofibroblasts. In TGFβ1-stimulated stromal fibroblasts, fibroblast activating protein-alpha (FAP-α) [Chen et al. 2009] was upregulated and has been identified as a myofibroblast marker. Thymus cell antigen-1 (Thy-1/CD90) was upregulated in TGFβ1-stimulated lung and liver fibroblasts [Fries et al. 1994, Dudas et al. 2007]. However, other groups have reported reduced Thy-1 expression [Zhou et al. 2004], suggesting that myofibroblast marker expression was tissue-specific. A consensus has evolved, and myofibroblast hallmark markers now include elevated collagen I production and the expression of contractile cytoskeletal proteins, α-SMA and F-actin [Hinz et al. 2001] (Figure 3a). TGFβ1 also promotes ECM deposition by enhancing synthesis, and altering the balance between ECM-preserving elements such as plasminogen-activator inhibitor-1 [Ghosh et al. 2012], tissue inhibitor of metalloproteinases (TIMPs) [Hemmann et al. 2007] and degradative cellular cues (proteases, Figure 3b). TGFβ1 also stimulates fibroblast proliferation [Biernacka et al. 2011] (Figure 3c).
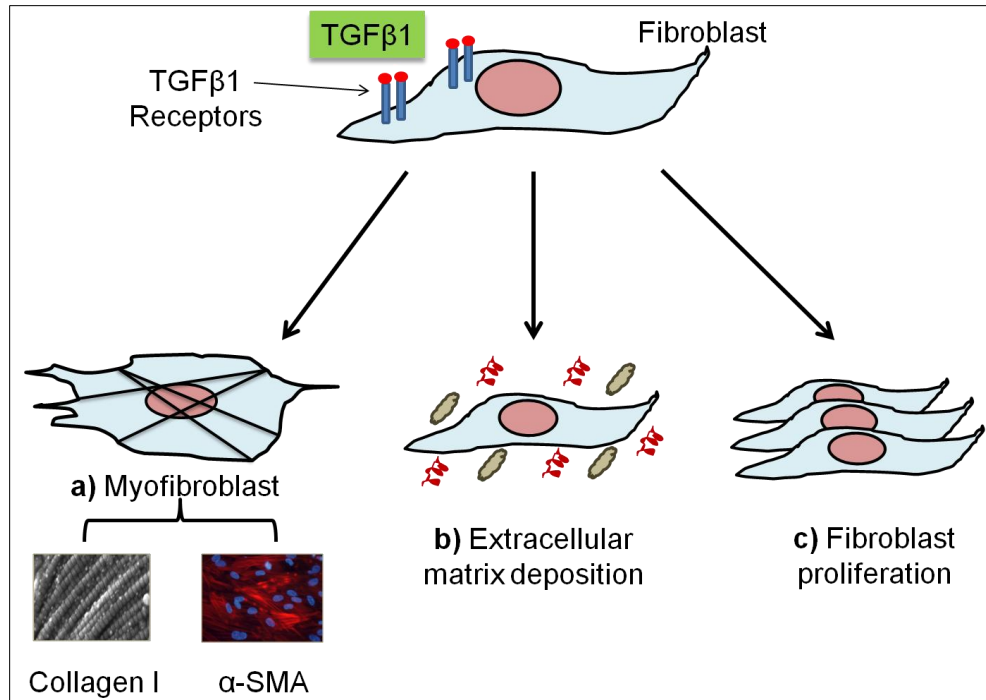
Figure 3. The effects of TGFβ1 on fibroblast function and phenotype. Under TGFβ1 stimulation, (a) fibroblasts adopt a myofibroblastic phenotype by expressing α-SMA and elevated collagen I production; (b) TGFβ1-stimulated fibroblasts increase ECM deposition; and (c) there is proliferation to achieve wound healing.

Other markers of the TGFβ1-mediated fibrogenic pathway include:

i. Frizzled-8 (FZD8): a downstream effector of the TGFβ1-signaling pathway and a receptor of the canonical Wnt pathway, FZD8 was demonstrated to induce canonical Wnt/β-catenin signaling leading to gene activation [Nam et al. 2006].

ii. NADPH-oxidase 4 (NOX4): The NADPH oxidase proteins are a source of reactive oxidative stress (ROS) and have been implicated in fibrogenesis. NOX4 was expressed in cardiac fibroblasts, pulmonary fibroblasts, hepatocytes and epithelial cells [Chan et al. 2009, Crestani et al. 2010]. In the lung, NOX4 maintained TGFβ1-induced myofibroblast activation and fibrogenic responses [Amara et al. 2010, Hecker et al. 2009, Bocchino M et al. 2010], and was elevated in the biopsies of IPF patients [Amara et al. 2010].

iii. Tetraspanin 2 (TSPAN2): TSPANs are transmembrane proteins and correlate to ECM production and regulation. To date, there is little evidence in the literature of the relationship between TSPANs and fibrosis.

In pathological conditions, activated myofibroblasts do not undergo apoptosis [Kis et al. 2011] and hence become key effectors of fibrosis, leading to increased contraction and ECM deposition in the wound bed (Figure 4).
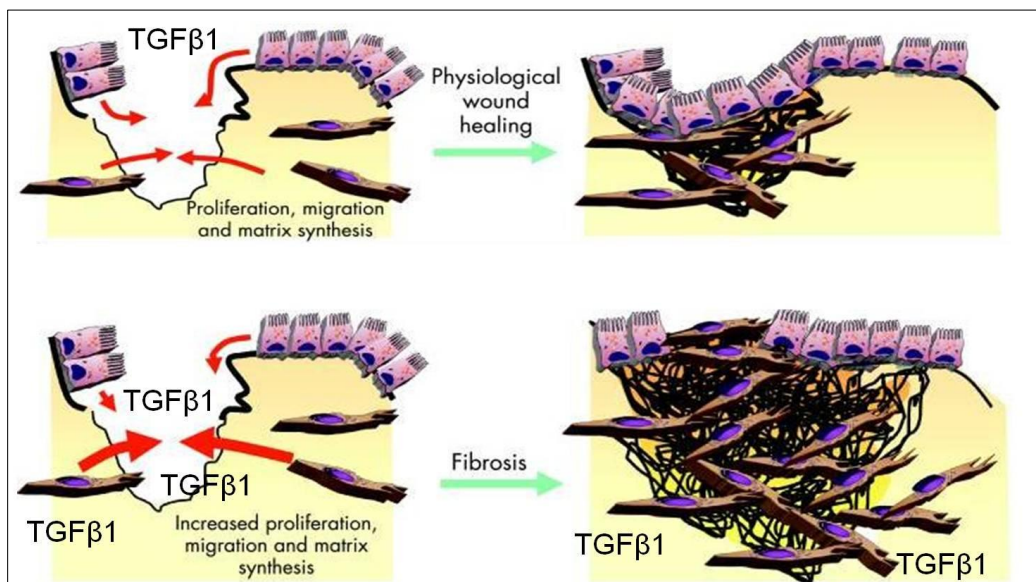
Figure 4. Physiological and fibrotic wound healing. In physiological wound healing, the production of TGFβ1 is well-regulated. In fibrosis, on-going TGFβ1 signaling leads to ECM accumulation and the persistence of myofibroblasts in the wound. Adapted from [Rieder et al. 2007].

2.3.3 TGFβ1-induced fibrogenesis *in vitro*: constraints in the current model

Pulsatile regulation occurs in most physiological systems and is most established in the endocrine system. In neuroendocrinology, neurohormone gonadotropin releasing hormone was demonstrated to work in a pulsatile manner to coordinate luteinizing hormone and follicle stimulating hormone production [Flanagan et al. 1998]; growth hormones were produced in individual bursts of between 30 – 90 min intervals [Martin et al. 1986]; and in the corticotropic

axis, the regulation of the coritcotropin-releasing hormone and arginin vasopressin led to the burst release of cortisol from adrenal cells [Veldhuis et al. 2008].

Similarly in wound healing, the production of TGFβ1 *in vivo* was demonstrated to be well-coordinated. TGFβ1 is a pleiotropic factor exerting a variety of biological functions and regulatory molecules are present in the signaling pathway of TGFβ1 to achieve homeostasis and avoid prolonged myofibroblast activation [Liu et al. 2011, Ruscetti et al. 2003]. *In vitro* studies traditionally employ TGFβ1 as a culture media additive for 4 days [Hinz et al. 2001]. However, TGFβ1 secretion in rat dermal healing wounds was shown to be short-lived and produced in a "burst-like" fashion [Yang et al. 1999] – a far cry from current established fibrosis *in vitro* models (Figure 5). To date, literature on cytokine regulation *in vivo* is limited and there has been only been one report [Yang et al. 1999] documenting *in vivo* cytokine regulation. Their work emphasizes the nature of TGFβ1, a cytokine which intricately coordinates tissue repair, and highlights the importance of developing a physiologically relevant platform for effective anti-fibrotic screening purposes.
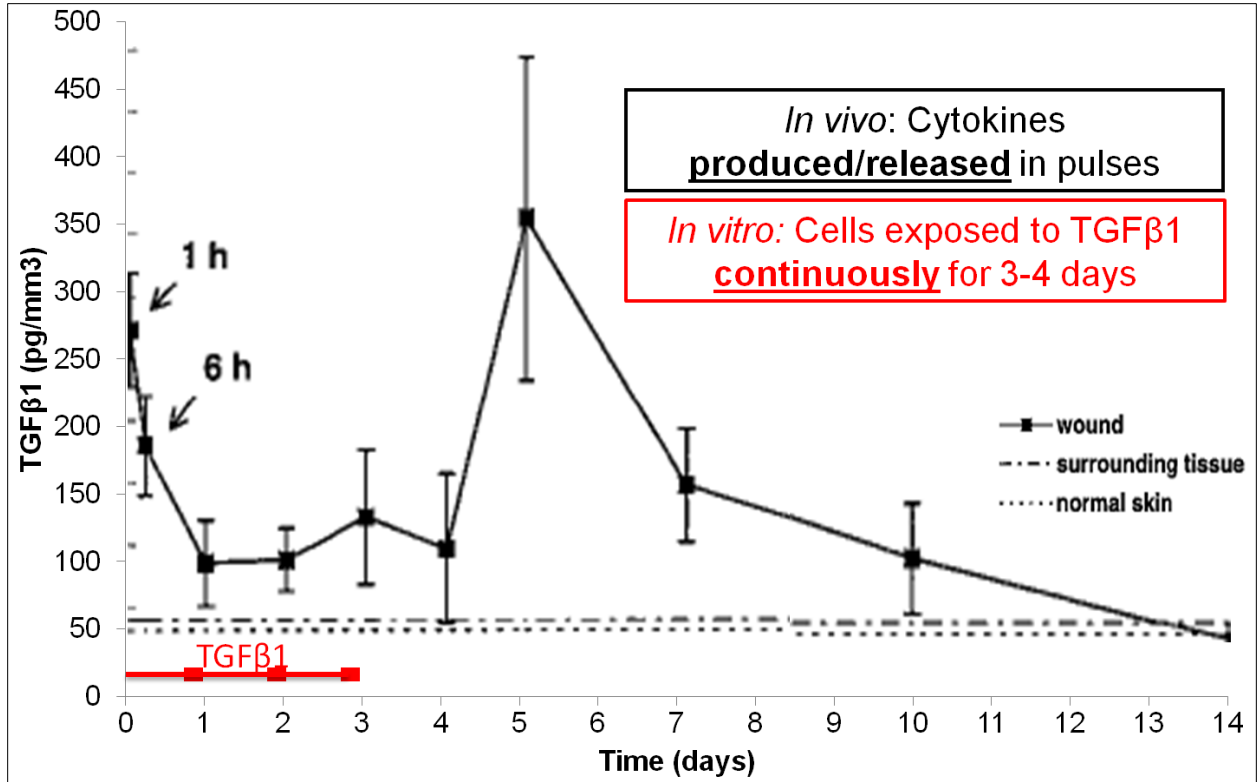
Figure 5. Pulsatile release of TGFβ1 in an *in vivo* rat dermal wound healing model assessed over a 14 day period. Current *in vitro* (red line) fibrosis models do not recapitulate *in vivo* (black line) conditions. Adapted from [Yang et al. 1999].

2.4 Cell – ECM interactions

2.4.1 The physiological ECM in wound repair

The ECM is more than just a scaffold for wound repair. Cellular genotype and phenotype is largely influenced by cellular interactions with the ECM, neighboring cells, and soluble local and systemic biochemical cues. For example, cancer cells were suppressed to form normal tissues by modifying their microenvironment [Mintz et al. 1975]. In turn, cells remodel the ECM. The ECM of a tissue or organ is highly dependent on its origin, context and state; generally consisting of interstitial connective tissue and the basement membrane, which is a meshwork of various molecular components such as proteoglycans, glycoproteins and fibres [Aumailley et al. 1998]. The wound microenvironment consists mainly of collagen I, which is functionally required to confer tensile strength and provide structural support. Resident fibroblasts contribute to the major development of the ECM and in turn, ECM components such as the ED-A domain of FN influence cellular phenotype [Serini et al. 1998].

2.4.2 Macromolecular crowding (MMC): recreating an *in vivo* microenvironment

The interior of cells, be they of eukaryotic or prokaryotic origin is highly crowded [Fulton 1986], mostly because of macromolecules such as proteins, lipids, nucleic acids and carbohydrates. In *ex vivo* culture, cells are harvested from tissue and placed in a highly aqueous environment on TCP – a condition far removed from the actual tissue state. Current solutions in cell culture technologies for the recapitulation of the microenvironment include surface modifications of TCP and/or 3D cultivation in ECM-derived scaffolds such as collagen gels [Simkovic 1959] and Matrigel [Kleinman et al. 1982].

2.4.2.1 MMC enhances ECM deposition and remodeling

An alternative approach towards the recreation of a highly dense microenvironment is the use of MMC. MMC have important effects in cell biology and can be broadly categorized as: **1)** accelerated protein folding under MMC [van den Berg et al. 2000]; **2)** increased enzyme – substrate half-lives and reaction kinetics leading to enhanced product formation [Norris et al. 2011, Lareu et al. 2007]; **3)** the restoration of cellular functions (e.g transcription and DNA replication) under compromised environments such as adverse pH or temperature [Zimmerman et al. 1987, 1993]; and **4)** the reversal of biochemical reactions [Somalinga et al. 2002]. Our group has previously demonstrated the efficacy of MMC in cell culture. MMC significantly enhance ECM deposition around mesenchymal stem cells [Zeiger et al. 2012] and fibroblasts [Chen et al. 2011]. Utilizing the biophysical approach of MMC in cell culture allows cells to recreate their own microenvironment to serve as a platform for advances in basic research and tissue engineering.

2.4.3   Dynamic cell – ECM reciprocity

Regulation of cellular function is characterized by close communication between cells and their environment (Figure 6) [Nelson et al. 2006, Bornstein et al. 2002]. This ongoing bi-directional crosstalk between cells and the ECM is coined as "dynamic reciprocity" [Bissell et al. 1982, Sage et al.1982].
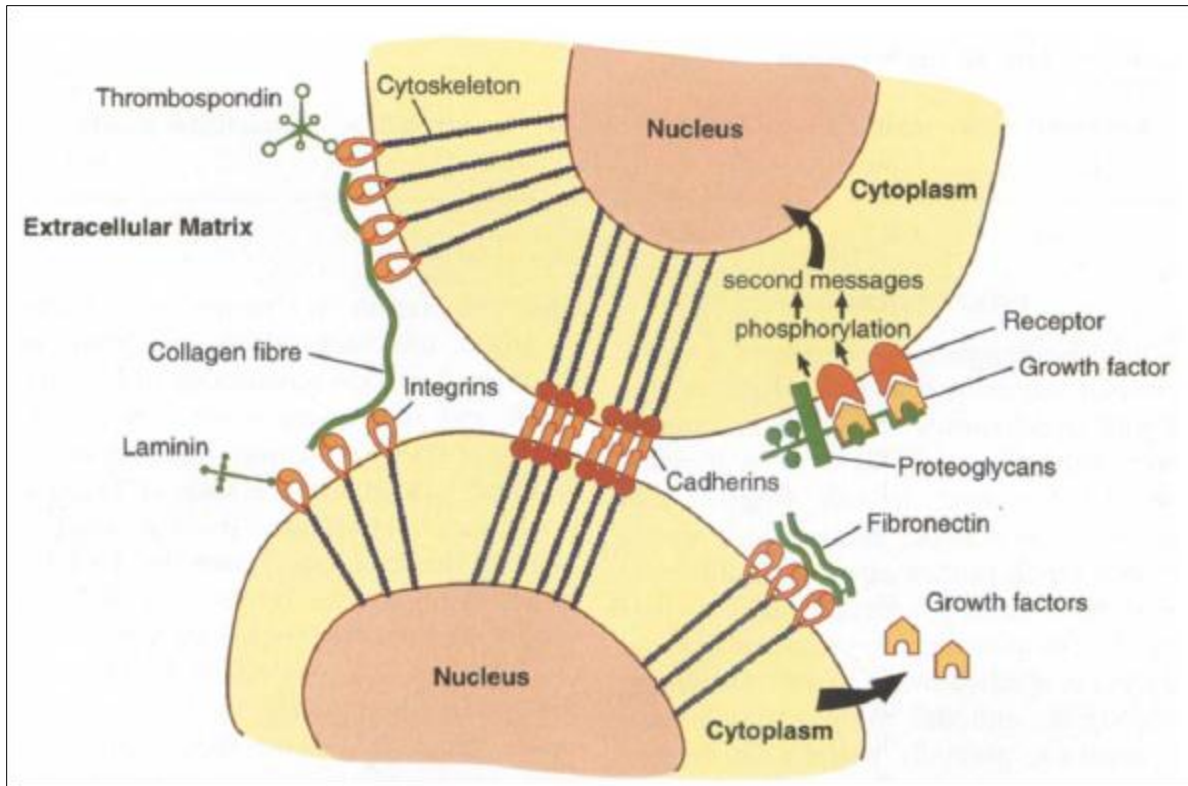
Figure 6. Cell – ECM interactions. Cells and their ECM interact through biochemical (cytokines or adhesion molecules) and mechanochemical stimuli to influence each other. The ECM regulates cellular tension, polarity, differentiation, migration, proliferation and survival. In turn, the cell synthesizes, degrades and remodels the ECM. Adapted from [Mutsaers et al. 1997].

The ECM compromises of a network of proteins with various structural and cell regulatory functions. Cells are directly linked to the ECM through integrins, which is mediated though FN, collagen and vitronectin, laminin, CD44, syndecans, cell adhesion molecules, selectins and discoidins [Widgerow et al. 2010, Schultz et al. 2011]. In the ECM, integrins constitute the most abundant receptors mediating cell – ECM interactions as they create the link between the "outer" and "inner" environment of the cell. Integrins are more than just mere hooks; they act as transducers to give cells critical signals about changes in mechanical stiffness, the release of growth factors and the nature of their surroundings [Schultz et al. 2011]. The ECM also affects cellular function and phenotype by providing spatial cues which guide cell migration, sequester signaling molecules such as locally released growth factors and cytokines, all of which govern

cell survival, proliferation, spindle orientation (development), differentiation and provide structural support to tissues and organs [Page-McCaw et al. 2007].

Cells also influence ECM regulation and tissue architecture by directing ECM synthesis, degradation and remodeling [Askari et al. 2009, Schultz et al. 2011]. Cells rapidly remodel the ECM by synthesizing and degrading connective tissue proteins. The ECM sequesters signaling cues which stimulates connective tissue synthesis. ECM degradation is in turn controlled by cells which secrete collagenase enzymes, proteases and MMPs [Daley et al. 2008]. A clear example of one such cell type is the fibroblast. Fibroblasts synthesize a host of ECM components, as well as the enzymes involved in ECM degradation. Taken together, dynamic reciprocity plays major roles in all forms of biological processes such as embryogenesis and development, angiogenesis, regeneration and fibrogenesis [Schultz et al. 2011].

2.4.3.1 Dynamic reciprocity: Focus on wound healing and fibrosis

Like most biological processes, wound healing and fibrosis involve cell – microenvironmental interactions, of which the ECM is a major component of. Cell – ECM communication is highly regulated and coordinated in order to orchestrate a band of signals to restore biological function and tissue integrity. A minor perturbation in this well-controlled physiological process can lead to fibrosis or simply, scar formation. The role of dynamic reciprocity in wound healing as defined by [Nguyen et al. 2009] is discussed in the preceding text. This section highlights cell – ECM interactions at various stages of wound healing.

2.4.3.1.1 Early Phase

Within minutes of tissue damage, a barrage of signals leads to a series of events designed to trigger inflammation and prevent major blood loss. Platelets infiltrate the wound site and release cytokines (TGFβ1, TNF-α) and chemokines which serve as chemoattractants for fibroblasts and

neutrophils [Widgerow et al. 2010], affecting ECM function [Ignotz et al. 1986]. FN and the fibrin clot, designed to halt blood loss, serve as a provisional ECM to incorporate adherent sites for cell attachment and act as a source of growth factors, proteases and protease inhibitors [Roberts et al. 1990].

2.4.3.1.2   Cellular Phase

Inflammation features in the early stages of the cellular phase of wound healing. Monocytes bind to the ECM, which enhances their phagocytic capacity and increases degradation of ECM debris [Zafiropoulos et al. 2008]. It also induces differentiation into macrophages, which increases profibrotic cytokine production [Li et al. 2006].

Formation of granulation tissue and angiogenesis follow. A key feature of dynamic reciprocity is the spatiotemporal regulation of integrin expression, leading to differential regulation patterns in cell adhesion dynamics, cytoskeletal organization and activation of signaling pathways [Truong et al. 2009]. The provisional ECM releases bioactive molecules to mediate fibroblast and vascular cell proliferation and fibroblast attachment to FN stimulates the production of ECM components – collagen, proteoglycans and hyaluronic acid [McDonald et al. 1982]. MMP production is a key feature at this stage, regulated by sphingosine-1 phosphate crosstalk with TGFβ1 to regulate MMP expression [Watterson et al. 2007]. In addition, integrin-mediated fibroblast attachment to collagen stimulates cellular production of MMPs [Steffensen et al. 2001], ultimately leading to ECM degradation and cell migration. This phase is also mediated by the proliferation of epithelial keratinocytes. MMPs dissolve ECM attachments so as to enable the keratinocytes to freely migrate through the ECM [Chen et al. 2009]. The migration of keratinocytes is mediated through highly specific integrin interactions as keratinocytes do not bind to the provisional ECM as they lack $\alpha_V\beta_3$ integrins [Kubo et al. 2001]. They instead express integrin subtypes which have an affinity to collagen, tenasin-C and vitronectin [Clark et al. 1996],

thereby relocating collagen-binding integrins from the lateral membrane of which is mediated by $\alpha_2\beta_1$ and $\alpha_3\beta_1$ integrins to the basal surface ($\alpha_V\beta_6$ integrins) of the wound. Angiogenesis occurs concurrently with granulation tissue formation, a process dependent on MMP-mediated ECM degradation that allows endothelial cell migration into the wound [Lafleur et al. 2003].

Mechanical tension represents another feature of dynamic reciprocity in fibrosis. This is largely modulated by the transition from collagen III to the stronger collagen I in the ECM, due to fibroblast remodeling in addition to changes in protein content of the ECM. MMP-mediated ECM degradation disrupts ECM tension and elasticity, which in turn, modulates cell shape (via the cytoskeleton), mediated through integrin anchors [Parker et al. 2002]. An important regulator of integrin-mediated tension is the small GTPase family member, RhoA [DeMali et al. 2003]. RhoA regulates stress-fibre formation and facilitates FN-ECM assembly [Zhong et al. 1998]. ECM-mediated cell shape changes affects the proliferative, migration (also mediated by cytokine gradients) and differentiation capabilities of the cells [Ingber et al. 1993], leading to changes in the mechanical properties of the remodeled ECM.

The final stage of the wound healing process is the contraction and remodeling phase. Upon stimulation by profibrogenic cytokines, commonly TGFβ1, fibroblasts differentiate into contractile α-SMA-expressing myofibroblasts and increase synthesis of ECM proteins (collagen I, ED-A FN) which enhance ECM tensile strength. The ED-A splice variant of FN has been demonstrated to induce and enhance myofibroblast differentiation [Serini et al. 1998], demonstrating the influence of the ECM on the myofibroblast phenotype. Latent TGFβ1 activation from ECM stores also mediates myofibroblast contraction [Wipff et al. 2008]. TGFβ1 interacts with ECM proteins, decorin [Yamaguchi et al. 1990] and the betaglycans, to induce the synthesis of decorin and biglycans [Okuda et al. 1990]. Feedback signals from increased ECM protein accumulation and ECM proteins (including fibrillins) – TGFβ1 interactions, reduces TGFβ1 bioavailability towards the tail end of the reparative process [Martinez-Ferrer et al. 2010]. Myofibroblasts also continue

to synthesize collagen until the ECM regains its structural integrity, mediated by ECM elasticity and tension.

Chronic wounds leading to scarring fail to exhibit the normal sequence of dynamic cell – ECM interactions due to aberrant protease levels involving the dysregulation in MMP production [Beidler et al. 2008, Liu et al. 2009, Rayment et al. 2008, Mwaura et al. 2006], or failed integrin switching at appropriates phases of wound healing [Larjava et al. 1993], ultimately leading to disease pathogenesis [Brem et al. 2007]. Although fibrosis cannot be solely attributed to dynamic cell – ECM interactions, the influence of the ECM in this well controlled physiological process should not be discounted.

2.5   Epigenetics

Epigenetics is defined as the study of heritable changes in gene expression or cellular phenotypes caused by mechanisms other than changes in the underlying DNA sequence.

2.5.1   Histone structure and function

Histones are the chief protein components of chromatin and play a role in gene regulation. Histones consist of DNA wound round 'spools' which package and order DNA into structural units, forming nucleosomes (Figure 7) [Felsenfeld et al. 2003]. Gene regulation is controlled through epigenetic or histone modifications which includes acetylation, methylation (on DNA and histones), phosphorylation, ubiquitination, SUMOylation, and ADP-ribosylation [Strahl et al. 2000].
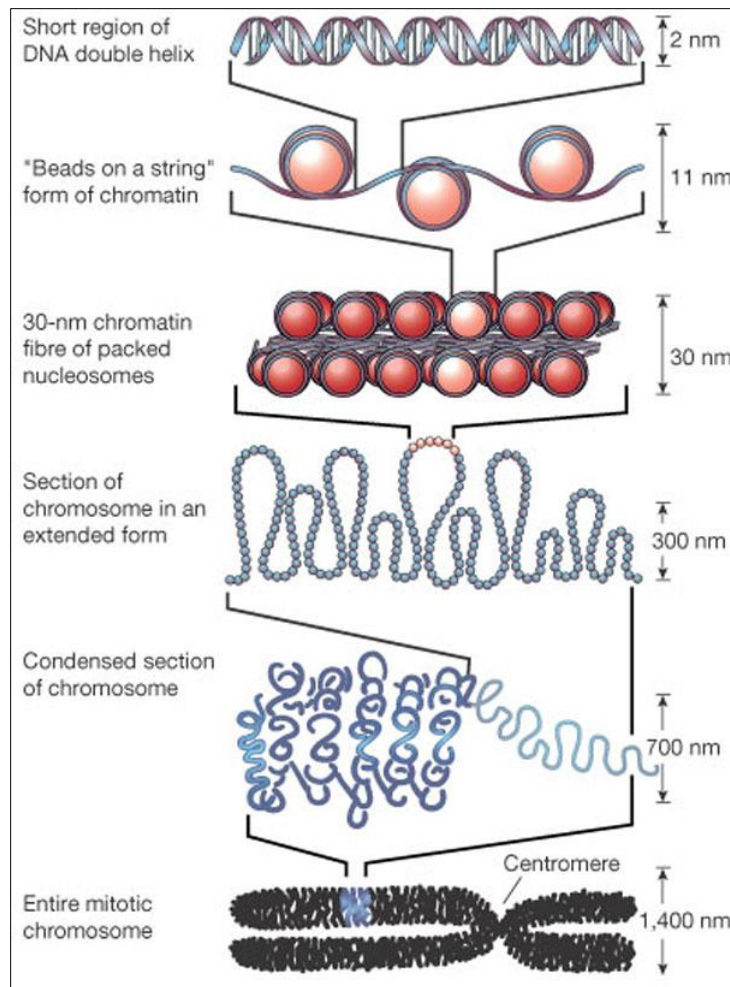
Figure 7. Organization of DNA within the chromatin structure. Adapted from [Felsenfeld et al. 2003].

2.5.2   Mechanisms of histone modifications

Histone acetylation and DNA methylation are the most appreciated forms of epigenetic modifications. Acetylation involves the addition of -$COCH_3$ group(s) on histone tails, a process mediated by the histone acetyltransferase (HAT) enzyme. HAT transfers the acetyl moiety onto the N-terminal tails of core histones, increasing histone hydrophobicity to facilitate the binding of transcriptional machinery to stimulate transcription. HDACs repress transcription by removing acetyl groups resulting in more densely packed chromatin [Eberharter et al. 2002]. The addition of methyl groups to cytosine-guanine (CpG) rich regions along the DNA strand, typically in the proximal to promoter regions, is known as DNA methylation. This is mediated by a class of

enzymes known as DNA methyltransferases (DNMT). It is generally held that histone acetylation increases transcription, but there are notable exceptions [Deckert et al. 2001]. In contrast, methylated CpG regions act, in general, as transcriptional repressors, leading to reduced gene transcription (Figure 8) [Eberharter et al. 2002].
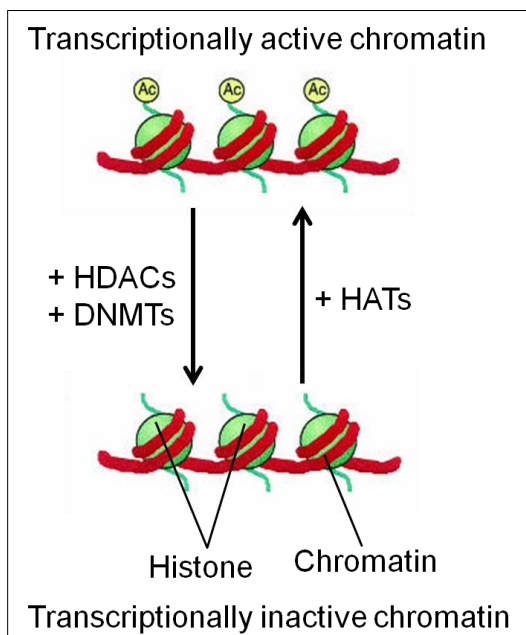
Figure 8. Histone modification switch. Acetylation by HAT renders chromatin in an 'open' state and permits the binding of chromatin remodeling factors to facilitate transcription. Deacetylation by HDAC or DNA methylation by DNMT renders chromatin in a 'closed' state. Adapted from [Eberharter et al. 2002].

2.5.3   Histone deacetylases (HDACs)

2.5.3.1 Classification of HDACs

HDACs are classified based on domain organization and sequence identity into classical and non-classical groups (Table 2) [de Ruijter et al. 2003].

Classification type	Class	Members	Subcellular Location	Tissue distribution	Classification basis
Classical	I	HDAC1, 2, 3, 8	Nucleus	Ubiquitous	Functions inhibited by HDACi trichostatin A (TSA)
Classical	IIA	HDAC4, 5, 7, 9	Nucleus / cytoplasm	Tissue specific	
Classical	IIB	HDAC6, 10			
Non-classical	III	Sirtuins in mammals (SIRT1-7); Sir2 in yeast	-	-	NAD^+-dependent proteins not affected by TSA
Classical	IV	HDAC11	Nucleus / cytoplasm	Tissue specific	Solely based on sequence identity

Table 2. Classification of HDACs. HDAC classification, the associated members, subcellular location, tissue distribution and the basis of classification type is presented. Classical HDACs share highly homologous zinc-dependent catalytic domains. Modified from [Marks et al. 2009].

2.5.3.2 The importance of HDACs in gene regulation

HATs and HDACs work in an orchestrated manner to regulate gene transcription (Figure 8). In general, HATs perform the role of transcriptional co-activators and HDACs, transcriptional de-activators. HDACs are actively involved in gene regulation and exert effects in cellular processes, environmental processing (i.e. signal transduction) and diseases [Eberharter et al. 2002]. HDAC1 and 2 are the most well studied, and play an important role in homeostasis. In mice, germ-line deletion of HDAC1 and HDAC3 causes early embryonic lethality [Dovey et al. 2010, Knutson et al. 2008] and cardiac-specific deletion of HDAC1 and 2 causes neonatal lethality [Montgomery et al. 2007].

HDACs also coordinate with DNA methylation to orchestrate regulation in gene repression. In certain cellular processes, HDACs are recruited by both DNMTs and methylated CpG binding proteins (such as MeCP2 and methyl-CpG binding domain proteins), resulting in histone deacetylation, DNA methylation and transcriptional repression [Eberharter et al. 2002]. Although a predominant function of HDAC is the modification of histone and chromatin structure, HDACs also interact with a variety of non-histone proteins such as transcription factors and co-regulators [Glozak et al. 2005]. Taken together, HATs and HDACs work in concert to regulate

gene transcription, and dysregulation of these factors can lead to aberrant processes and disease states.

2.5.3.3 The involvement of HATs and HDACs in fibrosis

In the lung, reduced HDAC activity and concomitant increased HAT activity was observed in bronchial biopsies obtained from patients with asthma [Ito et al. 2002], interestingly, the authors observed greater reduction in HDAC activity in asthmatic patients who smoked [Murahidy et al. 2005]. A marked reduction in HDAC activity in lung parenchyma biopsies was observed in chronic obstructive pulmonary disease patients [To et al. 2004]. Specifically, in IPF, defective histone acetylation was responsible for reduced COX-II expression and correlated with disease severity [Coward et al. 2009]. In a separate study, authors identified HDAC4 as an important regulator of TGFβ1-mediated myofibroblast differentiation in normal human lung fibroblasts [Guo et al. 2009]. In the epithelium, HDAC4 mediated the TGFβ1-induced myofibroblastic differentiation of human skin fibroblasts [Glenisson et al. 2007]; and it appeared that HDAC activity was required for the initiation and development of SSc [Huber et al. 2007]. Also, TGFβ1 treatment reduced histone 4 acetylation resulting in stimulation of dermal fibroblast collagen synthesis and myofibroblast differentiation [Bhattacharyya et al. 2009]. TGFβ1 treatment also induced acetylation of transcription factor Fli-1, leading to myofibroblast differentiation [Asano et al. 2007, Ghosh et al. 2007].

In primary myelofibrosis, both the transcriptional factor nuclear factor-κB (NF-κB) and HDAC1/3 were involved in the progression of myelofibrosis [Komura et al. 2005]. Further, the elevation of HDAC Class I, II and III isoforms suggested that HDACs were involved with disease progression [Wang et al. 2008]. In the heart, HDAC overexpression resulted in both atrial arrhythmia susceptibility and fibrosis in transgenic mice [Liu et al. 2008]. In a separate study, elevation of HDAC7a mRNA expression, together with increased TGFβ1 and collagen I production was

observed in mice with cardiac hypertrophy [Ellmers et al. 2007]. In renal fibrogenesis, HDAC2 was a key regulator of TGFβ1-induced myofibroblast differentiation, resulting in ECM accumulation and EMT in the kidney [Noh et al. 2004]. Lastly, in mice injured by urethral obstruction, increased expression of HDAC1 and 2 was observed [Yoshikawa et al. 2007]. Despite being a relatively new field, increasing evidence of HDAC activity during fibrosis, and the promise of novel ways for modulating HDAC activity may open new therapeutic avenues to combat this pathology.

2.5.4 DNA methylation: Focus on fibrosis

DNA methylation affects a wide range of fibrotic genes. Hypermethylation of the Thy-1 and its subsequent silencing was observed in lung fibroblasts [Sanders et al. 2011]. More specifically, in IPF cells, fibrotic fibroblasts exhibited increased global DNA methylation [Huang et al. 2010]. Hypermethylation of CpG islands in the Fli-1 promoter region in pathological fibroblasts and skin biopsy specimens suggested that DNA methylation mediated fibrotic manifestations in SSc [Wang et al. 2006]. Hypermethylation of RASAL1 (which encodes an inhibitor of the Ras oncoprotein), mediated by DNMT1, perpetuated fibroblast activation and renal fibrogenesis [Bechtel et al. 2010]. The DNA-binding protein, methyl-CpG-binding protein 2 (MeCP2) was demonstrated to bind directly to the α-SMA gene through DNMTs and was shown to be essential for myofibroblast differentiation and pulmonary fibrosis [Hu et al. 2010, 2011]. In the mouse model of early-stage liver fibrosis, genome-wide analysis revealed reduced DNA methylation, resulting in inflammation and fibrogenesis [Komatsu et al. 2012].

2.6 The current landscape: Advances into anti-fibrotic therapy

The mechanisms of fibrosis, biosynthesis of collagen and its essential regulation points are well characterized, and many of the key mechanisms regulating fibrogenic growth factor pathways have been elucidated. Yet, the need for an effective anti-fibrotic agent remains unmet. Current

anti-fibrotic treatments (both at the commercial and academic level) target three mechanisms – profibrotic cytokines (mainly TGFβ1), inflammation and collagen output.

Firstly, anti-growth factors, such as small molecule inhibitors of the TGFβ1 receptor kinases, neutralizing antibodies that interfere with ligand-receptor interactions, antisense oligonucleotides reducing TGFβ1 expression, and soluble receptor ectodomains that sequester TGFβ1 have been developed to intervene against excessive TGFβ1 signaling activity. A number of drugs are currently in clinical studies with relatively poor efficacy and it is clear that further mechanistic studies are required to reveal how TGFβ1 mediates fibrotic responses in order to better target locally acting TGFβ1 [Lukas et al. 2011]. In the commercial setting, strategies such as anti-connective tissue growth factor (CTGF) developed by Fibrogen Inc. and the blocking of TGFβ1 receptors (Renovo) have yet to produce convincing results in clinical trials [Huber et al. 2010, Varga et al. 2008, Shah et al. 1994]. Despite being a notorious profibrotic factor, the important physiological functions that are reliant on TGFβ1 means that inhibiting its activity may potentially lead to aberrant immune activation and impaired wound healing.

Inflammation is a first-phase response of fibrogenesis and anti-inflammatory approaches have been developed to target fibrosis. To target inflammation, strategies based on reducing inflammation with corticosteroids and immunosuppressive drugs have been in clinical trials, but with mixed reviews [Sivakumar et al. 2008]. In liver fibrosis, the only form of reversible fibrosis, glucocorticoids such as prednisone and the immunosuppressant azathioprine led to the reversion of fibrosis [Dufour et al. 1997]. The COX-II (cyclooxygenase-II) inflammation inhibitor has been reported as having no effect in a study conducted with transgenic mice [Yu et al. 2008]. The pathogenesis of fibrosis cannot be completely explained by inflammation, and anti-inflammatory approaches have had minimal therapeutic value in attenuating fibrosis – possibly due to the fact that the inflammation may have substantially resolved by the time fibrosis is established.

The collagen biosynthesis pathway is another target for anti-fibrosis therapy. The selective endothelin-A antagonist Darusentan reduced collagen accumulation in rat secondary biliary fibrosis but had no effect on α-SMA expression [El Bialy et al. 2011]. Current trials also include the use of prolyl hydroxylase inhibitors [Tschank et al. 1987]. Clinical trials with inhibitors (such as FG-4539) by Fibrogen Inc. [Langsetmo et al. 2006, FibroGen et al. 2006 *press release*, Nwogu et al. 2001] and C-proteinase inhibitors (Pfizer) have yet to produce convincing clinical results [Turtle et al.2004].

A new dimension in gene regulation has emerged with the discovery of microRNAs (miRNAs) and small-interfering RNAs (siRNAs). siRNA interference with the TGFβ1 signaling pathway has been explored. Sato et al. has outlined the knockdown of specific components involved in collagen biosynthesis, such as the collagen-specific intraendoplasmic chaperone HSP47, using vitamin-A-coupled liposomes for siRNA delivery in rats [Sato et al. 2008]. The potential of miRNA-29c in the down-regulation of collagen deposition in TGFβ1-induced myofibroblasts has also been described [Chen et al. 2009], and it is generally recognized that miRNAs are a promising approach towards modulating cell behavior; a plethora of possibilities exist. To the best of my knowledge, there has been no reported clinical miRNA trial to date, and targeting miRNAs *in vivo* will almost certainly prove to be yet another major challenge.

Recently, a new class of epigenetic modulators known as HDAC inhibitors have recently been described to possess anti-fibrotic potential [Pang et al. 2010], and this will be discussed in the preceding text.

2.6.1 Classification of HDACi

HDACi represent a new group of small organic agents that are able to modulate HDAC activity. They are broadly divided into four categories based on structural identity: hydroxymates, cyclic

peptides, aliphatic acids and benzamides (Table 3) [Pang et al. 2010]. HDACi of interest, SAHA (marketed as Vorinostat or Zolinza™, Merck) is outlined in bold.
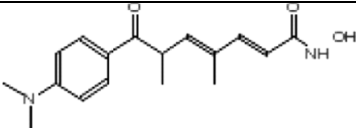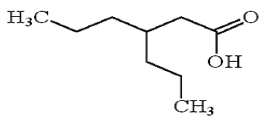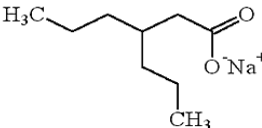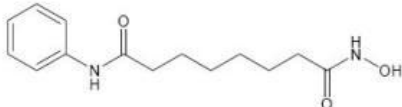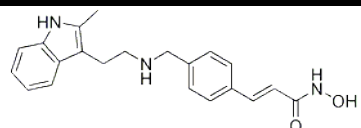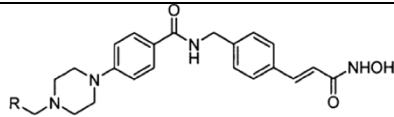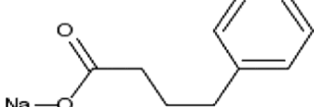
HDACi	Class Selectivity	Chemical structure	Reference
TSA	Class I/II HDACs		[Finnin et al. 1999]
Valproic acid	Class I HDACs		[Aiken et al. 2000]
Sodium valproate	Class I HDACs		[Aiken et al. 2000]
SAHA (Vorinostat)	**Class I/II HDACs**		**[Marks et al. 2009]**
LBH589 (Panobinostat)	Non-selective		[Atadja 2009]
SK-7041	Class I HDACs		[Pang et al. 2010]
Sodium 4-phenylbutyrate (4-PBA)	Non-selective		[Pang et al. 2010]

Table 3. Chemical structure of common HDACis. Modified from [Pang et al. 2010].

2.6.2 HDACi therapy in anti-fibrosis

Numerous investigations have been conducted to address the efficacy of HDACis for both anti-cancer therapy and neurodegenerative diseases. More recent work has described the emerging potential of HDACi in fibrosis.

Trichostatin A (TSA) is the most widely studied HDACi in both *in vitro* studies and *in vivo* models. In the skin, TSA downregulated TGFβ1-mediated α-SMA mRNA, protein expression and morphological change in cultured human skin fibroblasts [Glenisson et al. 2007]. In SSc fibroblasts, the inhibition of HDAC by TSA attenuated the expression of the ECM proteins collagen I and FN [Huber et al. 2007]. Another *in vivo* study demonstrated that TSA treatment prevented dermal accumulation of the ECM by silencing HDAC7 in the skin fibrosis mouse model [Hemmatazad et al. 2009]. Cystic fibrosis (CF) is an autosomal recessive genetic disorder caused by a mutation in the gene for the protein cystic fibrosis transmembrane conductance regulator (CFTR). Authors demonstrated that treatment with sodium 4-phenylbutyrate (4-PBA) corrected the deletion of phenylalanine-508 (responsible for the mutation of the CFTR gene) in primary cultures of CF patients [Hutt et al. 2011]. In addition, 4-PBA corrected cellular trafficking in CF epithelial cells [Rubenstein et al. 2000]. In the kidney, TSA decreased both the *in vitro* and *in vivo* activation and proliferation of renal interstitial fibroblasts, and reduced the expression of FN [Pang et al. 2009]. In renal tubulointerstitial injury, TSA and valproic acid (VPA) attenuated macrophage infiltration, colony stimulating factor-1 induction (a chemokine involved in macrophage infiltration) and profibrotic responses [Yoshikawa et al. 2009]. TSA also inhibited α-SMA expression, collagen type I and III synthesis in HSCs [Niki et al. 1999]. In the heart, both TSA and SK-7041 (a novel hybrid synthetic HDACi synthesized from TSA) blocked the development of cardiac hypertrophy, mediated by the anti-hypertrophic transcriptional regulator Krüppel-like factor 4 [Kee et al. 2006]. In pulmonary fibrosis, TSA prevented TGFβ1-mediated myofibroblast differentiation in normal human lung fibroblasts [Guo et al. 2009]. Lung fibroblasts from IPF patients show reduced COX-II expression; treatment with a combination of SAHA and Panobinostat (LBH589) was able to restore COX-II expression [Coward et al. 2009]. Lastly, our group has documented new evidence for the anti-fibrotic effects of SAHA [Wang et al. 2009].

History has dictated the precedence of HDACi therapy before the elucidation of its exact mechanism of action and HDACi are already clinically employed in certain disorders today. While the exact mechanisms are unclear, the involvement of epigenetic pathways has been proposed [Marks et al. 2009, Wanczyk et al. 2011, Nalabothula et al. 2011]. Taken together, the literature reports numerous investigations into the *in vitro* and *in vivo* potential of HDACi and they may prove to be effective and clinically useful anti-fibrotic agents.

2.7   SAHA: a potential epigenetic anti-fibrotic agent?

In an indication discovery approach, Wang et al. firstly described the anti-fibrotic effects of HDACi SAHA. When SAHA and TGFβ1 were added into cultures simultaneously, SAHA abrogated TGFβ1-effects in normal and pathological fibroblast lines by preventing the transition into myofibroblasts and normalized α-SMA expression and collagen deposition (Figure 9a, b). SAHA also inhibited serum-induced fibroblast proliferation and downregulated inflammatory cytokines [Wang et al. 2009]. However, SAHA was not able to attenuate or reduce α-SMA expression in fibroblasts exposed to TGFβ1 treatment 24h before SAHA treatment (i.e. myofibroblasts, Figure 9c, d).
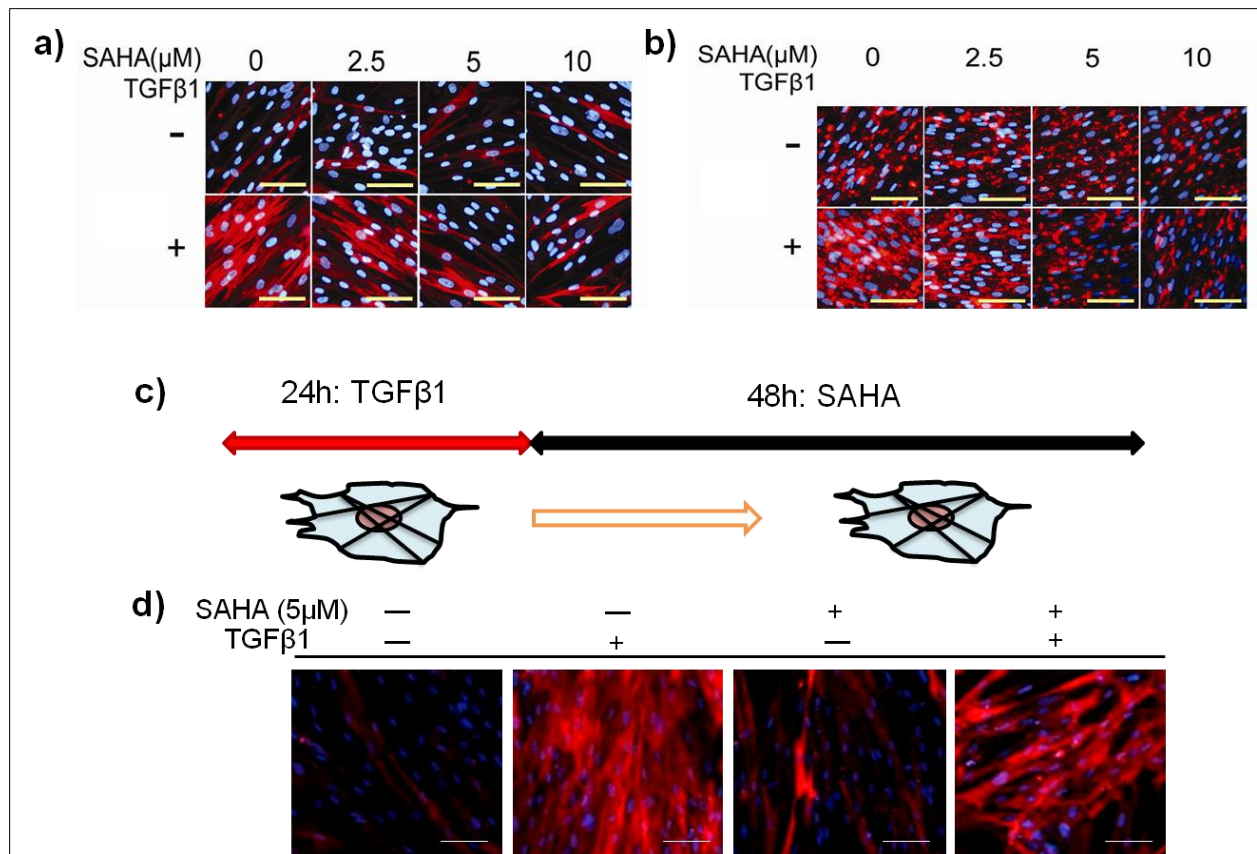
Figure 9. SAHA's emerging anti-fibrotic potential. SAHA abrogated TGFβ1-induced (a) α-SMA expression and (b) collagen I deposition in fibroblasts. SAHA was not able to attenuate TGFβ1-induced α-SMA expression in fibroblasts exposed to TGFβ1 24h before SAHA. Adapted from [Wang et al. 2009]. (c) Growth-arrested fibroblasts were treated with or without TGFβ1 for 24h prior to 48h SAHA treatment. (d) Representative ICC pictures (α-SMA, red; DAPI, blue) of the cell layer. Bars indicate 500µM. Data are represented from two independent studies in triplicates.

2.7.1   SAHA is cytotoxic and induces apoptosis in transformed cells

SAHA enhanced the cytotoxic effects of SN38 (topoisomerase I inhibitor) in glioblastoma cell lines [Sarcar et al. 2010], DAOY and PC3 tumour cells [Schmudde et al. 2008]. Independent studies also demonstrated SAHA's caspase-dependent apoptotic effects in T-cell lymphoma [Marks et al. 2009], breast cancer cells [Huang et al. 2000], Ewing's sarcoma [Sonnemann et al. 2007] and malignant pleural mesothelioma [Hurwitz et al. 2012]. Taken together, the literature suggests that SAHA is cytotoxic, and can induce apoptosis in transformed cells.

2.7.2 SAHA as a cytoskeletal modifier

SAHA hyperacetylated α-tubulin (Figure 10), a cytoskeletal component in fibroblasts [Wang et al. 2009]. This strongly suggested that HDAC6 (α-tubulin deacetylase), a microtubule-associated deacetylase was inhibited [Hubbert et al. 2002]. Independent studies have documented the compromised *in vitro* and *in vivo* stability of dynamic microtubules [Matsuyama et al. 2002], epithelial and fibroblast motility with HDAC6 inhibition [Lafarga et al. 2011, Tran et al. 2007].
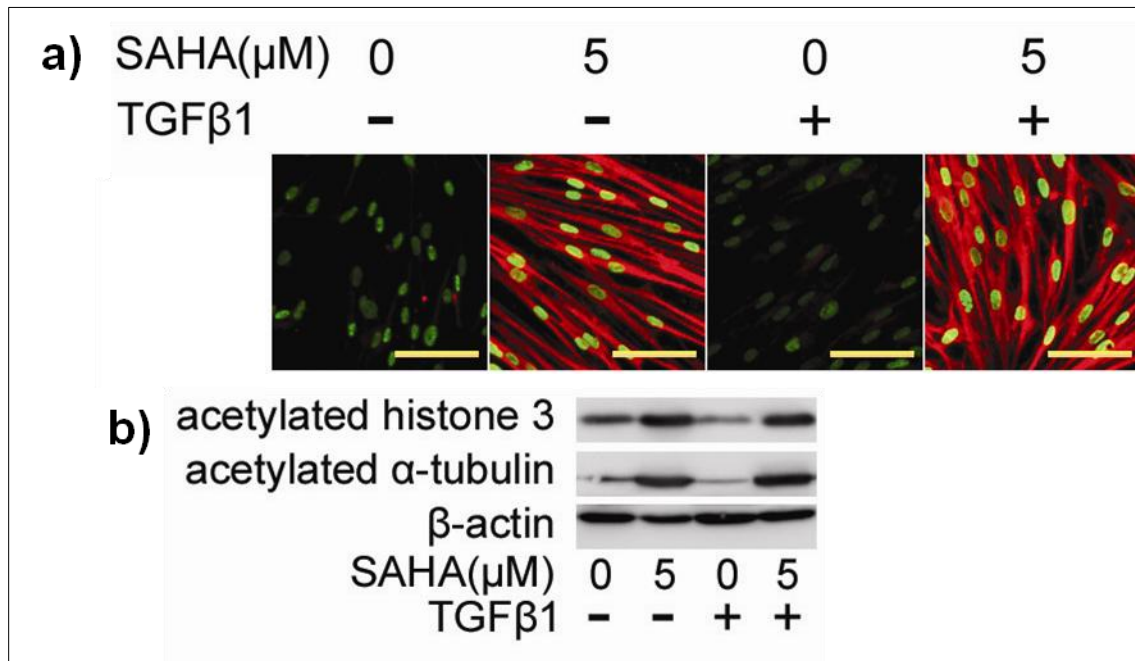
Figure 10. SAHA induced hyperacetylation of histone 3 and α-tubulin. Fibroblasts were treated with or without TGFβ1 and SAHA for 24h. Representative (a) ICC pictures (histone 3, green; α-tubulin, red) of cell layer. Bars indicate 50µM; (b) immunoblots of acetylated histone 3 and α-tubulin. Adapted from [Wang et al. 2009].

2.7.3 SAHA: Faster translation towards clinical therapy

The quest for an effective anti-fibrotic agent remains unfulfilled and the use of an FDA-approved drug currently in clinical use would shorten ethical and regulatory procedures, and significantly accelerate the time required to move into translational therapy. An FDA-approved drug means that: **1)** promising *in vitro* data can be moved into preclinical animals for good reason and **2)** *in vivo* data can lay the foundation for clinical studies in humans. Currently, HDACi are in clinical

use. For example, VPA (marketed as Depakote, Valparin and Stavzor by Pfizer, Abbott Laboratories and Noven Pharmaceuticals Inc. respectively) was approved as an anti-epileptic drug in 1967 in France and is employed as an anticonvulsant and mood-stabilising drug in the treatment of neuro-psychiatric and degenerative disorders [Perucca E 2002, Alvarez-Breckinridge 2012]. LBH589 is currently in clinical trials for the treatment of Hodgkin's Lymphoma, myelodysplatic syndromes and breast and prostate cancer [Revill et al. 2007]. Recently, SAHA (Vorinostat, marketed under the name Zolinza by Merck) [Marks et al. 2007] and romidepson (marketed as Istodax, FK228 by Celgene) [Hahnen et al. 2008], were FDA-approved in October 2006 and November 2009 respectively. Both drugs are currently in use for the treatment of refractory cutaneous T cell lymphoma.

Chapter 3

Materials and Methods

This chapter describes the materials and methods employed in the experiments outlined in this thesis.

3.1 Fibroblast cell culture

Normal human fetal lung fibroblasts WI-38 (CCL-75, ATCC, Manassas, VA, USA) were cultured in 10% fetal bovine serum (FBS) - Dulbecco's modified eagle's medium (DMEM) (GIBCO-Invitrogen, Grand Island, NY, USA) in 5% CO_2 at 37°C. The cells were sub-cultured using trypsin-EDTA (GIBCO-Invitrogen, Grand Island, NY, USA) at low passage (6-8). Fibroblasts were seeded at 5 x 10^4/well in 24-well plates or 1 x 10^5/well in 12-well plates in 10% FBS DMEM. Cells were seeded at 70% and 50% of the above mentioned density for days 7 and 14 analysis respectively. After 24h to allow for cell attachment in 10% FBS, the fibroblasts were growth-arrested using serum-free DMEM for 24h. Subsequently, they were treated with or without 5ng/ml of TGFβ1 (R&D Systems, Minneapolis, MN, USA) and 30 µg/ml L-ascorbic acid phosphate magnesium salt η-hydrate (Aca, Wako, Osaka, Japan) in serum-free DMEM (Figure 11). Thereafter, TGFβ1 treatment was removed and cultures washed twice with Hank's buffered salt solution (HBSS, GIBCO-Invitrogen, Grand Island, NY, USA). Cultures were maintained in 0.5% FBS DMEM and 30 µg/ml aca, with medium changes every 4 days. So as not to overlook any changes in gene and/or protein expression, the following end-points: days 1 (immediate), 7 (mid-term) and 14 (long-term) post-treatment were selected. *In vivo* TGFβ1

production tailed off towards day 14 [Yang et al. 1999], and this formed the basis of selecting

the last end-point at day 14.
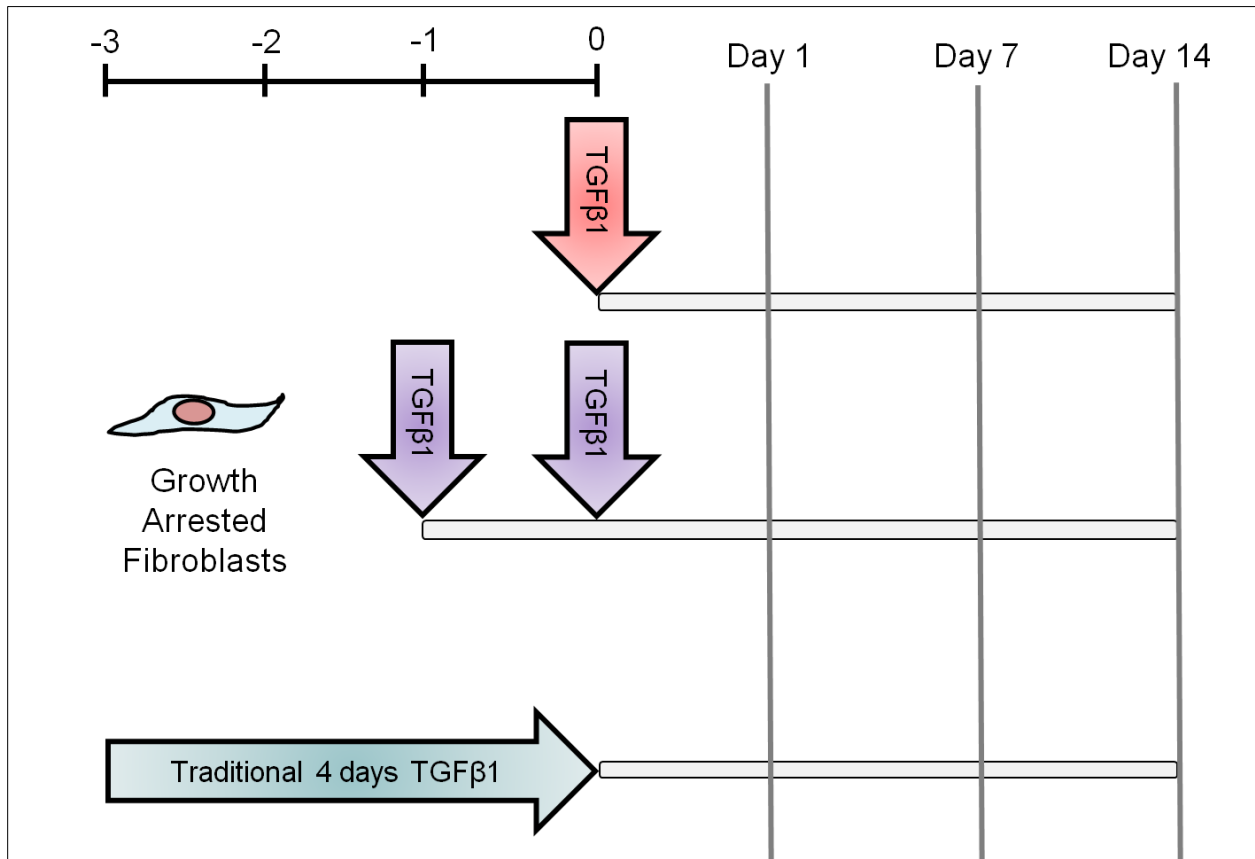
Figure 11. Cell culture setup of single (red) and double (purple) TGFβ1 pulse(s) on growth-arrested fibroblasts to simulate *in vivo* conditions. Currently, fibrosis *in vitro* studies employ TGFβ1 for 4 days (blue). Traditional 4 days TGFβ1 treatment was compared to pulsatile TGFβ1 treatment.

3.1.1 Myofibroblast generation

WI-38 fibroblast cells, pathological IPF fibroblasts (CCL-134, ATCC, Manassas, VA, USA) and

hypertrophic scar fibroblasts (HSF, gift from Prof. TT Phan, NUS Singapore) were cultured in 10%

FBS DMEM. To generate myofibroblasts, WI-38, IPF and HSF fibroblasts were treated with

5ng/ml TGFβ1 for 4 days and passaged using 1mg/ml dispase (Stemcell™ Technologies Inc.,

Vancouver, Canada).

3.1.2   SAHA treatment versus TGFβ1 pulse(s)

The kinetics of SAHA treatment versus TGFβ1 pulse(s) were evaluated using 3 independent models (Table 4). Fibroblast cultures were washed twice with HBSS following removal of SAHA or TGFβ1 and maintained in 0.5% FBS DMEM and aca till days 1 and 7 post-SAHA or TGFβ1 removal.

Model	SAHA (5µM) for 24h and/or 4h (single) or 2 x 4h (multiple) TGFβ1 pulse(s)	
SAHA pre-treat	Yes	No
SAHA post-treat	No	Yes
SAHA pre- & post-treatment	Yes	Yes

Table 4. Kinetics of SAHA treatment versus TGFβ1 pulse(s). SAHA pre-; post-; pre- and post-treatment in the TGFβ1 single (4h) and multiple (2 x 4h) pulse(s) model was evaluated.

3.2   *Sodium dodecylsulfate-polyacrylamide gel electrophoresis (SDS-PAGE)*

Serum-free DMEM in the last 24h of the culture period (Figure 12) was harvested and digested with 25µg/ml porcine gastrin mucosa pepsin (Roche, Basel, Switzerland). Collagen I deposition on the ECM was digested *in situ* with 250µg/ml porcine gastric muscosa pepsin. Extracts were digested in 0.1N HCl for 2h and neutralized with 1N NaOH. Extracts were then visualized under non-reducing conditions using 5% resolving/3% stacking SDS-PAGE gel electrophoresis as outlined in [Raghunath et al. 1994]. Protein bands were stained with the SilverQuest™ kit according to manufacturer's protocol (Invitrogen, Carlsbad, USA). Densitometric analysis of wet gels was performed on the collagen α1(I)-bands with the GS-800™ calibrated densitometer and analyzed by the Quantity One v4.5.2 image analysis software (Bio-rad, Hercules, CA).
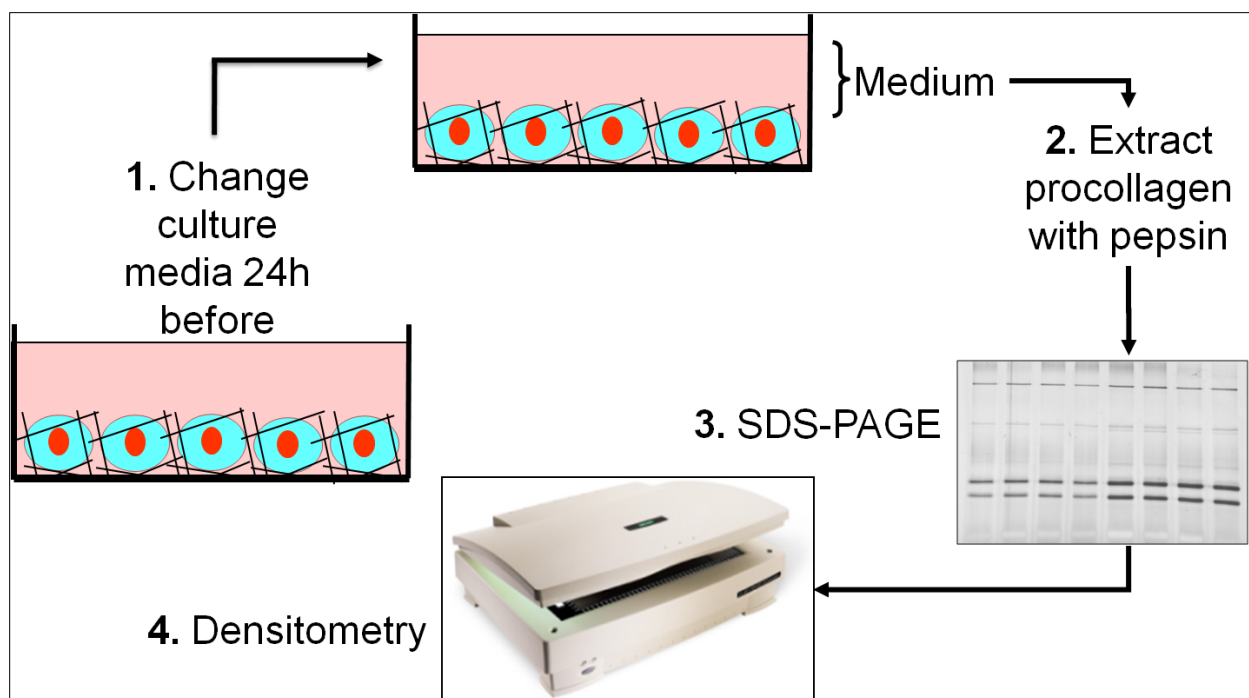
Figure 12. Biochemical analysis of collagen content. Serum free DMEM was used to assess the collagen content in culture media of the indicated follow up day, where the culture media was changed and harvested after 24h to analyse the collagen content. Samples were resolved using a 5%/3% SDS-PAGE electrophoresis.

3.3 Optical analysis: adherent cytometry

To normalize collagen I secretion rate, fibroblasts were stained with 4′, 6-diamidino-2-phenylindole (DAPI, Molecular Probes OR, USA) after absolute methanol fixation. Nine image sites covering 71% of the total well area were acquired at 2x magnification using a Nikon TE600 fluorescence microscope with an automated Ludl stage (BioPrecision 2, Ludl Electronic Products Ltd) and analyzed using the Metamorph® Imaging System software (Molecular Devices, Downingtown, PA) as described in [Chen et al. 2009]. A nucleus was defined as a fluorescent region with a length of 10 – 20μM and pixel intensity value of 10 units above background. Normalization was evaluated as collagen I output per nuclear counts in triplicate wells. All collagen I secretion rate data in this thesis is reported as collagen I secretion rate / cell.

3.4   *Immunoblotting*

Western blots were performed according to [Lareu et al. 2007]. Briefly, proteins were extracted from the cell layer with loading buffer comprising of 50mM Tris-HCl pH 6.8, 2% SDS, 0.1% bromophenol blue and 10% glycerol and protease inhibitor cocktail (Roche, Basel, Switzerland). Extracts were separated under non-reducing conditions on 12% resolving/3% stacking SDS-PAGE gel electrophoresis with 5mM DTT. Proteins were electroblotted onto a nitrocellulose membrane. Immuno-detection was carried out in Tris-buffered saline Tween-20 at pH 7.6 (50mM Tris-base, 150mM NaCl and 0.05% Tween 20). Membrane was blocked with 5% non-fat milk for 1h. Primary antibodies against α-SMA (1:500) and β-actin (1:1000) were from mouse (Sigma-Aldrich, St. Louis, MO) and incubated for 1.5h. Membrane was incubated for 1h with secondary antibody goat anti-mouse HRP (1:3000, Dako, Glostrup, Denmark). Membrane was washed with buffer 3 times after antibody incubation. Blots were developed with the Pierce Western blotting detection system (Pierce-Thermo Scientific, Rockford, IL, USA) and chemiluminescence signal captured with the VersaDoc Imaging System model 5000 and analysed with the Quantity One v4.5.2 image analysis software (Bio-Rad, Hercules, CA). α-SMA was detected using immunoblotting, and calibrated against β-actin within the same blot.

3.5   *Immunocytochemistry (ICC)*

Cell layers were washed with HBSS and fixed with methanol-free 3.7% formaldehyde (Pierce-Thermo Scientific, Rockford, IL, USA) at room temperature for 15mins. The cell membrane was permeabilized with 0.1% Triton X-100 for 3 mins. After washes with PBS, non-specific sites were blocked with 3% BSA for 1h followed by incubation with primary antibody, α-SMA (1:100, Dako, Glostrup, Denmark) for 1.5h. Secondary antibodies were goat anti-mouse AlexaFluor594 (1:400, Molecular Probes, OR, USA) and AlexaFluor488 phalloidin (1:100, Molecular Probes, OR, USA). To assess protein deposition on ECM, primary antibodies were against mouse anti-

collagen I (1:1000, Sigma-Aldrich, St. Louis, MO), rabbit anti-fibronectin (1:100, Dako, Glostrup, Denmark) and rabbit anti-LTBP-1 (1:200, gift from Dr. Carl-Henrik Heldin, Helsinki, Finland). Secondary antibodies were from goat anti-mouse AlexaFluor594, chicken anti-rabbit AF488, goat anti-rabbit AlexaFluor594 (1:400, Molecular Probes, OR, USA) and AF488 phalloidin. Cell nuclei were counterstained with DAPI. Images were acquired with an Olympus LX71 epifluorescence microscope (Olympus, Tokyo, Japan). All digital images were background subtracted based on conjugate control.

3.6 Quantitative molecular analysis: RNA extraction, Reverse Transcription – Polymerase Chain Reaction (RT-PCR)

Total RNA was isolated from cell extracts using Trizol® reagent (Invitrogen, Grand Island, NY) and the RNeasy mini kit (Qiagen, Valencia, CA). RNA concentration was determined using NanoDrop (NanoDrop Technologies, Wilmington, DE). 100ng of total RNA was reverse-transcribed using the SuperScript III reverse transcriptase (Invitrogen, Grand Island, NY) with oligo(dT) primers according to manufacturer's protocol. Real time PCR was carried out using 2µL of cDNA, 10µL of Maxima® SYBR Green/ROX qPCR Master Mix (Thermo Fisher Scientific, MA, USA) and 0.3µM of primers, in a reaction volume of 20µL. All reactions were performed on the real-time Mx3000P (Strategene, La Jolla, CA). The thermal cycling program for all PCRs was: 95°C for 15mins, followed by 40 cycles of amplifications, which consisted of a denaturating step at 94°C for 15s, an annealing step at 55°C for 30s, and an extension step at 72°C for 30s. Fibrogenic genes analyzed were α-SMA, FZD8, NOX4 and TSPAN2. Primers are listed in Table 5. The level of expression of the target genes, normalized to GAPDH was calculated using the $\Delta\Delta C_T$ formula and expressed as fold-change controls.

Gene	Primer sequence
GAPDH	Forward Primer: 5'- GTCCACTGGCGTCTTCACCA -3' Reverse Primer: 5'- GTGGCAGTGATGGCATGGAC -3'
α-SMA	Forward Primer: 5'- TTCAATGTCCCAGCCATGTA -3' Reverse Primer: 5'- GAAGGAATAGCCACGCTCAG -3'
FZD8	Forward Primer: 5'- AGACAGGCCAGATCGCTAACT -3' Reverse Primer: 5'- AAGCGCTCCATGTCGATAAG -3'
NOX4	Forward Primer: 5'- GGCCAGAGTATCACTACCTCC -3' Reverse Primer: 5'- GTTCGGCACATGGGTAAA -3'
TSPAN2	Forward Primer: 5'- TTCATGTGTGATCTGCGTGTT -3' Reverse Primer: 5'- TGGGAGCGAAATAGGTTGT-3'

Table 5. Primer sequences of selected fibrogenic genes for quantitative RT-PCR analysis. Primers were designed using the Oligo6.0 bioinformatics program.

3.7   TGFβ1 enzyme-linked immunosorbent assay (ELISA)

Cultures were treated with 4h and 2 x 4h TGFβ1 pulse(s) and the expression of TGFβ1 determined with a commercially available ELISA kit (Human TGFβ1 Quantikine ELISA Kit, R & D Systems). In accordance with the model, culture media was changed and harvested after 24h to analyse TGFβ1 content in the supernatant by sandwich ELISA according to specialized procedures as described in the manufacturer's protocol.

3.8   Epigenetic Assays

3.8.1   Acetylated-Histone 3 quantitation

Global acetyl-histone 3 (H3) was determined with a commercially available ELISA kit (PathScan Acetylated Histone 3 Sandwich ELISA kit, Cell Signaling Technologies). At the indicated endpoint, cell layers were lysed and histones extracted. Acetylated H3 levels were quantified according to specialized procedures as described in the manufacturer protocol.

3.8.2   MassARRAY: DNA extraction, Bisulfite Conversion – PCR, Spot-fire[1]

Genomic DNA was isolated from cell extracts using the DNeasy mini kit (Qiagen, Valencia, CA).,

and concentration determined using the NanoDrop (NanoDrop Technologies, Wilmington, DE).

DNA methylation was measured with the Sequenom MassARRAY Compact System [Coolen et

al. 2007].   Briefly, gene-specific amplification of bisulfite-treated DNA was followed by *in vitro*

transcription and subsequent analysis by ECM-assisted laser desorption ionization time-of-flight

(MALDI-TOF) mass spectrometry. Sequenom assay design and methods were according to

procedures outlined in the manufacturer's protocol. Briefly, 1µg DNA was bisulfite converted

using the EZ DNA Methylation kit (Zymo Research, Irvine, CA). PCR primers specific (Table 6)

for bisulfite converted DNA were designed using the UCSC Genome Browser [Kent et al. 2002]

and Methprimer [Li et al. 2002]. Each of the reverse primer's contains a T7-promoter tag for *in*

vitro transcription (5'-cagtaatacgactcactatagggagaaggct-3'), and the forward primer was tagged

with a 10mer to balance Tm (5'-aggaagagag-3'). Bisulfite-treated DNA was PCR amplified using

the HotStar Taq Polymerase (Qiagen, Valencia, CA) in 5µL reactions and treated with Shrimp

Alkaline Phosphatase (Sequenom, San Diego, CA) for 20 mins at 37°C and then at 85°C for

5mins. *In vitro* transcription/uracil-cleavage reaction was carried out in 7µL reactions using

Sequenom T-cleavage reagent mix. Transcription cleavage products were desalted with 6mg of

CLEAN-Resin and 20nL spotted on a 384-pad SpectroCHIP (Sequenom, San Diego, CA) using

a MassARRAY nanodispenser (Samsung, Seoul, South Korea). Mass spectra was acquired

using a MassARRAY MALDI-TOF MS (Bruker-Sequenom, San Diego, CA) and peak detection,

signal-to-noise calculations and quantitative CpG site methylation performed using proprietary

EpiTyper software v1.0 (Sequenom, San Diego, CA). Samples that failed to give reliable PCR

product or produced spectra with low confidence levels (<2.9 in EpiTyper) were excluded from

analysis. For fragments that contained a single CpG site, DNA methylation was calculated by

---

[1] Experiment was performed in collaboration with Dr. Allan Sheppard and Ms. Leticia Castro, Liggins Institute, University of Auckland, New Zealand.

the ratio of methylated to unmethylated fragments. Lower boundary limitations imposed by Sequenom analysis treat cleavage products containing multiple CpG sites as single units and methylation values reported were weighted averages across the unit (referred to as a CpG group). DNA quality and no-template controls, 0% and 100% methylated DNA was included in all assays.

Amplicon	Genomic Coordinates	Primer Sequence		CpG
ACTA2 (1)	chr10:90,750,1 87-90,750,540	Fwd	5'-TAGTTAGGGTTGGTTTTAGGGTGT-3'	19
		Rev	5'-CCTAAAATAAACATACCAACCACTACA-3'	
ACTA2 (2)	chr10:90,750,8 28-90,751,169	Fwd	5'-TTTGTTTTGAAGGTTGTAGGTTTTTT-3'	26
		Rev	5'-ACTATTAAAACCTTCCCTCAAACCC-3'	
COL1A1 (1)	chr17:48,278,6 03-48,278,899	Fwd	5'-AGTTTATATGTTTAGGGTTTAGATATGTT-3'	19
		Rev	5'-CCAAAATAAACTCCCTCCTATCTCA-3'	
COL1A1 (2)	chr17:48,278,8 60-48,279,232	Fwd	5'-AGTATTTTTGGTTTAGGTTGGG-3'	17
		Rev	5'-CACAAAACTAAACATATCTAAACCCT-3'	

Table 6. Amplicons, genomic coordinates, primer sequences and predicted CpGs sites covered for the extended promoter regions measured. PCR specific primers were designed using the UCSC Genome Browser and CpG sites predicted using the Methprimer algorithm.

3.9   *Decellularization of the TGFβ1-pulsed ECM*

Fibroblasts were pulsed with or without TGFβ1 and maintained for either 1 day (early ECM, M1) or 7 days post-pulse (late ECM, M7); end-points derived from TGFβ1 pulse(s) characterization. Monolayers were washed with PBS twice then treated with 0.5% DOC (Prodotti Chimici E Alimentari, S.P.A. 2003030085) and supplemented with 0.5x protease inhibitor cocktail in water for 15 mins on ice for a total of four times. This was followed by 0.5% DOC in PBS for 15 mins on ice with gentle agitation for a total of two times. ECM was then washed with PBS thrice and incubated with 0.5mg/ml DNAse (USBiological, Massachusetts, USA) for 1h at 37°C. ECM was washed with PBS thrice to remove residual detergent and DNAse activity before untreated fibroblasts were seeded onto the ECM (Figure 13).
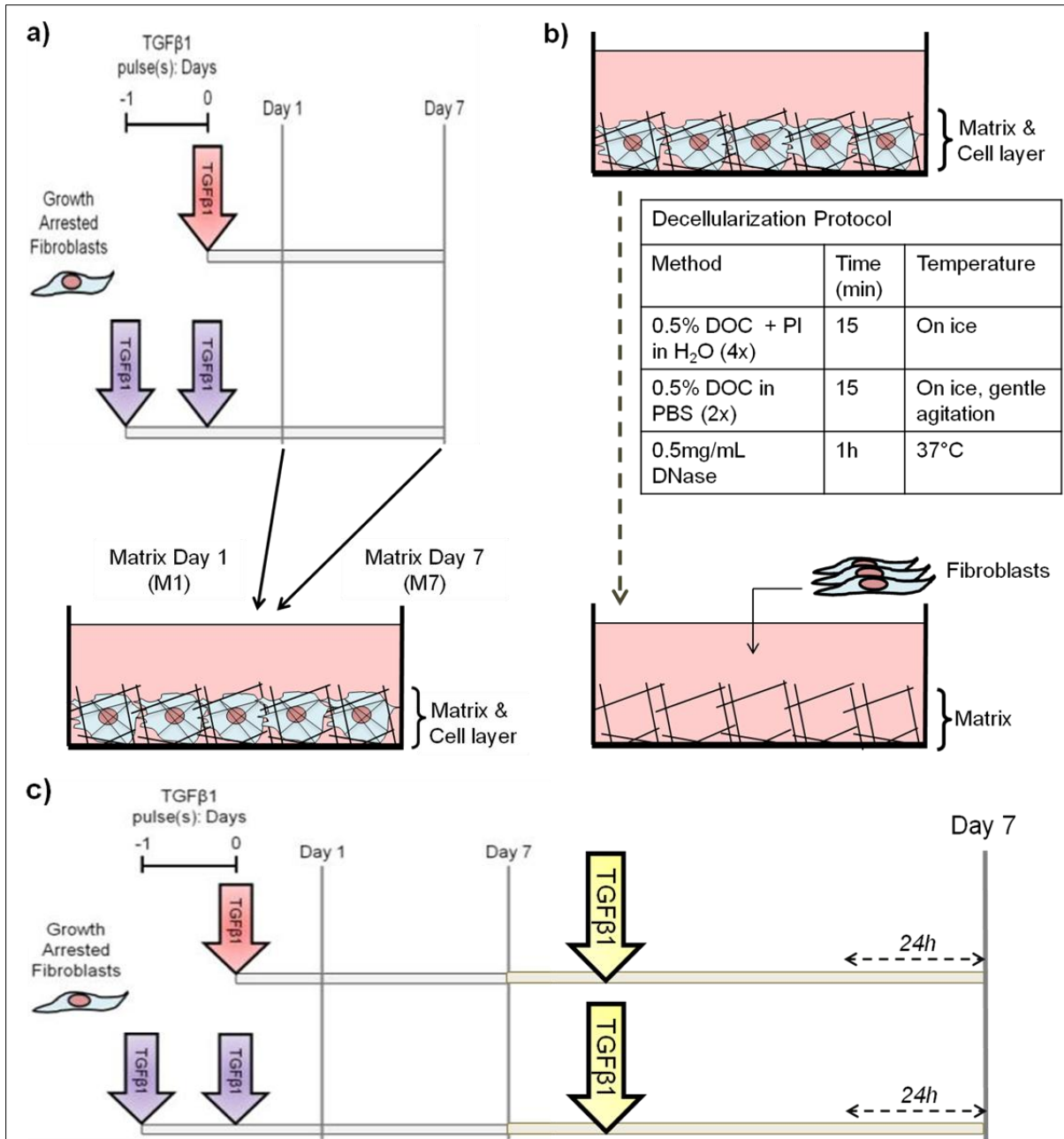
Figure 13. Decellularization of TGFβ1-pulsed ECM and overall cell culture setup. (a) ECM was lysed at 2 end-points: 1 day (M1, early ECM) and 7 days post-pulse (M7, late ECM); (b) schematic of lysis protocol denoting the lysis procedure. Untreated fibroblasts were seeded onto the decellularized ECM; and (c) treated with or without a 24h TGFβ1 pulse to analyse the ECM effects on myofibroblast induction and maintenance. Serum free DMEM in the last 24h of the culture period and α-SMA expression was used to assess myofibroblast differentiation.

3.10 Decellularization of MMC fibroblast ECM[2]

To generate the fibroblast ECM, fibroblasts were seeded at 5 x 10^4/ well in 24-well plates in 10% FBS DMEM. 24h later, media was replaced with 0.5% FBS DMEM and neutral crowder cocktail according to [Chen et al. 2009, Chen et al. 2011, Zeiger et al. 2012] in the presence of ascorbic acid for enhanced ECM deposition. Briefly, crowder cocktail comprised of 37.5mg/ml Ficoll (Fc) 70 and 25mg/ml Ficoll 400. After 6 days, the fibroblast ECM was washed with PBS twice, then treated with 0.5% DOC and supplemented with 0.5x protease inhibitor cocktail in water for 15 mins on ice for a total of four times. This was followed by 0.5% DOC in PBS for 15 mins with gentle agitation. ECM was washed with PBS thrice and incubated with 0.5mg/ml DNAse for 30 mins at 37°C. ECM was washed with PBS for three times to remove residual detergent and DNAse activity before myofibroblasts were seeded onto the decellularized ECM (Figure 14).

---

[2] Experiment (technical assistance) was performed by Mr. Sebastian Kress (Bayerische Julius-Maximilians-Universität, Würzburg, Germany under day-to-day supervision by Ariel Tan.
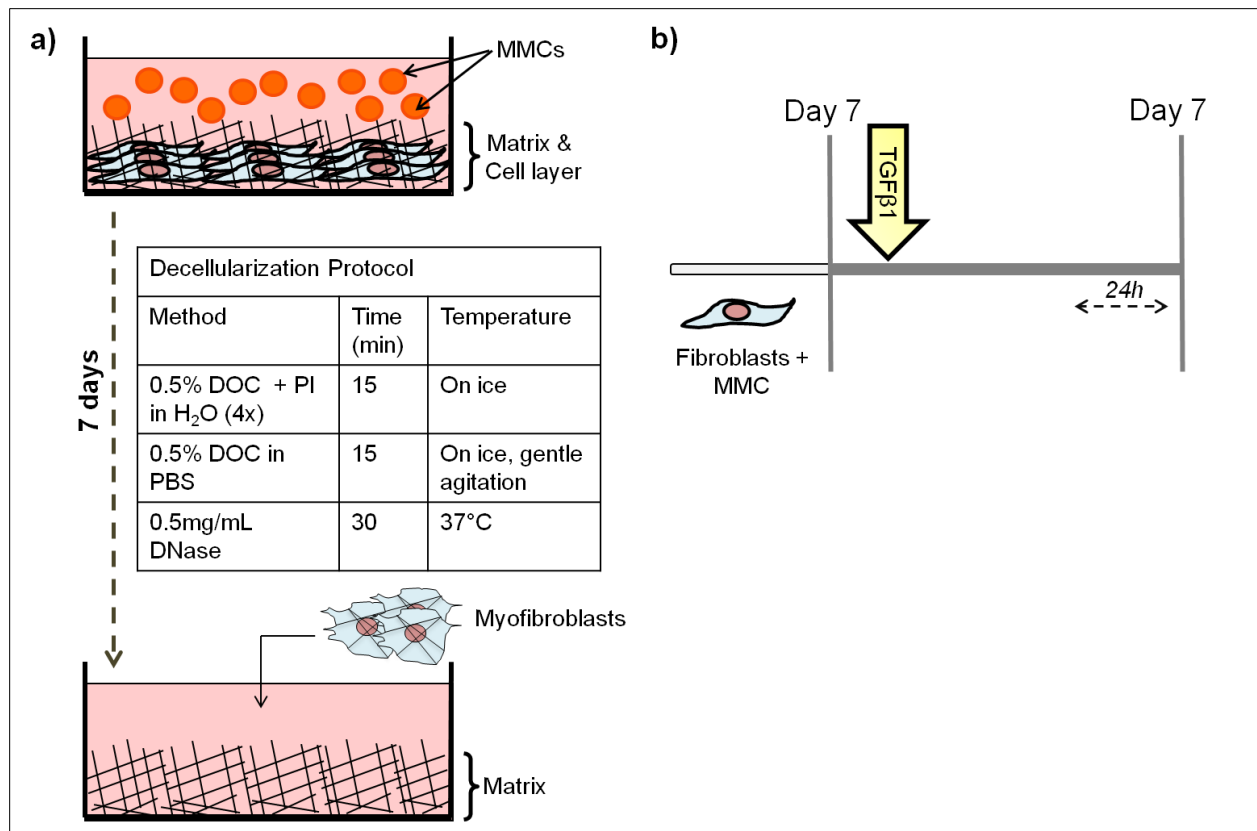
Figure 14. Decellularization of fibroblast ECM. (a) Schematic of lysis protocol denoting lysis steps. Myofibroblasts were seeded onto decellularized fibroblast ECM; (b) fibroblasts were treated with or without a 24h TGFβ1 pulse to analyse ECM effects on re-seeded myofibroblasts. Serum free DMEM in the last 24h of the culture period and α-SMA expression was used to assess the effects of the normal fibroblast ECM on the myofibroblast phenotype.

3.11 MTS Assay

Fibroblasts were treated with 4 days of TGFβ1 treatment to induce myofibroblast formation (Figure 11). Thereafter, TGFβ1 was removed and the myofibroblasts treated with SAHA (Alexis Biochemicals, Exeter, UK) at concentrations of 0, 1, 2.5, 5 and 10μM. Cell viability was determined using a commercially available colorimetric MTS (3-(4,5-dimethylthiazol-2-yl)-5-(3-carboxymethoxyphenyl)-2-(4-sulfophenyl)-2H-tetrazolium) CellTiter 96® AQueous One Solution Cell Proliferation Assay kit (Promega, Madison, Wisconsin, USA) at days 3 and 7 post-SAHA treatment.

3.12 Apoptosis and cytotoxicity analysis

SAHA-induced apoptosis and cytotoxicity was measured in fibroblasts and myofibroblasts. Growth-arrested fibroblasts were treated with and without TGFβ1 for 4 days (Figure 11). Thereafter, media was replaced with 5μM SAHA and cultures harvested and analysed at days 1, 2 and 4 post treatments. Apoptosis and cytotoxicity was determined using the commercial ApoTox-Glo™ assay (Promega, Madison, Wisconsin, USA) as indicated by the manufacturer protocol.

3.13 Mechanical and locomotion analysis[3]

3.13.1 Cell migration analysis

A wound healing assay was used to analyse cell migration. Commercial cell culture inserts of width 500μM ± 50μM (Ibidi GmBH, Martinsried, Germany) surrounded by two chambers were adhered in the center of uncoated 12-well plates (Figure 15). 70μL of fibroblast cell suspension was seeded/chamber and the remainder outside the chambers to a final density of 1 x 10^5/well. Cultures were maintained in 10% FBS DMEM to permit cell adhesion. After 24h, culture medium was removed and replaced with or without 5ng/ml of TGFβ1 in 0.5% FBS DMEM for 3 days as indicated by the manufacturers' protocol. Subsequently, culture inserts and cytokine containing medium was removed and replaced with or without 5μM of SAHA in 0.5% FBS DMEM. Wound closure was monitored at various time intervals until day 3 post-SAHA treatment. Images were acquired with an inverted Nikon Eclipse TS100 microscope (Nikon, Tokyo, Japan) and Nikon Digital Sight camera (Nikon, Tokyo, Japan). Cell migration into scratch area was quantitated using ImageJ analysis.

---

[3] Technical assistance was provided by Ms. Stella Chee. Experimental design and analysis of results was done by Ariel Tan.
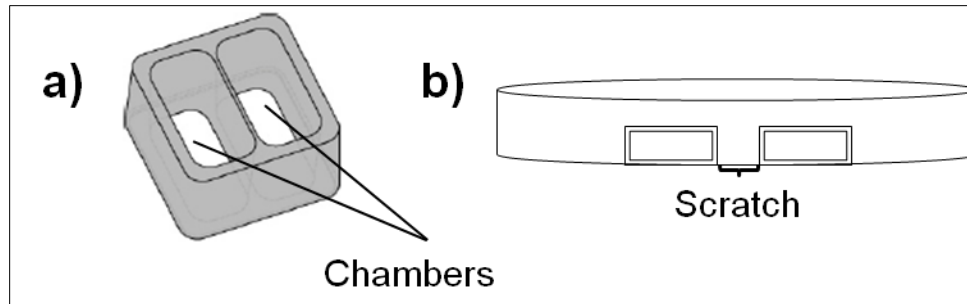
Figure 15. Cell culture inserts simulating an *in vitro* wound healing assay. (a) Schematic of Ibidi cell culture inserts; (b) 2D schematic of cell culture insert in culture plates. Fibroblasts are seeded in and out of the chambers and migration monitored by live cell imaging into scratch area at various time intervals.

3.13.2 Gel contraction analysis

SAHA-induced myofibroblast contractility was determined using the commercial gel contraction kit (Cell Bio Labs, San Diego, CA, USA) according to manufacturers' protocol. Briefly, fibroblasts were mixed in collagen I gels and treated with or without TGFβ1 in 0.5% FBS DMEM. After 48h required for stress to develop in the ECM, stressed gels were released (using a sterile spatula) and cytokine containing culture media replaced with or without 5μM of SAHA. Using a ruler, the contraction index (diameter of gel) was measured at various time intervals until 3 days post-SAHA treatment.

3.14 Statistical Analysis

Statistical analysis was performed using the GraphPad Software Inc. (San Diego, CA, USA). The statistical significance between groups was determined using the Student's t-test, two-tailed distribution with unequal variance. Probability values of $p<0.05$ (95% confidence interval) in comparison with controls were accepted as the level of statistical significance.

Chapter 4

Results

This chapter presents the results of the core findings of the project. An in vitro fibrosis model focusing on pulsatile TGFβ1 release is presented. SAHA's anti-fibrotic and cytoskeletal effects are presented.

4.1 Development of a physiologically relevant in vitro fibrosis model

Currently, no *in vitro* fibrosis model accurately depicts the physiological nature of TGFβ1 secretion *in vivo* and it is essential to develop an *in vitro* platform for wound healing and fibrosis. The aim of the platform is one that **a)** models *in vivo* pulsatile regulation of TGFβ1 as reported by [Yang et al. 1999]; and simulates **b)** physiological; and **c)** pathological wound healing. Classical myofibroblast markers α-SMA and F-actin expression, collagen I production and selected fibrogenic genes from a microarray on TGFβ1-treated fibroblasts were used to characterize the model.

4.1.1 Short-term analysis of TGFβ1 pulse showed no overt increase in α-SMA expression

To select pulse time-points and endpoints to investigate, it was important to understand the short-term kinetics of TGFβ1. Growth-arrested fibroblasts were exposed to a TGFβ1 pulse for selected time periods. Short-term analyses of a TGFβ1 pulse showed no overt increase in α-SMA expression immediately after a pulse. However, after 16h, a slight increase in α-SMA expression was observed (Figure 16). Results suggested that cells required more than 16h to

differentiate and upregulate the synthesis of the α-SMA protein. Therefore, short-term analysis after a TGFβ1-pulse was insufficient for an *in vitro* screening platform.
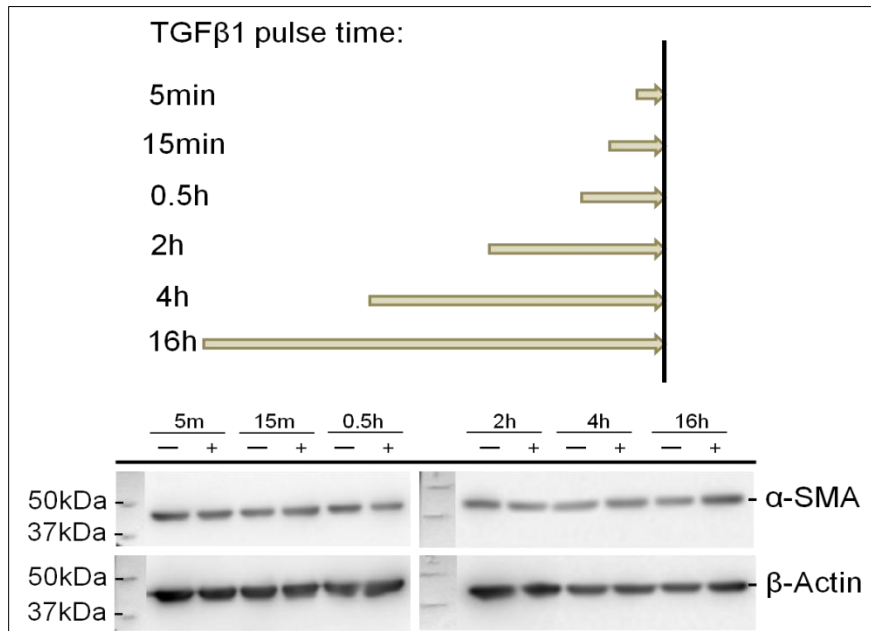
Figure 16. Short-term analysis of α-SMA expression immediately after TGFβ1 pulse showed no overt increase in α-SMA expression. After the pulse, cytokine containing medium was withdrawn, cell cultures washed and analyzed thereafter. This figure illustrates the raw data. For all other results, both raw and densitometric data are shown.

4.1.2   4 days TGFβ1 treatment lasts for 14 days

Fibroblasts are traditionally exposed to 4 days of TGFβ1 treatment to generate myofibroblasts [Hinz et al. 2001]. We therefore, assessed the effects of 4 days TGFβ1 treatment on the creation and maintenance of the myofibroblast phenotype (Figure 11) and established that classical myofibroblast markers remained elevated 14 days post-pulse (Figure 17).

59
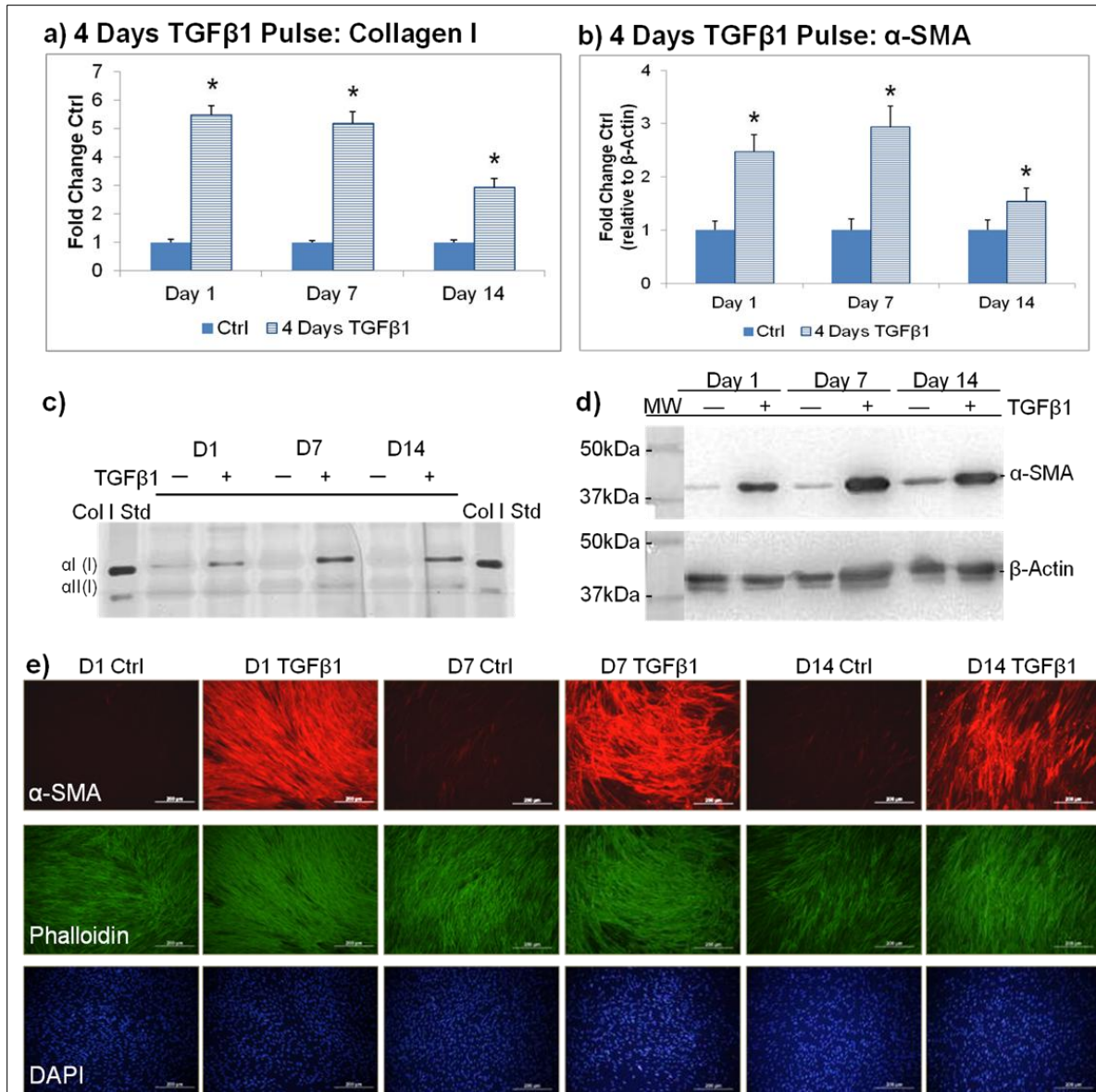
Figure 17. 4 days of TGFβ1 treatment had long-lasting effects. (a) Normalized densitometric SDS-PAGE analysis of the 24h collagen secretion rate by induced fibroblasts; (b) densitometric analysis of α-SMA was normalized to β-actin expression; (c) representative SDS-PAGE; (d) representative immunoblots at days 1, 7 and 14 post-treatment and (e) representative ICC pictures (α-SMA, red; phalloidin, green; DAPI, blue) of cell layer. Bars indicate 500μM. *$p < 0.05$ versus respective untreated controls. Data are represented as mean ± S.D, calculated from three independent studies in triplicates, and expressed as -fold changes over respective controls.

4.1.3 A 0.5h TGFβ1 pulse lasted for up to 7 days

We proceeded to investigating the effects of a single TGFβ1 pulse on the creation and maintenance of the myofibroblast phenotype. Here, we demonstrated that a single TGFβ1 pulse,

as short as 0.5h, induced myofibroblast phenotype maintenance as indicated by increased expression of α-SMA and collagen I production, for up to 7 days post-pulse (Figure 18). Collagen I production and α-SMA expression was reversed to baseline level 14 days later.
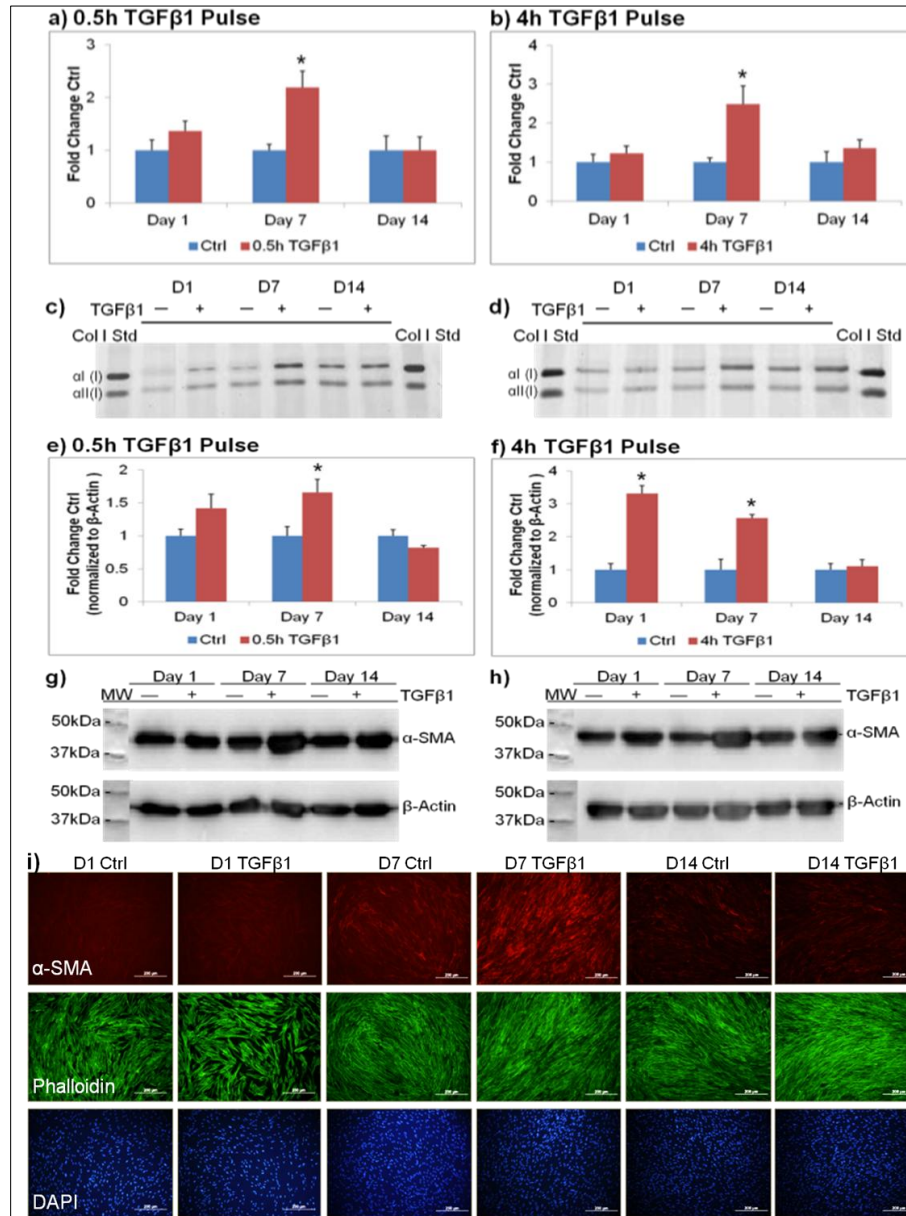
Figure 18. A single pulse of TGFβ1 had long-lasting effects. Normalized densitometric SDS-PAGE analysis of the 24h collagen secretion rate by induced fibroblasts after (a) 0.5h, (b) 4h TGFβ1 pulse; (c – d) representative SDS-PAGE of the 0.5h and 4h pulse respectively. Densitometric analysis of α-SMA was normalized to β-actin expression for the (e) 0.5h, (f) 4h TGFβ1 pulse; (g – h) representative immunoblots of 0.5h and 4h pulse respectively and (i) representative ICC pictures (α-SMA, red; phalloidin, green; DAPI, blue) from the 4h TGFβ1-pulsed cell layers. Bars indicate 500µM. *$p < 0.05$ versus respective untreated controls. Data are represented as mean ± S.D, calculated from three independent studies in triplicates, and expressed as -fold changes over respective controls.

To better characterize the single pulse model, I selected other fibrotic genes pertaining to the TGFβ1 signaling pathway or collagen regulation. mRNA levels of α-SMA (ACTA2), FZD, NOX4 and TSPAN2 were found to be elevated 24h post-TGFβ1 pulse (Figure 19).
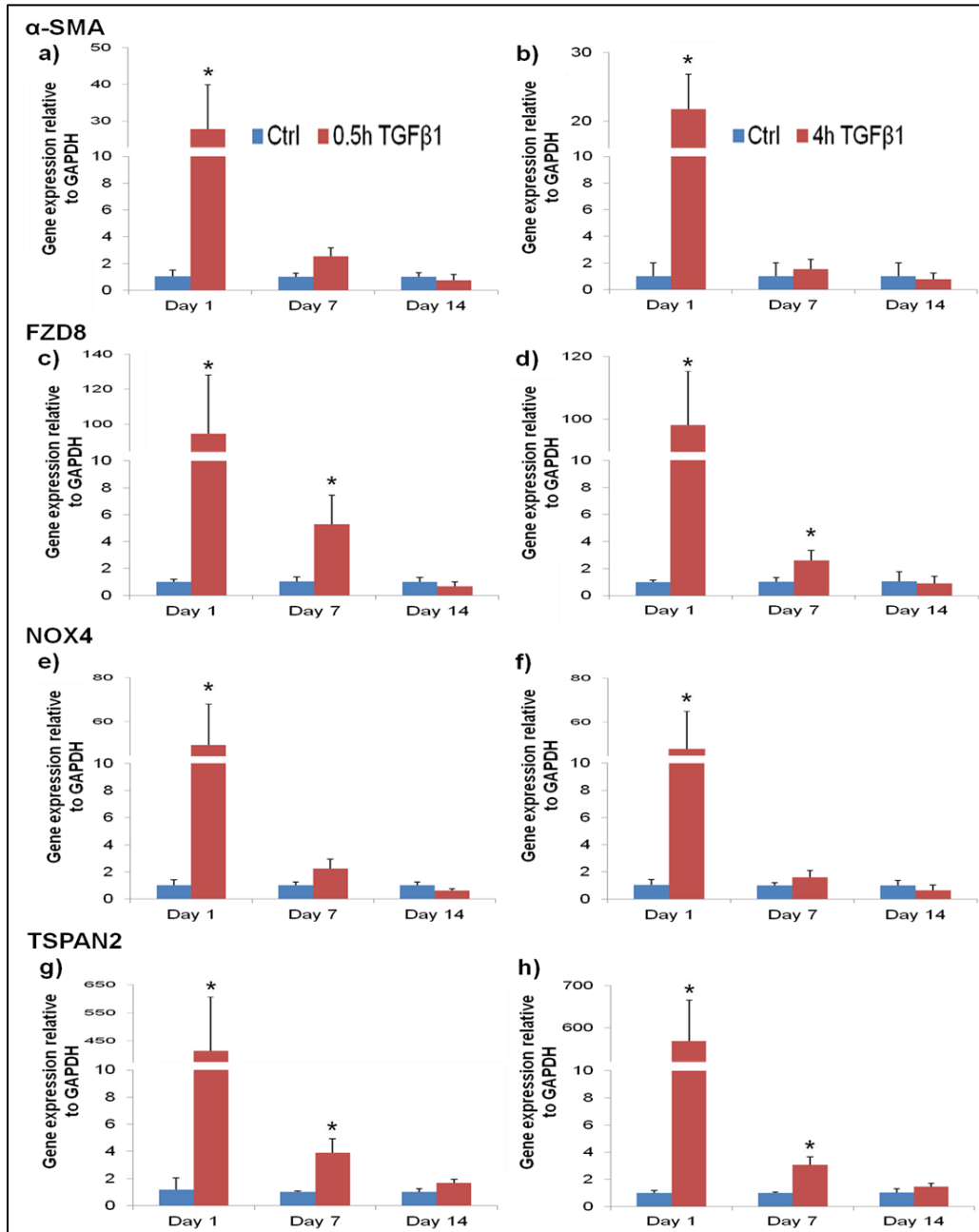
Figure 19. Selected fibrogenic genes were markedly increased 24h post-pulse. mRNA expression of α-SMA: (a) 0.5h, (b) 4h; FZD8: (c) 0.5h, (d) 4h; NOX4: (e) 0.5h, (f) 4h; and TSPAN2: (g) 0.5h, (h) 4h TGFβ1 pulse. With the exception of FZD8 and TSPAN2, mRNA expressions of the aforementioned fibrotic genes were at baseline levels at days 7 and 14. *$p < 0.05$ versus respective untreated controls. Data are represented as mean ± S.D, calculated from three independent studies in triplicates, and expressed as -fold changes over respective controls.

4.1.4 Multiple pulses potentiated effects

Further, we investigated the effects of an additional TGFβ1 pulse and demonstrated that an additional TGFβ1 pulse, administered 24h later, potentiated the myofibroblast phenotype maintenance as observed from persistent increased collagen I production and α-SMA expression up to 14 days post-pulse (Figure 20).
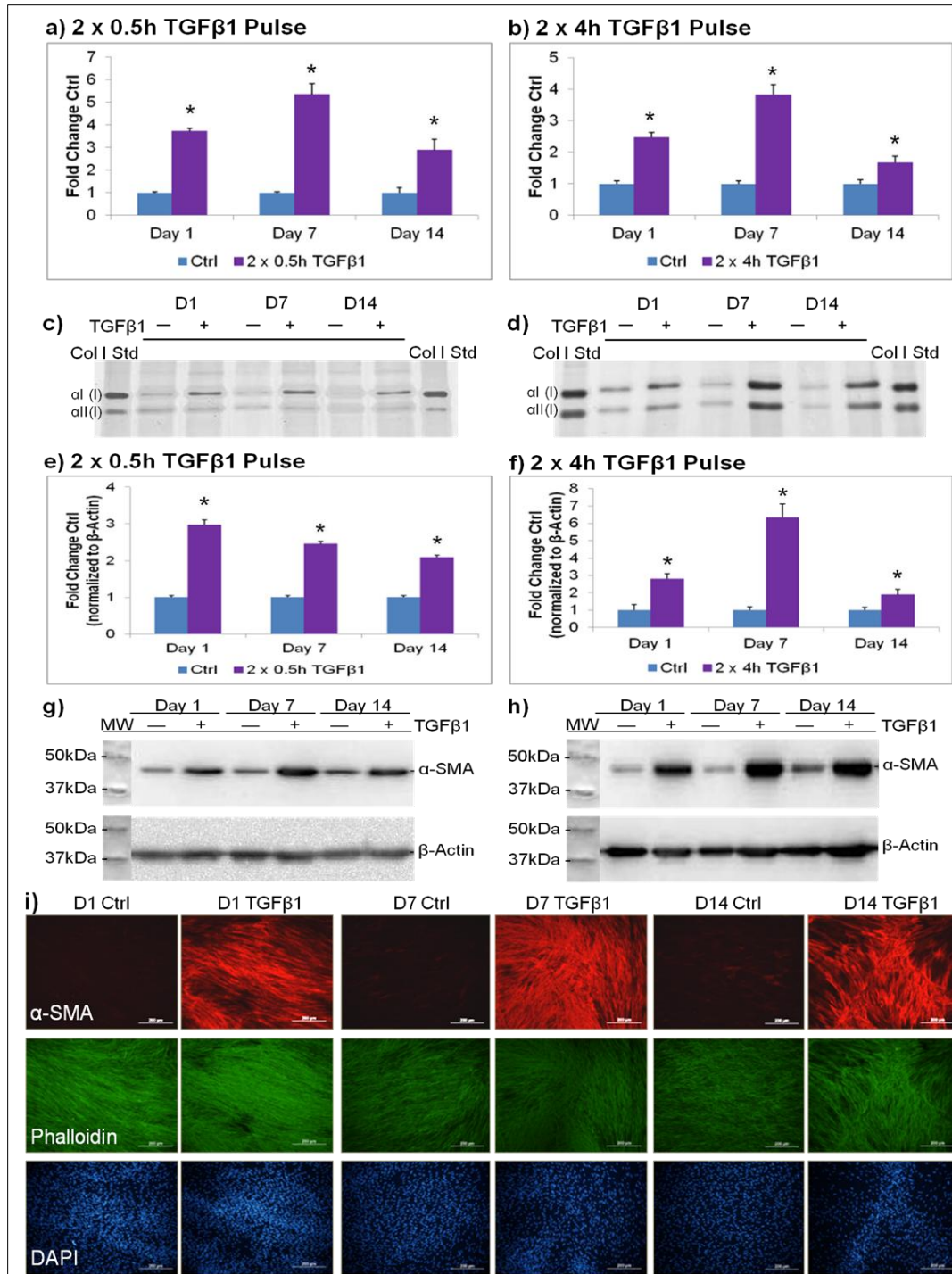
Figure 20. Multiple pulses of TGFβ1 potentiated effects. Normalized densitometric SDS-PAGE analysis of the 24h collagen secretion rate by induced fibroblasts after (a) 2 x 0.5h, (b) 2 x 4h TGFβ1 pulses; (c – d) representative SDS-PAGE of 2 x 0.5h and 2 x 4h pulses respectively. Densitometric analysis of α-SMA was normalized to β-actin expression for the (e) 2 x 0.5h, (f) 2 x 4h TGFβ1 pulses; (g – h) representative immunoblots of 2 x 0.5h and 2 x 4h pulses respectively and (i) representative ICC pictures (α-SMA, red; phalloidin, green; DAPI, blue) of the 2 x 4h TGFβ1-pulsed cell layers. Bars indicate 500μM. *$p < 0.05$ versus respective untreated controls. Data are represented as mean ± S.D, calculated from three independent studies in triplicates, and expressed as -fold changes over respective controls.

64

mRNA expression of selected fibrogenic genes were quantified and established to be elevated up to 7 days post-TGFβ1 pulses (Figure 21).
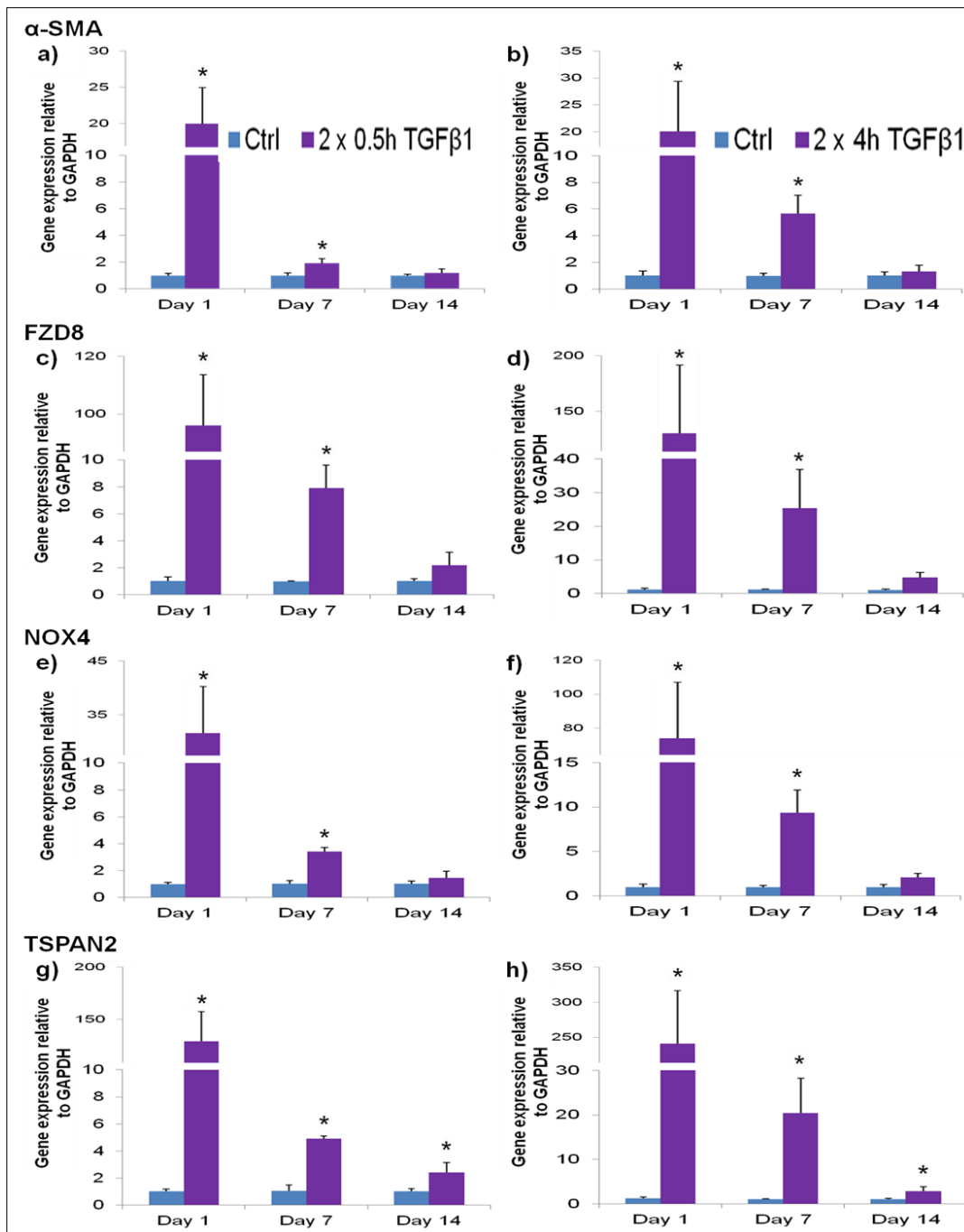
Figure 21. Selected fibrogenic genes were increased for up to 7 days post TGFβ1-pulses. mRNA expression of α-SMA: (a) 2 x 0.5h, (b) 2 x 4h; FZD8: (c) 2 x 0.5h, (d) 2 x 4h; NOX4: (e) 2 x 0.5h, (f) 2 x 4h; and TSPAN2: (g) 2 x 0.5h, (h) 2 x 4h TGFβ1 pulses. With the exception of TSPAN2, mRNA expressions of the aforementioned fibrotic genes were at baseline levels at days 7 and 14. *$p < 0.05$ versus respective untreated controls. Data are represented as mean ± S.D, calculated from three independent studies in triplicates, and expressed as -fold changes over respective controls.

4.2 Investigating the memorized effects of TGFβ1 pulses

The previous results suggests the establishment of a stable phenotype after TGFβ1 pulses and allows for further exploration of the mechanistic effects underlying the model. Fibroblast – myofibroblast differentiation is complex and highly regulated but understanding the mechanism will allow precise targeting for future anti-fibrotic therapies. Here, we focus on the 4h and 2 x 4h pulses to investigate: 1) autocrine TGFβ1 production; 2) epigenetic effects and 3) cell – ECM interactions based on the notion of matrix reciprocity.

4.2.1 Single TGFβ1 pulses triggered sustained autocrine TGFβ1 production

Cell layers were washed extensively with HBSS to remove recombinant TGFβ1. However, substantial levels of endogenously produced of active TGFβ1 levels were detectable in culture media 24h post-pulse and had reverted to baseline at days 7 and 14 (Figure 22a – b). In contrast, we observed an increased amount of latent TGFβ1 levels at all assessed timepoints as revealed when latent TGFβ1 in the samples were (Figure 22c – d).
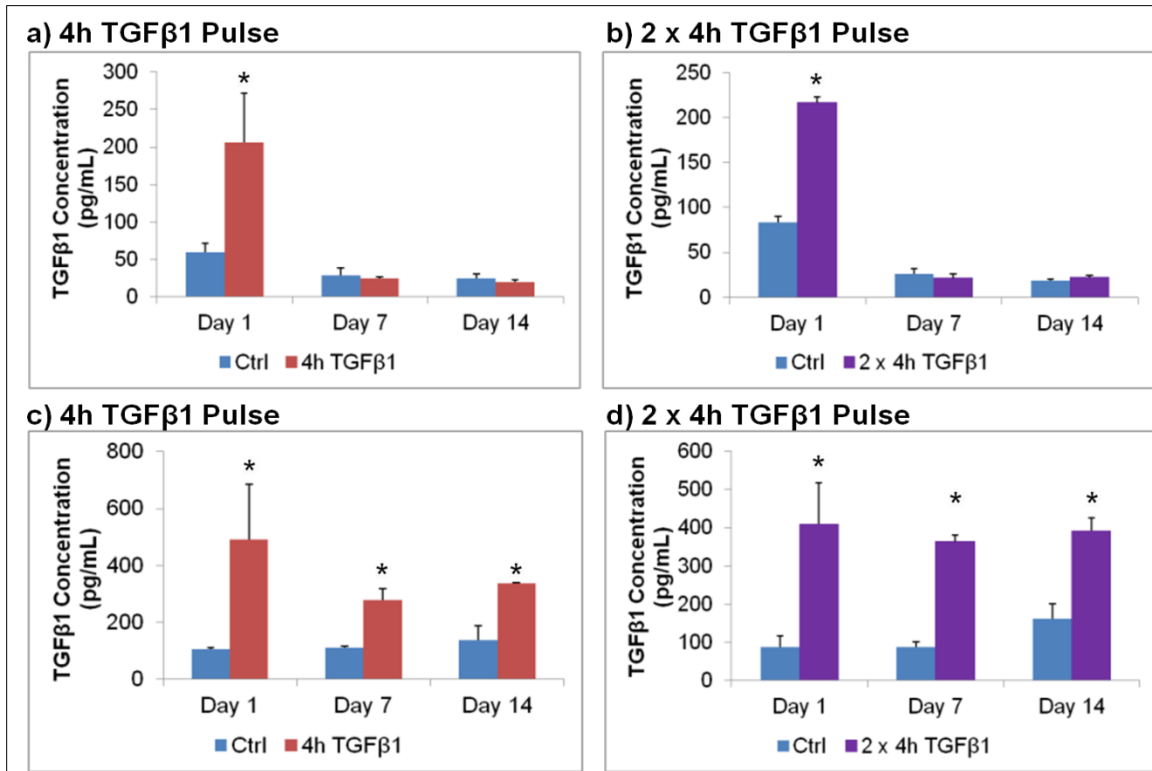
Figure 22. TGFβ1 pulse(s) induced elevated active and latent TGFβ1 secretion in fibroblasts. Circulating active TGFβ1 was elevated 24h post-pulse in the (a) 4h; and (b) 2 x 4h TGFβ1-pulsed fibroblasts. Acid treatment activated latent TGFβ1 storage and resulted in elevated expressions of TGFβ1 levels at all assessed end-points in the (c) 4h; and (d) 2 x 4h model. *$p < 0.05$ versus respective untreated controls. Data are represented as mean ± S.D, calculated from four independent studies in triplicates, and expressed as -fold changes over respective controls.

4.2.2 No apparent evidence for epigenetic modifications in selected fibrosis-related genes after TGFβ1 pulsing

SAHA hyperacetylated histone-3 [Wang et al. 2009] leading to the speculation that acetylation changes mediated gene transcription after TGFβ1 treatment. However, we demonstrated that a single 4h TGFβ1 pulse did not affect global H3 acetylation levels when cultures were analysed immediately after SAHA treatment and 24h post-SAHA treatment. HDACi SAHA was used as a positive control in this assay (Figure 23).
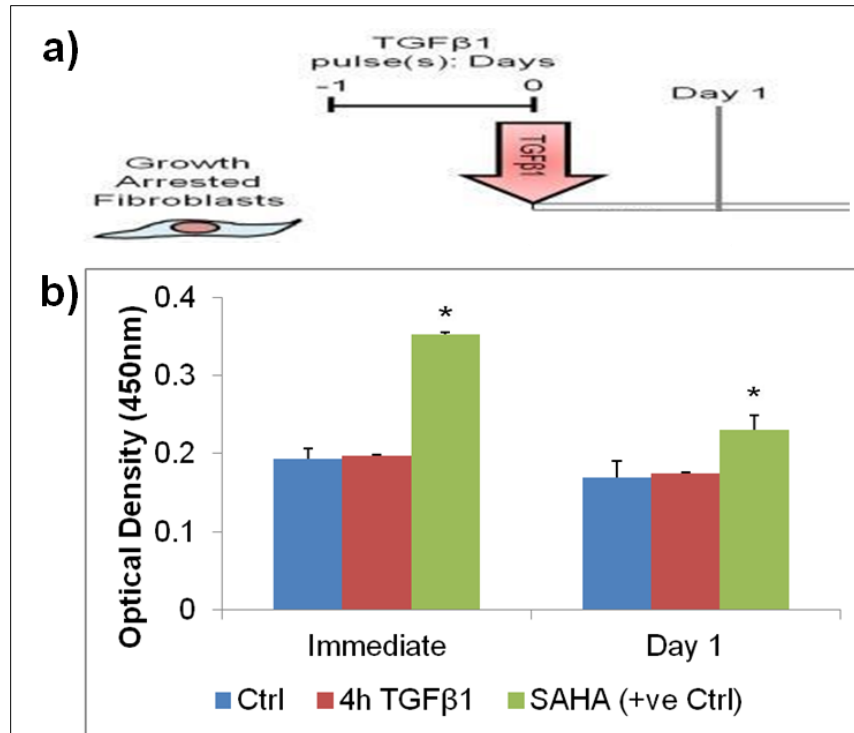
Figure 23. H3 acetylation levels remain unchanged after a TGFβ1 pulse. Acetylation levels in TGFβ1-pulsed fibroblasts were analyzed immediately and 1 day post-pulse. SAHA (HDACi) was used as the positive control in this assay. *$p < 0.05$ versus respective untreated controls. Data are represented as mean ± S.D, calculated from two independent studies in triplicates, and expressed as optical density 450nm.

We proceeded onto investigating DNA methylation changes and assessed the DNA methylation profiles in the proximal promoter regions of the ACTA2 and COL1A1 genes after TGFβ1 pulse(s). DNA methylation levels in these two genes were established to be unaffected by TGFβ1 pulse(s) (Table 7).

Amplicon	Targeted CpG's	4h TGFβ1 pulse			2 x 4h TGFβ1 pulse		
		Day 1	Day 7	Day 14	Day 1	Day 7	Day 14
ACTA2 (1)	19	=	=	=	=	=	=
ACTA2 (2)	26	=	=	=	=	=	=
COL1A1 (1)	19	=	=	=	=	=	=
COL1A1 (2)	17	=	=	=	=	=	=

Table 7. ACTA2 and COL1A1 were not regulated by DNA methylation changes in response to TGFβ1 pulse(s). Changes in methylation levels > 10% were considered significant. ACTA2 and COL1A1 genes express low methylation levels and displayed no overt changes with TGFβ1 pulse(s).

4.2.3   Trypsin-EDTA passaging attenuated the myofibroblast phenotype

If the memory was due to cell intrinsic factors, the myofibroblast phenotype should be propagated over passages. We therefore, investigated if the phenotype was maintained after trypsin-EDTA passaging and established the attenuation of the myofibroblasts phenotype after 4 days to TGFβ1 treatment to generate myofibroblasts (Figure 24). These results indicate that the memorized effects after TGFβ1 pulses were not due an intrinsic change in the cell, but likely dependent on the microenvironment of the cell. We therefore proceeded to investigate the phenotypic influence of TGFβ1-pulsed ECM on myofibroblast induction and maintenance.
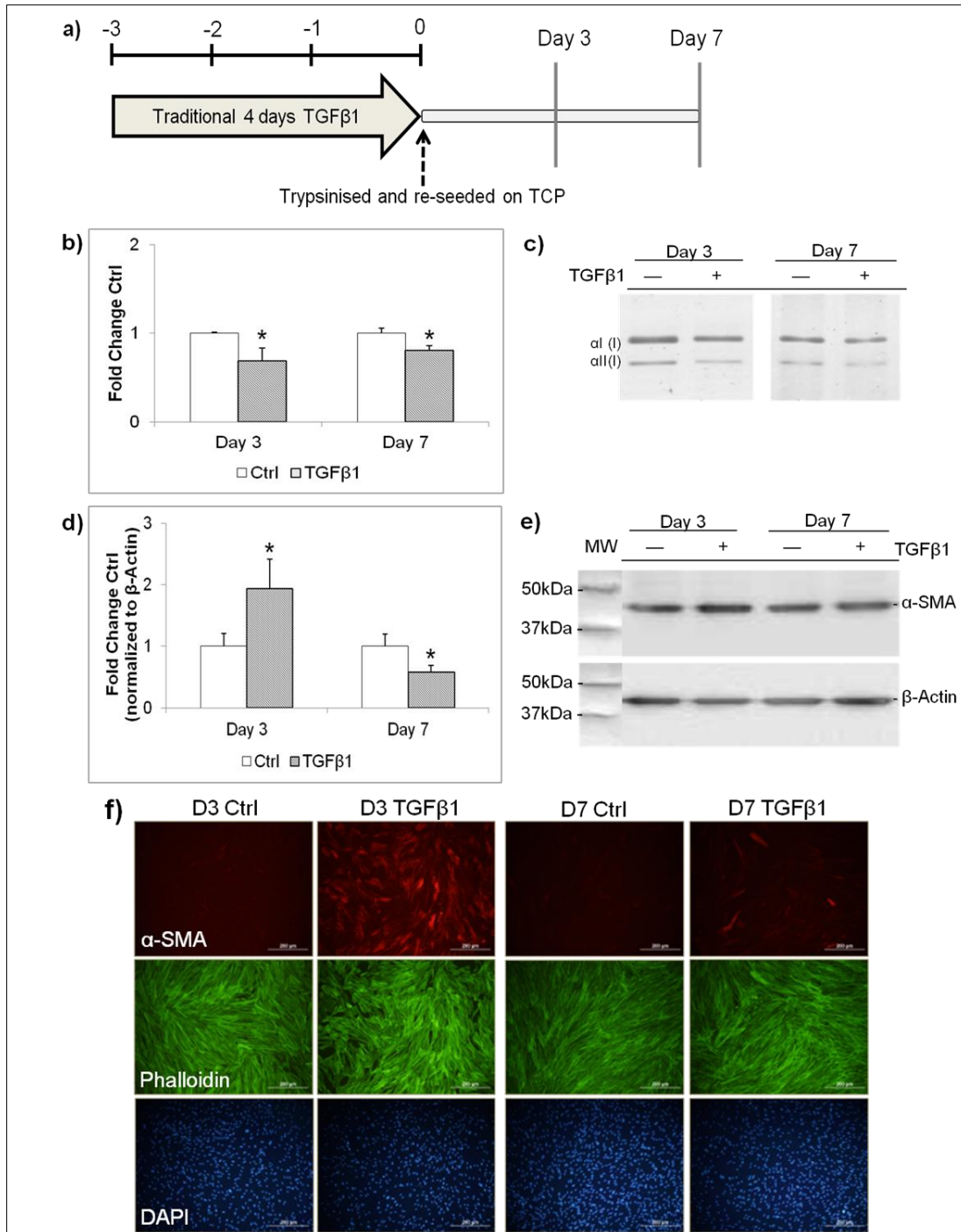
Figure 24. Trypsin-EDTA passaging attenuated the myofibroblast phenotype. (a) Cell culture setup of TGFβ1 treated myofibroblasts and subsequent sub-culture. Briefly, cells were treated with and without TGFβ1 for 4 days (benchmark for myofibroblast culture) and subsequently trypsin-EDTA passaged and re-plated onto TCP. (b) Normalized densitometric SDS-PAGE analysis of the 24h collagen secretion rate by induced fibroblasts; (c) representative SDS-PAGE; (d) densitometric analysis of α-SMA normalized to β-actin expression; (e) representative immunoblots and (f) ICC pictures (α-SMA, red; phalloidin, green; DAPI, blue) of sub-cultured myofibroblasts. Bars indicate 500μM. *$p < 0.05$ versus respective untreated controls. Data are represented as mean ± S.D, calculated from three independent studies in triplicates, and expressed as -fold changes over respective controls.

4.2.4   ECM generated under TGFβ1-pulses induced the myofibroblast phenotype

To investigate the phenotypic influence of ECM-mediated (produced after TGFβ1-pulses) myofibroblast induction, fibroblasts were pulsed with or without TGFβ1 for 4h and 2 x 4h and then removed by detergent treatment. The resulting decellularised ECM (Figure 25) was re-seeded with previously untreated fibroblasts. We observed that particularly doubly TGFβ1-pulsed matrices were able to induce a myofibroblastic phenotype (Figure 26). Furthermore, myofibroblast-inducing properties were strongest in matrices decellularised 1 day post-pulse and were slightly diminished (only α-SMA expression increased, Figure 26a, d, g) in matrices 7 days after decellularisation. We proceeded onto identifying a protein which may be responsible for myofibroblast induction in the untreated fibroblasts, and speculated that the induction of phenotype was attributed to latent TGFβ1 storage on the ECM. Here, we demonstrated elevated LTBP-1 expression on the M1, but not on the M7 ECM (Figure 27a).
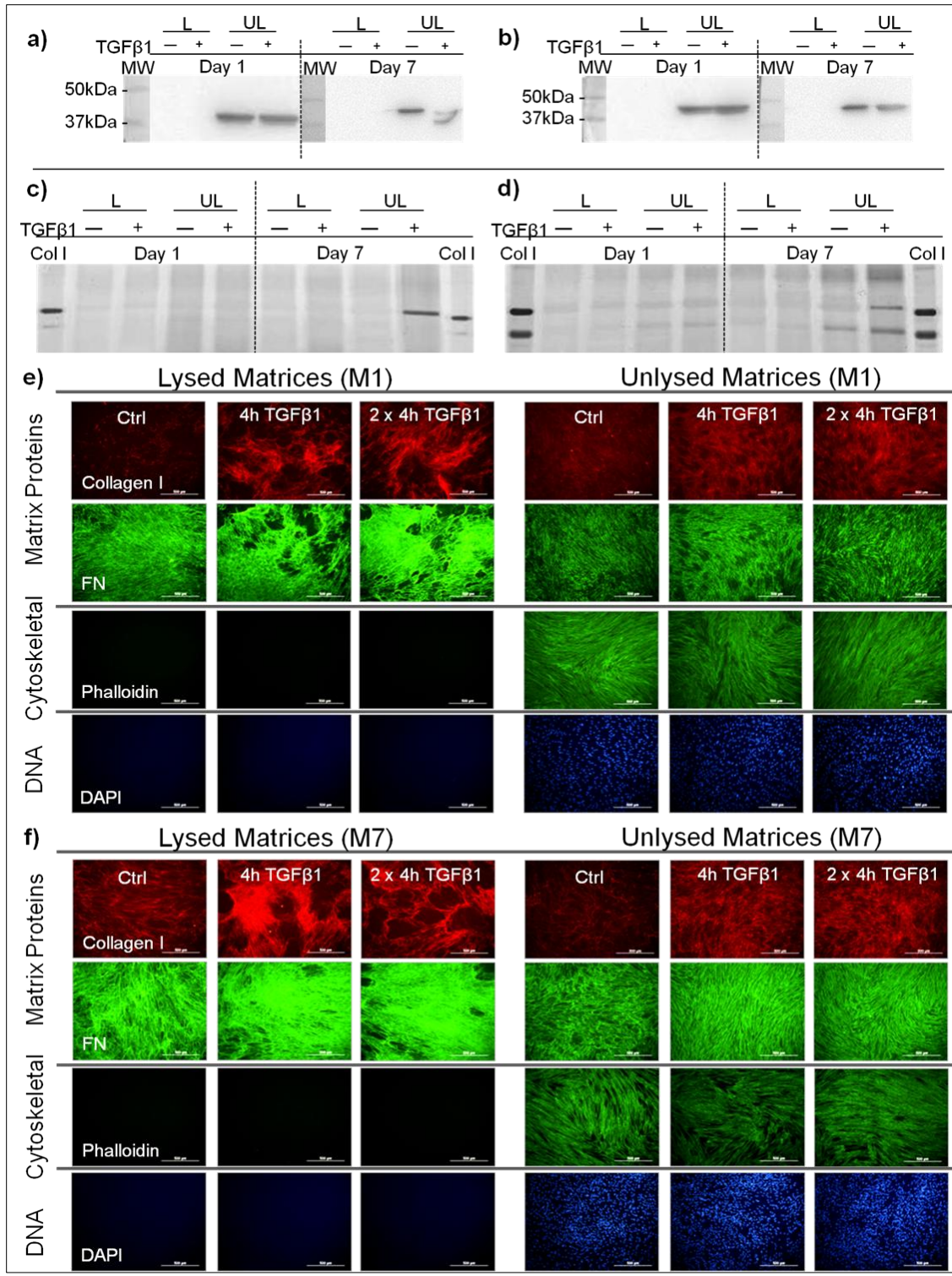
Figure 25. TGFβ1-pulsed ECM was free from DNA and actin residues. Representative immunoblots of (a) 4h; and (b) 2 x 4h TGFβ1-pulsed ECM. Elevated collagen I and FN expression was observed in TGFβ1-treated ECM; representative SDS-PAGE gels of (c) 4h; and (d) 2 x 4h TGFβ1 ECM; and representative ICC pictures of (e) early (decellularised 1 day post-pulse); and (f) late (decellularised 7 days post-pulse) ECM (collagen I, red; FN and phalloidin, green; DAPI, blue). *Legend: "L" denotes decellularized ECM and "UL" the unlysed ECM (positive ECM control).*
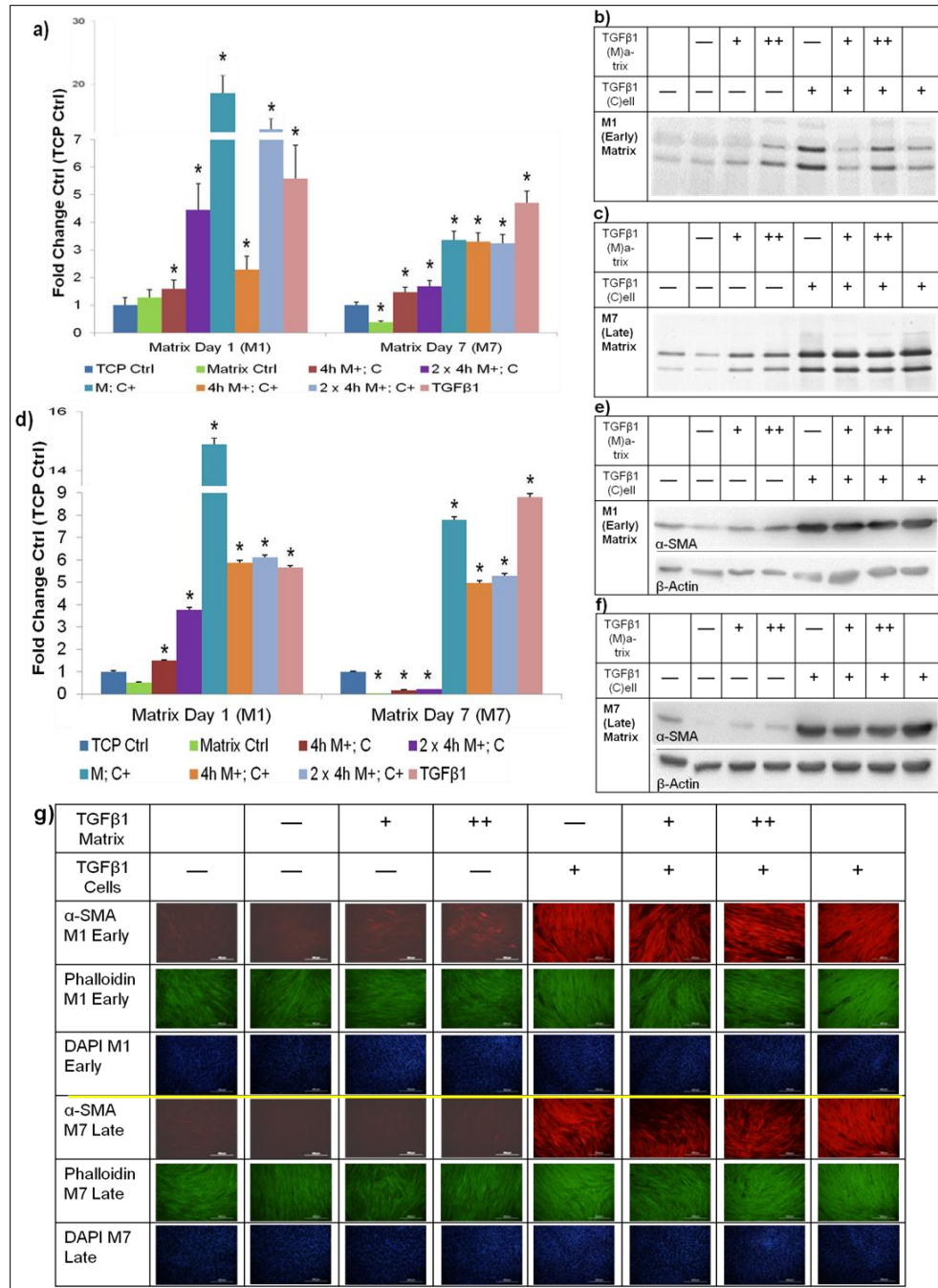
Figure 26. TGFβ1-pulsed ECM influenced the myofibroblast phenotype, with pronounced effects with multiple pulses and the early (M1) ECM. (a) Normalized densitometric SDS-PAGE analysis of the 24h collagen secretion rate; representative SDS-PAGE gels of (b) early M1; and (c) late M7 ECM. (d) Densitometric analysis of α-SMA was normalized to β-actin expression; representative immunoblots of (e) M1; and (f) M7 ECM. (g) Representative ICC pictures (α-SMA, red; phalloidin, green; DAPI, blue) of the cell layer. Tissue culture plastic (TCP) ctrl, ECM ctrl and cells reseeded onto 4h and 2 x 4h TGFβ1-pulsed ECM ICC images were modified to highlight α-SMA expression. Bars indicate 500μM. *$p < 0.05$ versus respective untreated controls. Data are represented as mean ± S.D, calculated from three independent studies in triplicates, and expressed as -fold changes over respective TCP controls. *Legend: TGFβ1 ECM: "+" denotes a 4h; and "++" 2 x 4h TGFβ1 pulse(s) on decellularized ECM. TGFβ1 Cells: "+" denotes a 24h TGFβ1 pulse on seeded fibroblasts.*
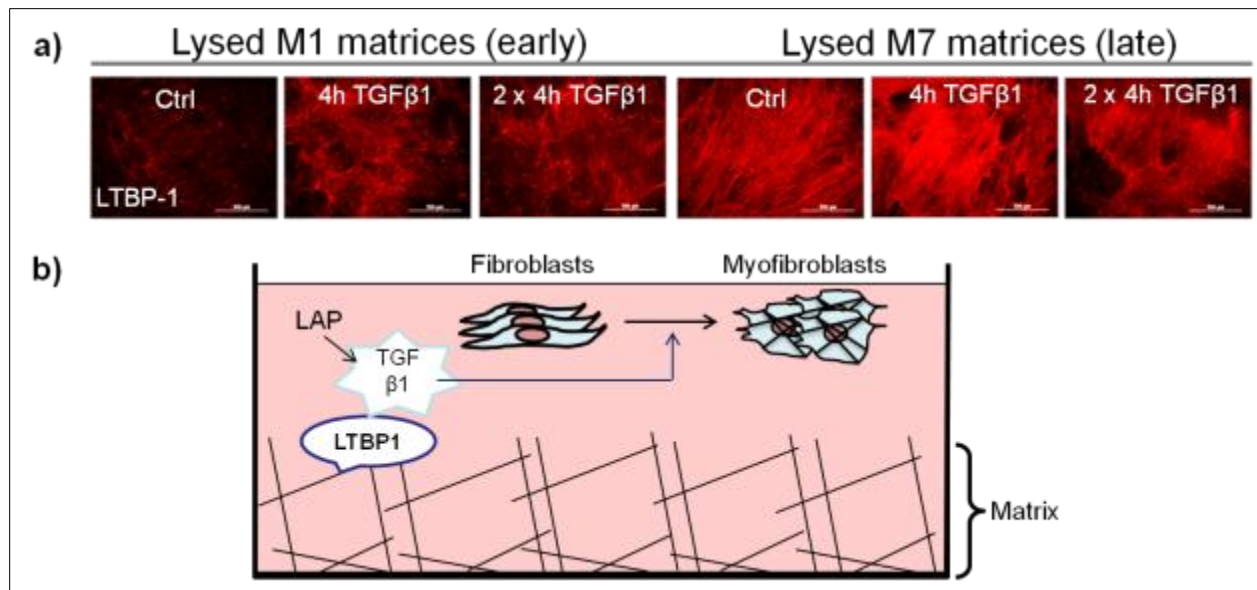
Figure 27. ECM decellularised 1 day post-pulse exhibited elevated LTBP-1 expression. (a) Representative ICC pictures (LTBP-1, red) of the 4h and 2 x 4h TGFβ1-pulsed M1 and M7 ECM. (b) Schematic illustrating the proposed mechanism. TGFβ1-pulsed M1 ECM expressed elevated levels of LTBP-1. We propose that LAP releases TGFβ1 and this in turn, activates fibroblast – myofibroblast differentiation.

4.2.5 Normal fibroblast ECM down-modulated the myofibroblast phenotype

From a therapeutic perspective, it would be beneficial if the ECM could normalize or down-modulate myofibroblast expression. In these studies, MMC (Fc cocktail) was employed to enhance ECM deposition (Figure 28). Subsequently, normal fibroblast ECM were decellularized and confirmed to be free from DNA and actin residues (Figure 29). Fibroblasts (WI-38, and pathological: hypertrophic scar (HSF) and idiopathic pulmonary (IPF) fibroblasts) do not intrinsically express α-SMA when cultured without TGFβ1 on TCP. Therefore, fibroblasts were treated with TGFβ1 for 4 days (current 'gold standard') to generate myofibroblasts and passaged using the *bacillus polymyxa*-derived protease, Dispase, as α-SMA expression was preserved when the correct enzyme treatment was applied (Figure 30). This is likely because Dispase does not disrupt the integrity of the cell membrane as it cleaves collagen IV, FN and to a lesser extent, collagen I [Ludwig et al. 2006]. Decellularized fibroblast ECM was observed to reduce to and reduce below fibroblast levels, collagen I production in fetal lung WI-38 (Figure 31)

and HSF myofibroblasts (Figure 32) respectively. α-SMA expression, however, remained unchanged from TCP test control (myofibroblasts) expression. In contrast, normal fibroblast ECM appeared to have no effect on the phenotype of IPF myofibroblasts (Figure 33).
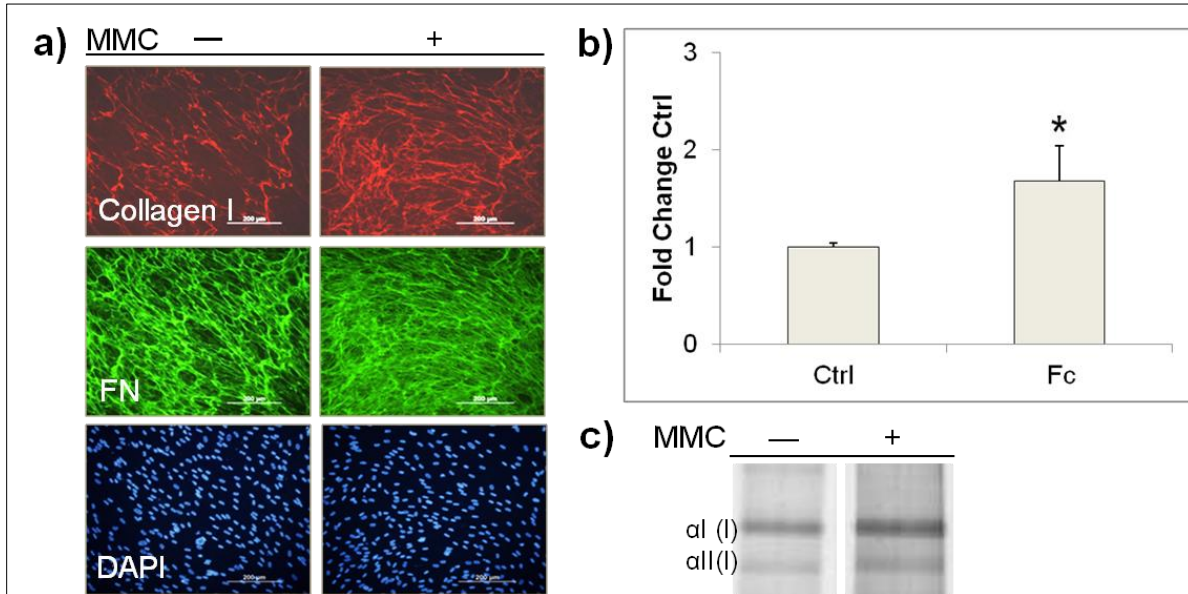
Figure 28. Collagen I and FN deposition on ECM were increased in the presence of a Fc cocktail. Fibroblasts were cultured for a total of 7 days. (a) Representative ICC pictures (collagen I, red; FN, green; DAPI, blue). (b) Normalized densitometric SDS-PAGE analysis and (c) representative SDS-PAGE of collagen deposition by fibroblasts. Bars indicate 500µM. *$p < 0.05$ versus uncrowded control. Data are represented as mean ± S.D, calculated from three independent studies in triplicates, and expressed as -fold changes over respective controls.
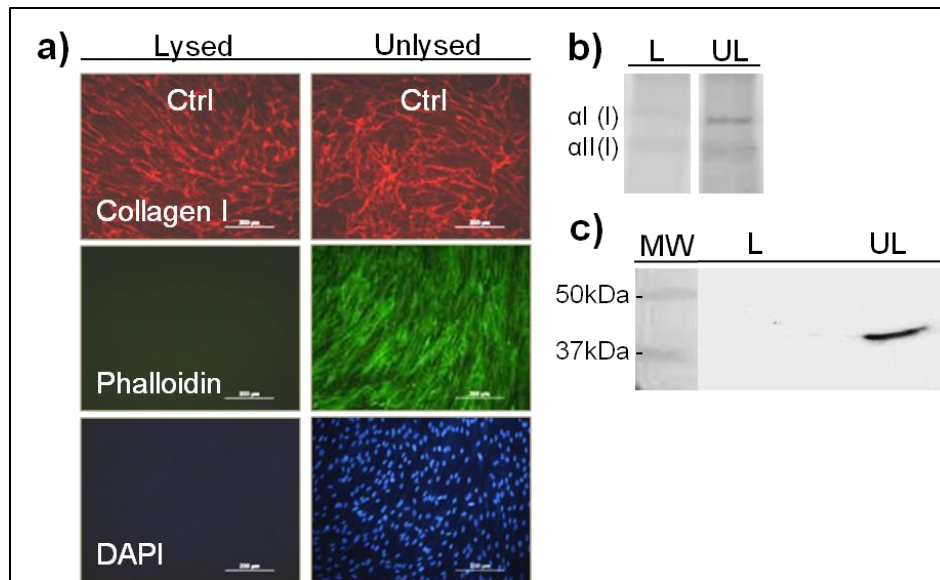
Figure 29. Decellularization of MMC normal fibroblast ECM. Fibroblasts were cultured in the presence of MMC for 7 days and decellularized thereafter. The absence of actin and DNA residues was observed in the decellularised ECM. Representative (a) ICC pictures (collagen I, red; phalloidin, green; DAPI, blue); (b) SDS-PAGE of collagen I deposition; and (c) β-actin immunoblot. *Legend: "L" denotes decellularized ECM and "UL" the unlysed ECM (positive ECM control).*

Figure 30. Dispase passaging reduced but preserved the myofibroblast phenotype. Fibroblasts (WI-38, HSF and IPFs) were treated with or without TGFβ1 for 4 days. Thereafter, cultures were passaged using Dispase and re-seeded onto TCP. Cultures were maintained for further 7 days. Representative ICC pictures (α-SMA, red; DAPI, blue).

76
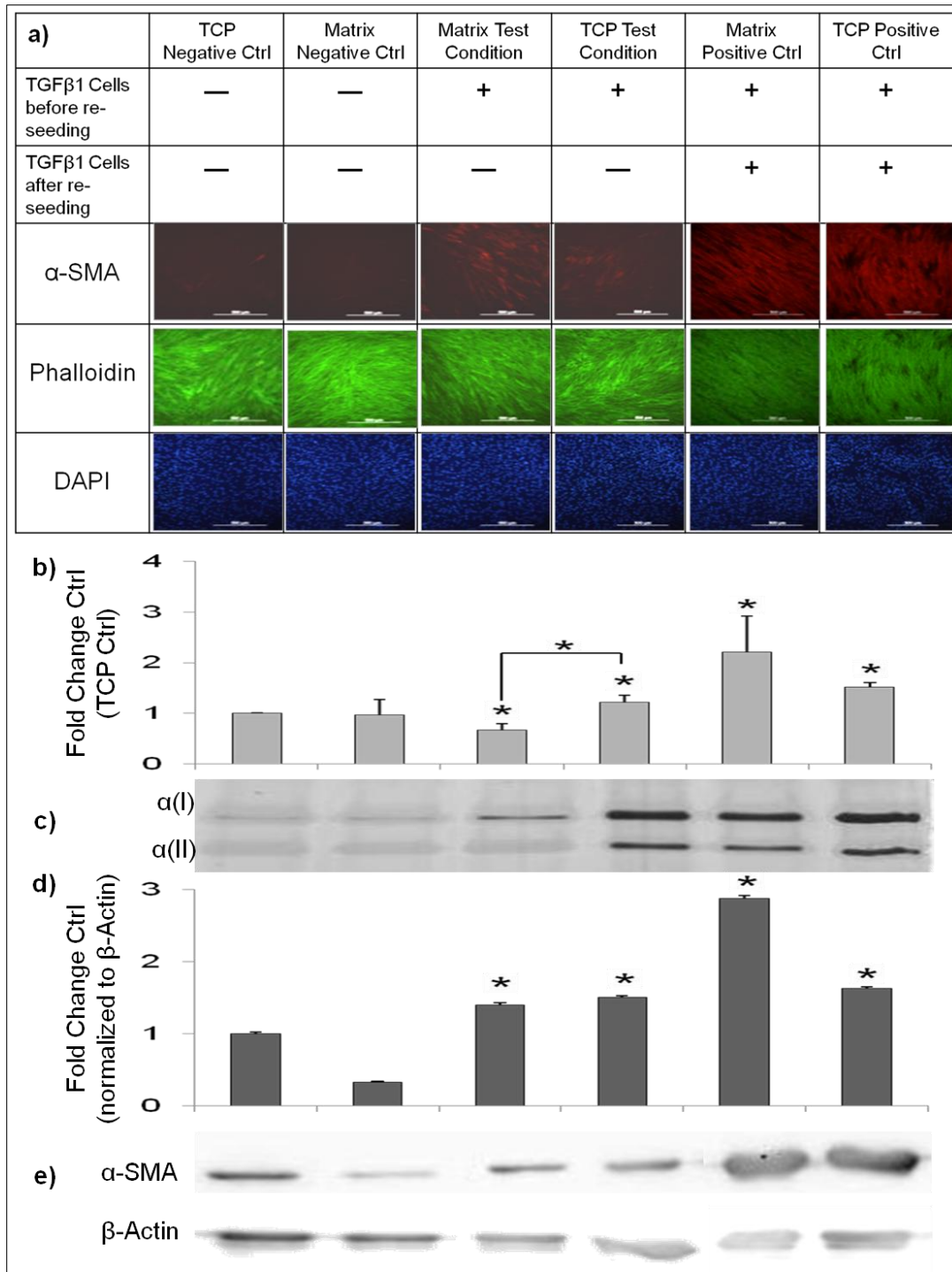
Figure 31. Fibroblast ECM reduced to fibroblast level collagen I production in WI-38 myofibroblasts. (a) Representative ICC pictures (α-SMA, red; phalloidin, green; DAPI, blue). Bars indicate 500μM. Negative controls and test conditions images were modified to highlight α-SMA expression (first 4 columns). (b) Normalized densitometric SDS-PAGE analysis of the 24h collagen secretion rate; (c) representative SDS-PAGE; (d) densitometric analysis of α-SMA normalized to β-actin expression; and (e) representative immunoblots. *$p < 0.05$ versus TCP negative control. *$p < 0.05$ versus TCP test control (myofibroblasts). Data are represented as mean ± S.D, calculated from duplicate studies in triplicates, and expressed as -fold changes over respective controls.

Figure 32. Fibroblast ECM reduced below fibroblast levels collagen I production in HSF myofibroblasts. (a) Representative ICC pictures (α-SMA, red; phalloidin, green; DAPI, blue). Bars indicate 500μM. Negative controls and test conditions images were modified to highlight α-SMA expression (first 4 columns). (b) Normalized densitometric SDS-PAGE analysis of the 24h collagen secretion rate; (c) representative SDS-PAGE; (d) densitometric analysis of α-SMA normalized to β-actin expression; and (e) representative immunoblots. *$p < 0.05$ versus TCP negative control. *$p < 0.05$ versus TCP test control (myofibroblasts). Data are represented as mean ± S.D, calculated from duplicate studies in triplicates, and expressed as -fold changes over respective controls.

78

Figure 33. Fibroblast ECM had no effect in IPF myofibroblasts. (a) Representative ICC pictures (α-SMA, red; phalloidin, green; DAPI, blue). Bars indicate 500μM. Negative controls and test conditions images were modified to highlight α-SMA expression (first 4 columns). (b) Normalized densitometric SDS-PAGE analysis of the 24h collagen secretion rate; (c) representative SDS-PAGE; (d) densitometric analysis of α-SMA normalized to β-actin expression; and (e) representative immunoblots. *$p < 0.05$ versus TCP negative control. Data are represented as mean ± S.D, calculated from duplicate studies in triplicates, and expressed as -fold changes over respective controls.

4.3 Revisiting SAHA's anti-fibrotic potential

We have shown that epigenetic modifications (histone acetylation / DNA methylation) were not responsible for the memorized effects of TGFβ1-pulsed treatments. However, HDACi SAHA has been described to affect myofibroblast differentiation and collagen targets [Wang et al. 2009]. Alternative targets of SAHA are microtubules which are important for cell locomotion properties. Although SAHA was not able to abrogate TGFβ1 effects after cells were treated with TGFβ1, and this appears to be due to physiological limitations. We therefore aimed to: **a)** assess the anti-fibrotic effects of SAHA in conjunction with TGFβ1-pulses in fibroblasts; and to **b)** establish the mechano-effects of SAHA on myofibroblasts as this may provide an additional consideration for anti-fibrotic therapy.

4.3.1 IC50 of SAHA was 5μM

Long-term exposure to SAHA (i.e. more than 72h) was observed to result in cell death. The IC50 (half maximal inhibitory concentration) value of SAHA in fibroblasts was 5μM [Wang et al. 2009]. Growth-arrested fibroblasts were treated with 4 days to TGFβ1 to generate myofibroblasts. Thereafter, cytokine containing media was removed and replace with varying concentrations of SAHA. Cultures were harvested at days 3 and 7 post-SAHA treatment. The IC50 concentration of SAHA in myofibroblasts was assessed using the MTS assay, and determined to be 4.5μM ≈ 5μM (Figure 34). 5μM of SAHA was employed for the remaining experiments.
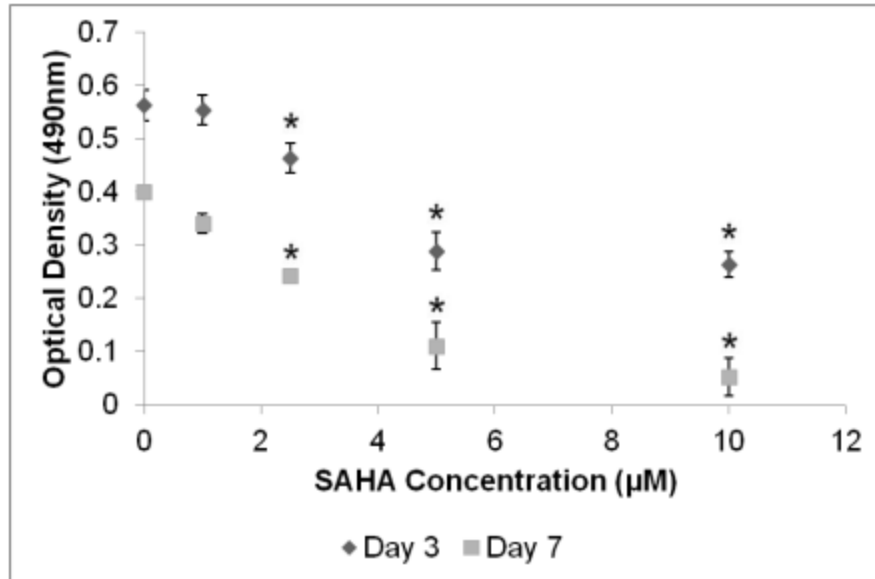
Figure 34. IC50 value of SAHA in myofibroblasts was 5µM. Fibroblasts were treated with 4 days of TGFβ1 to generate myofibroblasts and the IC50 value of SAHA evaluated from the best-fit linear equation at days 3 (where y = -0.0328x + 0.5485) and 7 (where y = -0.0346x + 0.3579) post-treatment. *$p < 0.05$ versus respective untreated controls. Data are represented as mean ± S.D, calculated from two independent studies in triplicates, and expressed as optical density 490nm.

4.3.2 SAHA induced early apoptosis in myofibroblasts

Previous reports documented that SAHA induced apoptosis in transformed cells. We therefore sought to compare SAHA's cytotoxic and apoptotic effects in fibroblasts and myofibroblasts using an MTS assay. Cytotoxicity was quantitated by measuring dead cell protease activity released from cells that have lost its membrane integrity (bis-AAF-R110: bis-alanylalanyl-phenylalanyl-rhodamine 110. Apoptosis was determined by measuring luminogenic caspase-3/7 activity. SAHA was non-cytotoxic and induced early (24h after SAHA treatment) apoptosis in myofibroblasts (Figure 35). This effect however, was not sustained over the following 2 days of SAHA treatment.
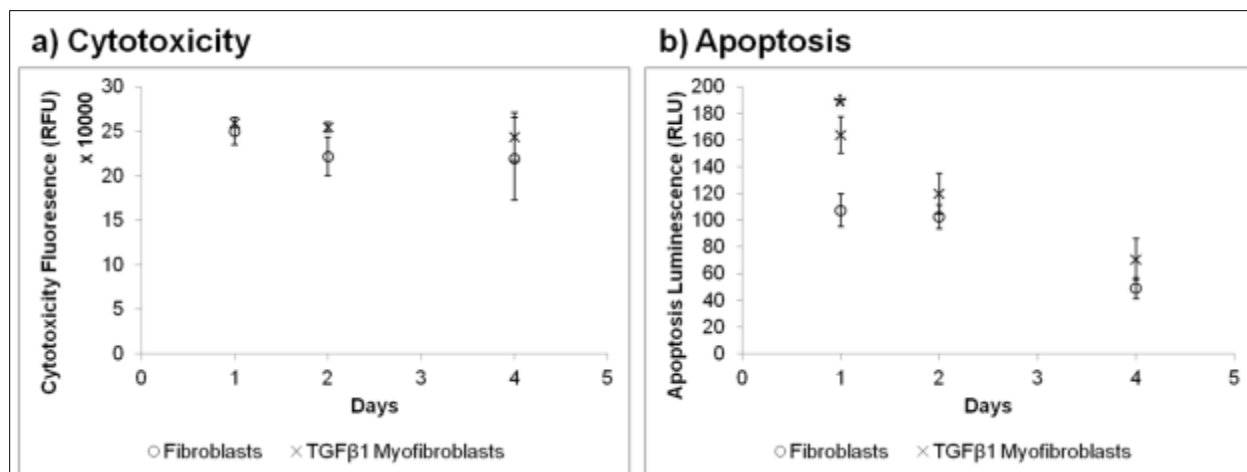
Figure 35. 5μM SAHA was non-cytotoxic and induced early apoptosis in myofibroblasts. (a) Fluorogenic bis-AAF-R110 (bis-alanylalanyl-phenylalanyl-rhodamine 110) was used to measure dead cell protease activity released from cells that have lost its membrane integrity. (b) Apoptosis was determined by measuring luminogenic caspase-3/7 activity. 24h post-SAHA treatment, myofibroblasts expressed elevated levels of capase-3/7 activity. *$p < 0.05$ versus respective untreated fibroblasts controls. Data are represented as mean ± S.D, calculated from two independent studies in triplicates, and expressed as relative fluorescence or luminescence units.

4.3.3   SAHA treatment versus TGFβ1 pulse(s)

Using the *in vitro* wound healing platform based on the long-lasting effects of TGFβ1 pulses, SAHA efficacy in conjunction with 4h or 2 x 4h TGFβ1 pulse(s) was investigated.

4.3.3.1 SAHA pre-treatment displayed short-term TGFβ1 effects with a single pulse

To investigate SAHA's protective effects on pulsed myofibroblast formation, we assessed the efficacy of 24h of SAHA pre-treatment before the administration of TGFβ1 pulse(s). We observed that 24h of SAHA treatment before a 4h TGFβ1 pulse reduced below fibroblast levels, collagen I and α-SMA expression 1 day, but not 7 days post-pulse (Figure 36). However, 24h of SAHA pre-treatment appeared to have no effect on myofibroblast differentiation when administered in conjunction with double TGFβ1 pulse(s) (Figure 37).
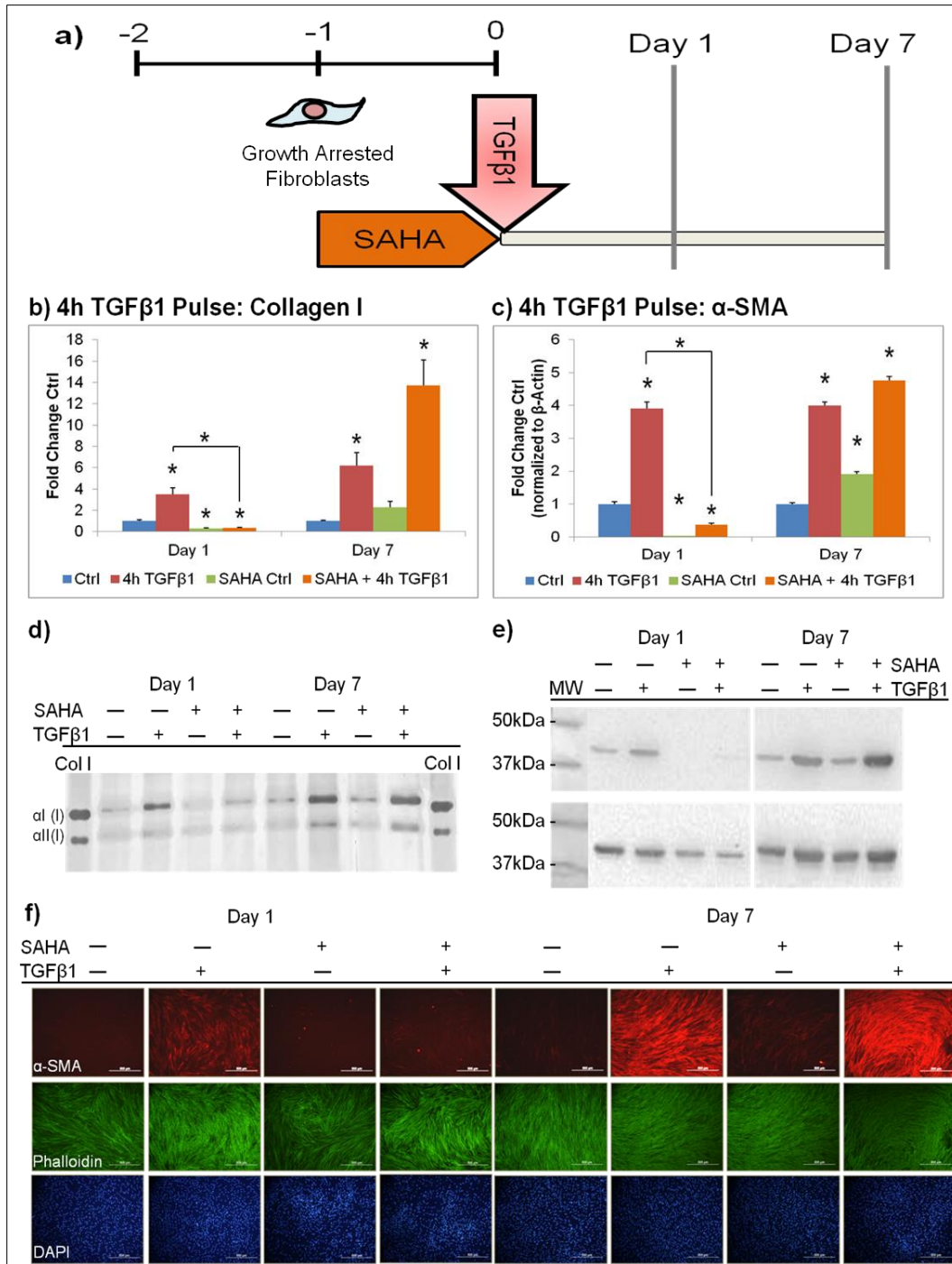
Figure 36. SAHA pre-treatment reduced to fibroblast levels, collagen I production and α-SMA expression after a single TGFβ1 pulse. (a) Cell culture setup of SAHA pre-treatment on growth-arrested fibroblasts for 24h followed by a 4h TGFβ1 pulse. (b) Normalized densitometric SDS-PAGE analysis of the 24h collagen secretion rate by induced fibroblasts; (c) densitometric analysis of α-SMA normalized to β-actin expression; representative (d) SDS-PAGE; (e) immunoblots and (i) ICC pictures (α-SMA, red; phalloidin, green; DAPI, blue) of the 4h TGFβ1-pulsed cell layers. Bars indicate 500μM. *$p <$ 0.05 versus respective untreated controls. *$p < 0.05$ versus respective TGFβ1 (positive) myofibroblast controls. Data are represented as mean ± S.D, calculated from three independent studies in triplicates, and expressed as -fold changes over respective controls.
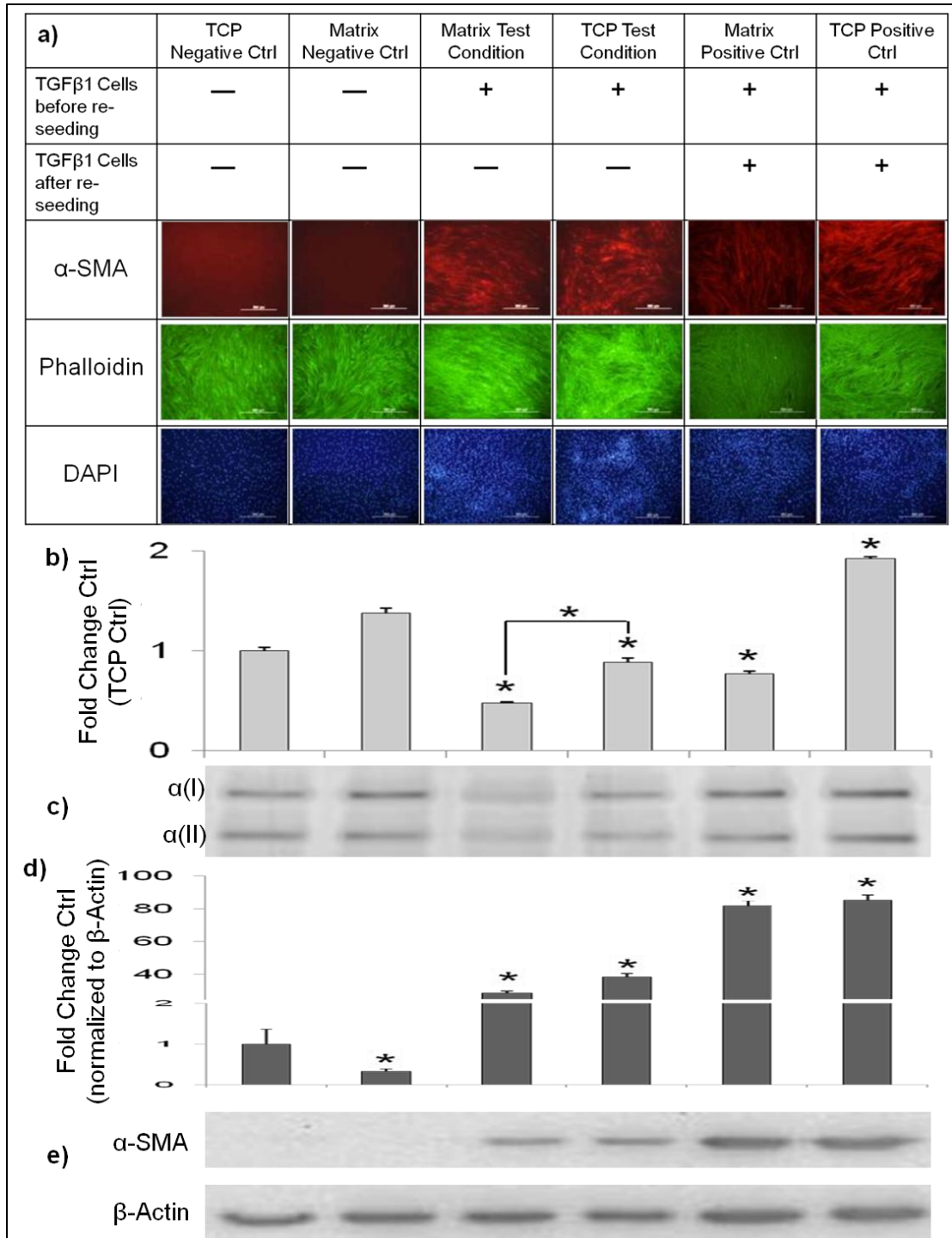
Figure 37. SAHA pre-treatment had no effect on double TGFβ1 pulses. (a) Cell culture setup of SAHA pre-treatment on growth-arrested fibroblasts for 24h followed by 2 x 4h TGFβ1 pulses, administered over 2 consecutive days. (b) Normalized densitometric SDS-PAGE analysis of the 24h collagen secretion rate by induced fibroblasts; (c) densitometric analysis of α-SMA normalized to β-actin expression; representative (d) SDS-PAGE; (e) immunoblots and (i) ICC pictures (α-SMA, red; phalloidin, green; DAPI, blue) of 2 x 4h TGFβ1-pulsed cell layers. Bars indicate 500μM. *$p < 0.05$ versus respective untreated controls. Data are represented as mean ± S.D, calculated from three independent studies in triplicates, and expressed as -fold changes over respective controls.
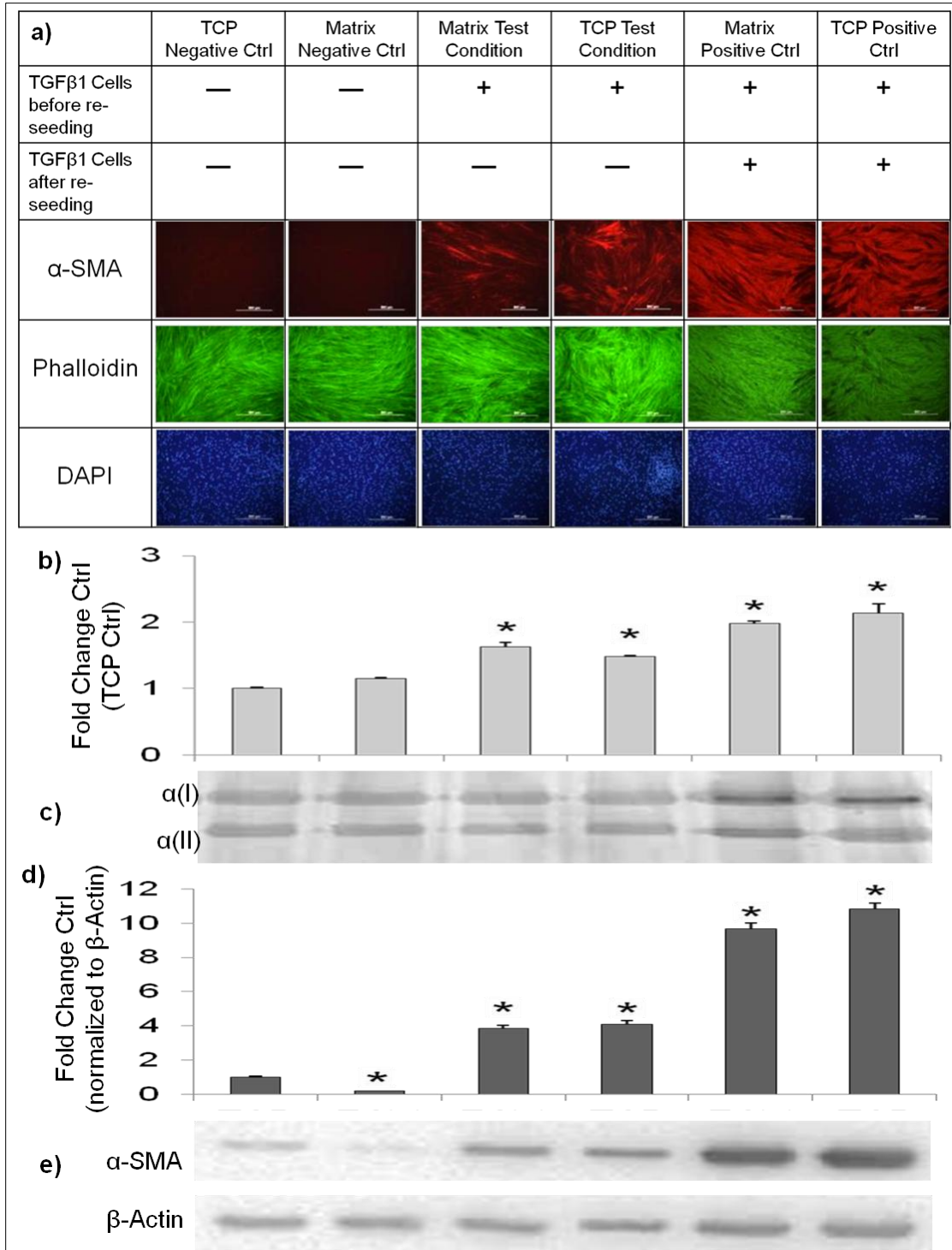
4.3.3.2 SAHA post-treatment normalized short-term TGFβ1 effects

We proceeded to assess if SAHA would prevent myofibroblast induction and maintenance after fibroblasts were treated with pulse(s) of TGFβ1. To do so, we treated fibroblasts with SAHA immediately after treatment with TGFβ1 pulses. Here we show that in comparison with the TGFβ1-induced myofibroblasts, SAHA post-treatment normalized and reduced collagen I production 1 and 7 days, respectively, post-SAHA treatment. α-SMA expression however, was only reduced 1 day post a single 4h TGFβ1 pulse (Figure 38). Characterising the effects of SAHA post-treatment in conjunction with double TGFβ1 pulses, we demonstrate that in comparison with the myofibroblast controls, SAHA post-treatment reduced collagen I production 1 and 7 days post-pulse, and reduced α-SMA expression 1 day post-pulse only (Figure 39), suggesting the transient short-term effects of SAHA post-treatment on myofibroblast induction and maintenance.
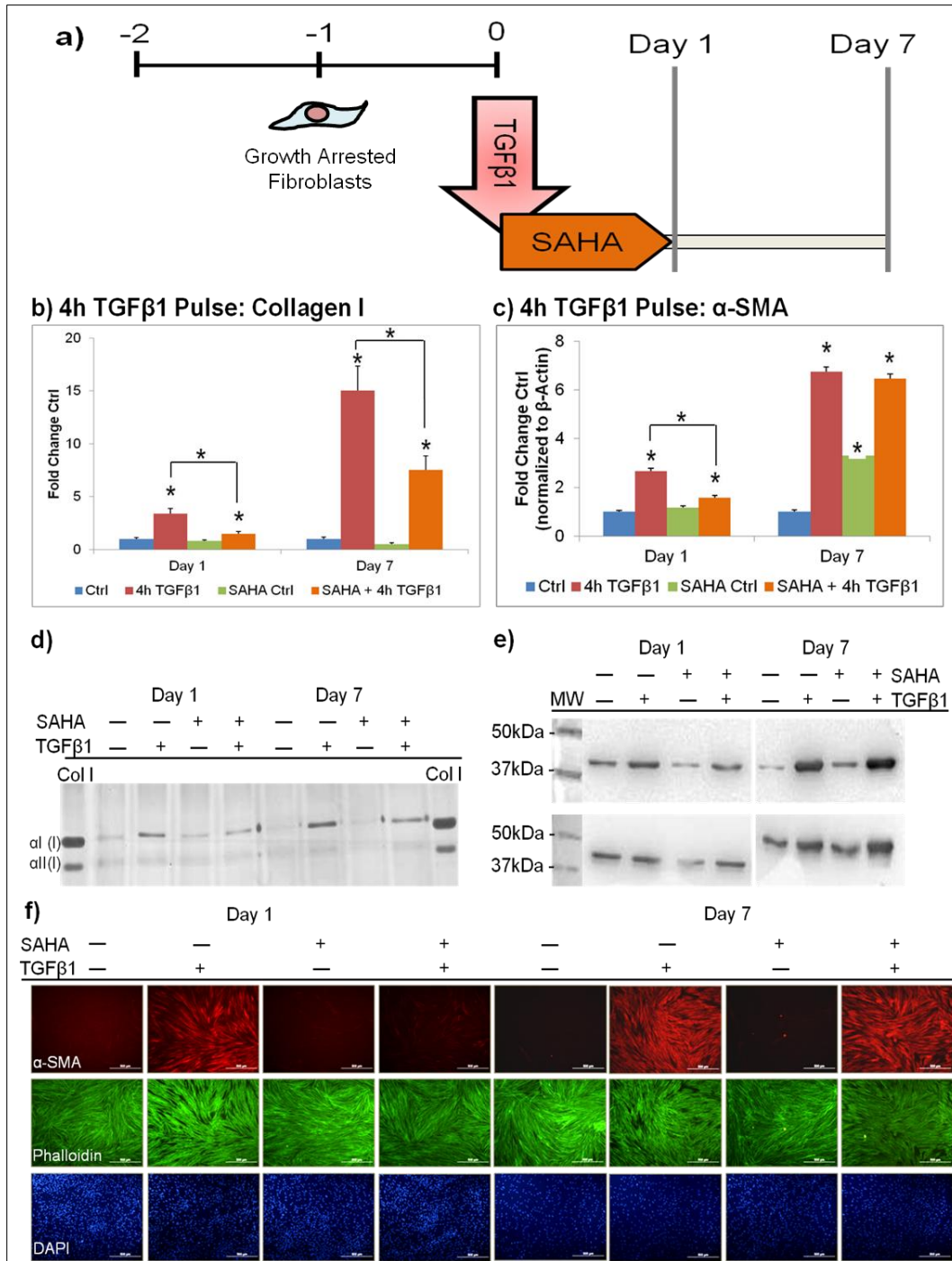
Figure 38. SAHA post-treatment normalized short-term TGFβ1-effects in the single pulse model. SAHA exhibited limited effects on α-SMA expression but reduced collagen production. (a) Cell culture setup of a 4h TGFβ1 pulse on growth-arrested fibroblasts, followed by SAHA post-treatment for 24h. (b) Normalized densitometric SDS-PAGE analysis of the 24h collagen secretion rate by induced fibroblasts; (c) densitometric analysis of α-SMA normalized to β-actin expression; representative (d) SDS-PAGE; (e) immunoblots and (i) ICC pictures (α-SMA, red; phalloidin, green; DAPI, blue) of 4h TGFβ1-pulsed cell layers. Bars indicate 500µM. *$p < 0.05$ versus respective untreated controls. *$p < 0.05$ versus respective TGFβ1 (positive) myofibroblast controls. Data are represented as mean ± S.D, calculated from three independent studies in triplicates, and expressed as -fold changes over respective controls.

Figure 39. In comparison with the myofibroblast controls, SAHA post-treatment reduced short-term TGFβ1-effects in the multiple pulses model. SAHA exhibited limited effects on α-SMA expression but reduced collagen production. (a) Cell culture setup of a 2 x 4h TGFβ1 pulse on growth-arrested fibroblasts, administered over 2 consecutive days, followed by SAHA post-treatment for 24h. (b) Normalized densitometric SDS-PAGE analysis of the 24h collagen secretion rate by induced fibroblasts; (c) densitometric analysis of α-SMA normalized to β-actin expression; representative (d) SDS-PAGE; (e) immunoblots and (i) ICC pictures (α-SMA, red; phalloidin, green; DAPI, blue) of the 2 x 4h TGFβ1-pulsed cell layers. Bars indicate 500µM. *$p < 0.05$ versus respective untreated controls. *$p < 0.05$ versus respective TGFβ1 (positive) myofibroblast controls. Data are represented as mean ± S.D, calculated from three independent studies in triplicates, and expressed as -fold changes over respective controls.

4.3.3.3 SAHA pre- & post-treatment acted in synergy to normalize long-term TGFβ1 effects

From the independent results obtained with SAHA pre- and post-treatment, we proceeded to combine both SAHA pre- and post-treatment to assess if this combination had synergistic effects on TGFβ1-pulsed myofibroblast induction and maintenance. In comparison with the myofibroblast control cells, the administration of SAHA before and after a 4h TGFβ1 pulse was observed to abrogate collagen I production and reduced α-SMA expression at all assessed end-points (Figure 40). When administered with double pulses, SAHA pre- and post-treatment normalized and reduced collagen production at days 1 and 7, respectively. However, α-SMA expression was observed to be reduced only 24h post-pulses (Figure 41).
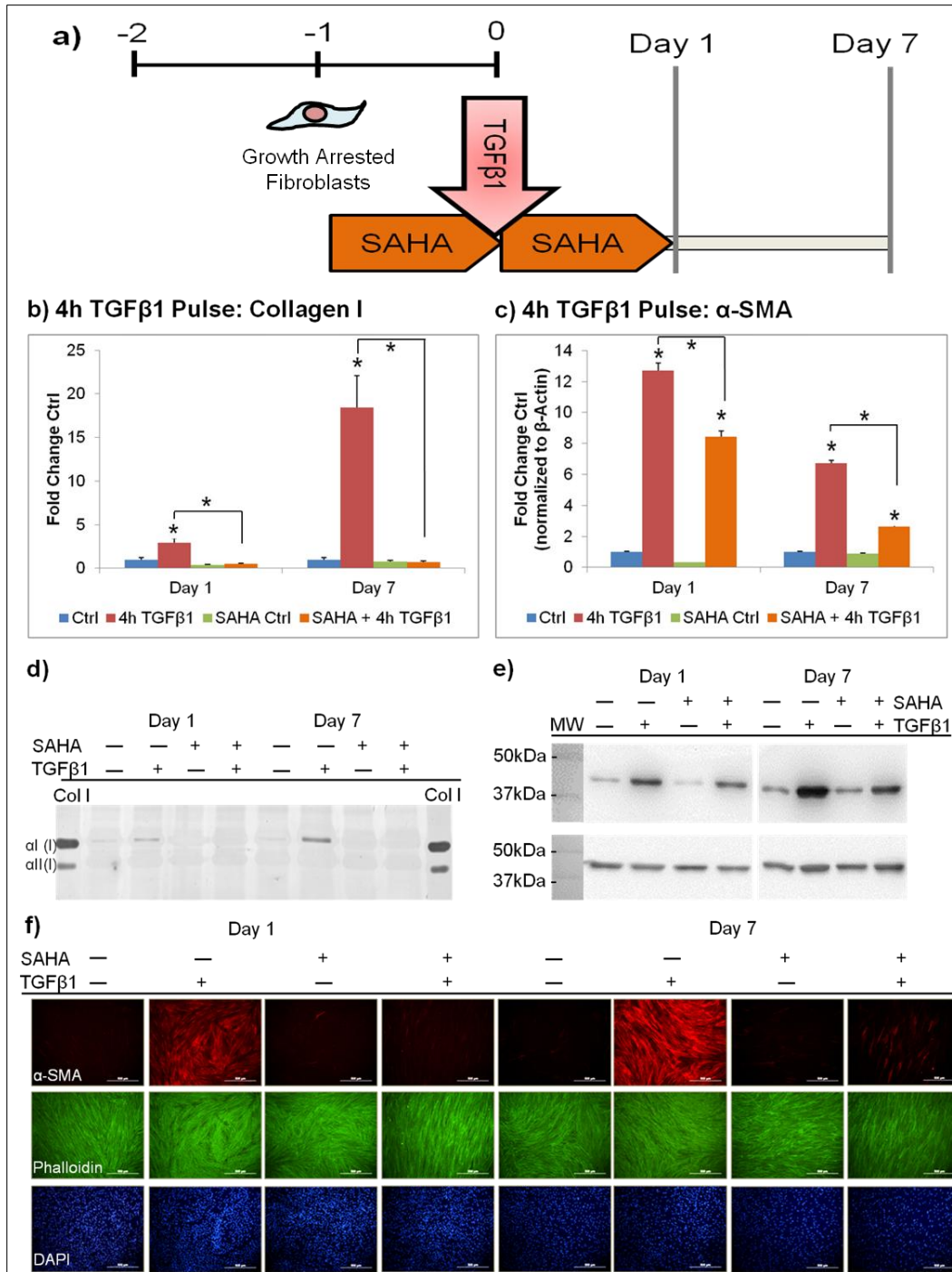
Figure 40. SAHA pre- and post-treatment normalized collagen I production and reduced α-SMA expression when administered with a 4h TGFβ1 pulse. (a) Cell culture setup of 24h SAHA treatment – 4h TGFβ1 pulse – 24h SAHA post-treatment on growth-arrested fibroblasts. (b) Normalized densitometric SDS-PAGE analysis of the 24h collagen secretion rate by induced fibroblasts; (c) densitometric analysis of α-SMA normalized to β-actin expression; representative (d) SDS-PAGE; (e) immunoblots and (i) ICC pictures (α-SMA, red; phalloidin, green; DAPI, blue) of 4h TGFβ1-pulsed cell layers. Bars indicate 500μM. *$p < 0.05$ versus respective untreated controls. *$p < 0.05$ versus respective TGFβ1 (positive) myofibroblast controls. Data are represented as mean ± S.D, calculated from three independent studies in triplicates, and expressed as -fold changes over respective controls.

Figure 41. SAHA pre- and post-treatment normalized short-term TGFβ1-effects when administered with 2 x 4h TGFβ1 pulses. As compared to the myofibroblast control, SAHA treatment normalizedcollagen I production and reduced α-SMA expression 1 day post pulse. Collagen production but not α-SMA expression was reduced 7 days post-pulse. (a) Cell culture setup of 24h SAHA treatment – 2 x 4h TGFβ1 pulse – 24h SAHA post-treatment on growth-arrested fibroblasts. (b) Normalized densitometric SDS-PAGE analysis of the 24h collagen secretion rate by induced fibroblasts; (c) densitometric analysis of α-SMA normalized to β-actin expression; representative (d) SDS-PAGE; (e) immunoblots and (i) ICC pictures (α-SMA, red; phalloidin, green; DAPI, blue) of the 2 x 4h TGFβ1-pulsed cell layers. Bars indicate 500μM. *$p < 0.05$ versus respective untreated controls. *$p < 0.05$ versus respective TGFβ1 (positive) myofibroblast controls. Data are represented as mean ± S.D, calculated from three independent studies in triplicates, and expressed as -fold changes over respective controls.

4.3.4 SAHA impeded myofibroblast motility

To assess SAHA's effects on myofibroblast motility, we employed the use of a wound healing assay on TGFβ1-treated myofibroblasts. Live phase contrast imaging demonstrated that SAHA impeded myofibroblasts migration (Figure 42). Using a linear best fit analysis to quantitate myofibroblast migration rates, we observed that myofibroblasts exhibited the fastest migration rate, while fibroblasts (regardless of SAHA treatment) migrated at a slightly slower rate. SAHA treated myofibroblasts was found to display the slowest migration rate (Figure 42c).

Condition	Ctrl	TGFβ1	SAHA	TGFβ1 + SAHA
Rate of migration (μM^2/h)	11928	11989	11634	6645
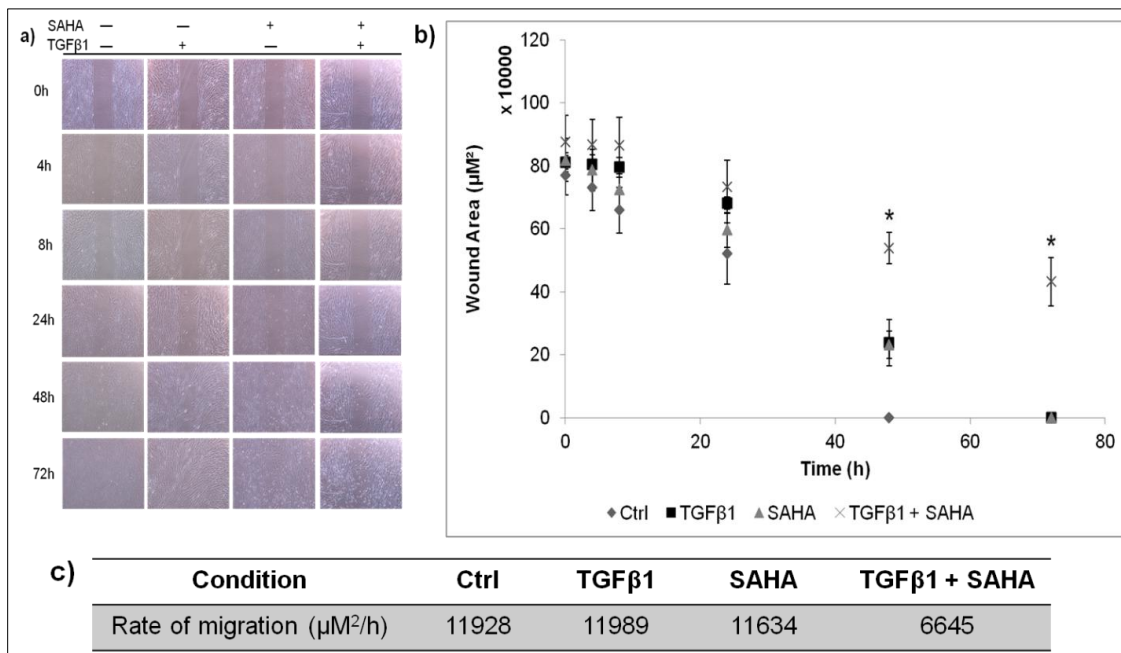
Figure 42. SAHA impeded myofibroblast migration into the wound area. Fibroblasts were treated with and without TGFβ1 for 3 days. Cytokine containing media was removed and cultures treated with and without SAHA before removal of the 'scratch', and monitored for a further 3 days. (a) Representative phase contrast images (4x magnification) of cell migration into wound area; (b) quantitation of cell migration into wound area, evaluated by ImageJ at various time intervals after release. (c) Rate of migration was evaluated by plotting the linear best-fit curve to obtained data. *$p < 0.05$ versus respective untreated controls. Data are represented as mean ± S.D, calculated from three independent studies in triplicates, and expressed as -fold changes over respective controls.

4.3.5 SAHA had no effect on myofibroblast contraction

Another property of myofibroblast locomotion is contraction. Using an *in vitro* 3D polymerized collagen I gel to assess SAHA's effects on TGFβ1-induced myofibroblast contractility, we observed that SAHA does not have an effect on myofibroblast contraction (Figure 43).
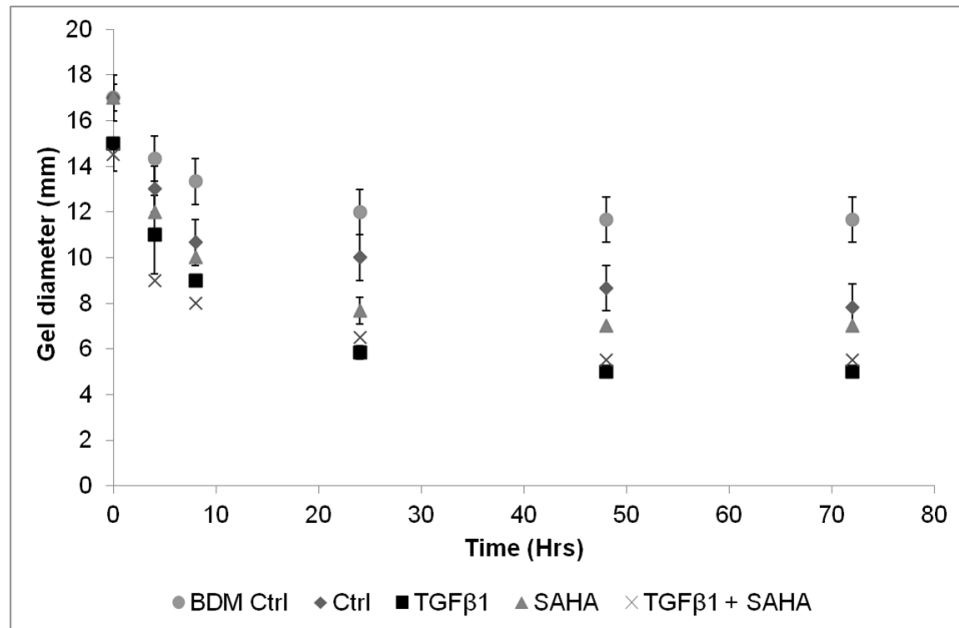
Figure 43. SAHA had no effect on myofibroblast contraction. Fibroblasts in collagen gel lattices were treated with and without TGFβ1 for 2 days to allow for polymerization and stress formation within the lattice. Prior to contraction initiation, cytokine containing culture media was removed and replaced with or without SAHA. Quantitation of gel contraction was evaluated by measuring the gel diameter with a ruler at various times after release, over a span of 3 days. 10mM BDM (contraction inhibitor) was utilized for the assay negative control. Data are represented as mean ± S.D, calculated from three independent studies in triplicates, and expressed as -fold changes over respective controls.
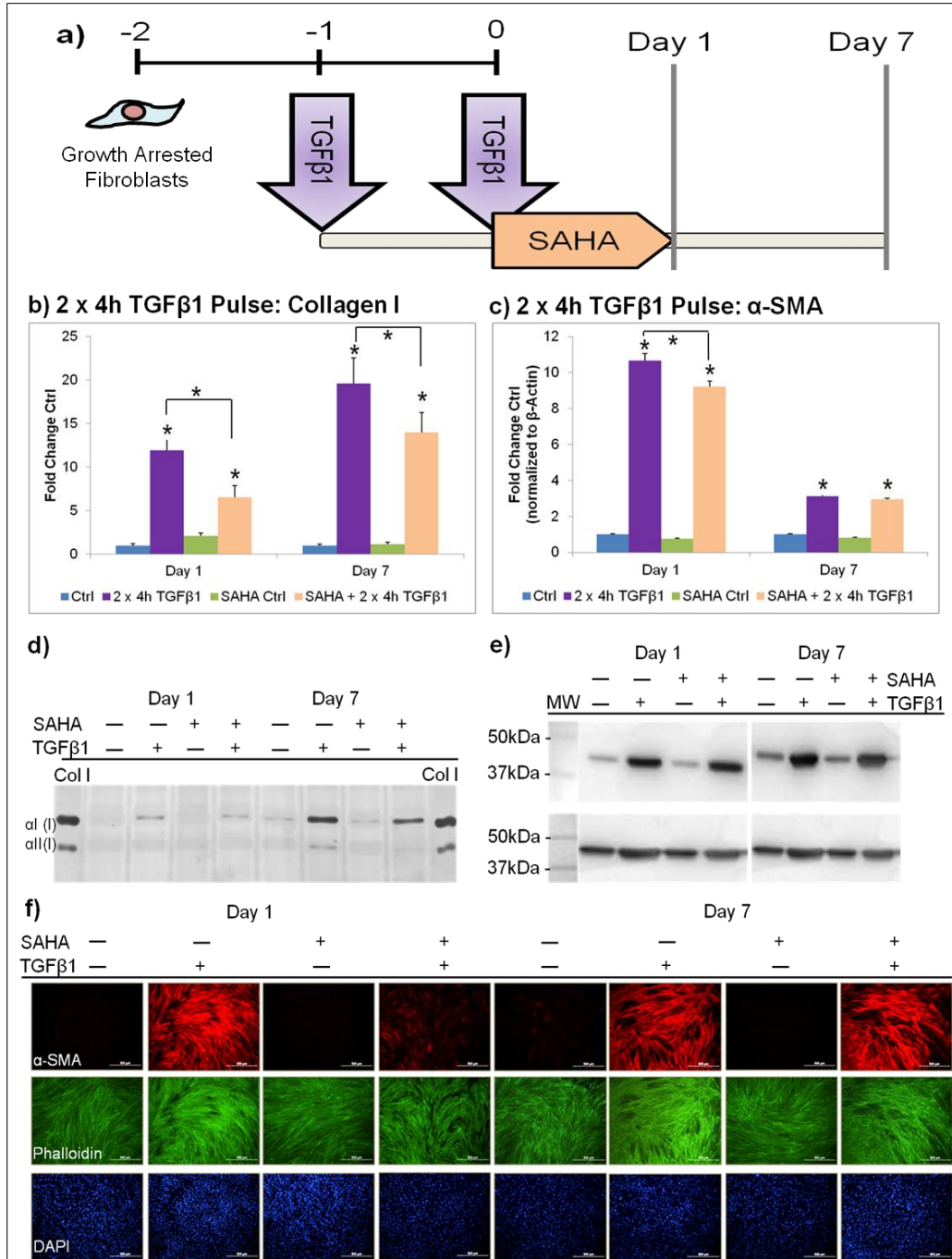
Chapter 5

Discussion

This chapter discusses the core findings of the project in relation to the memorized effects of TGFβ1 and SAHA's anti-fibrotic effects when administered with TGFβ1 pulses.

.

5.1 Development of a physiologically relevant in vitro fibrosis model

In this study we considered the effects of pulsed TGFβ1 on WI-38 cells and made two significant observations. Firstly, a short TGFβ1 pulse had surprisingly long lasting effects as evidenced by the generation of a *bona fide* myofibroblast phenotype. This suggests some phenotypical signal retention mechanism or information storage in or around the cell. Secondly, this effect was transient; it wears off (Figure 44). We suggest here that the single pulse model comes closer to the actual physiological wound healing situation. Upon a TGFβ1 insult, affected fibroblasts differentiate into myofibroblasts to fulfill the functional requirement of ECM production and contraction; these cells subsequently undergo apoptosis in physiological healing [Rieder et al. 2007]. In a similar manner, collagen I production and α-SMA expression remain elevated 7 days post-pulse and subsequently, production of collagen I and α-SMA was scaled down. Myofibroblast reversibility also occurs in liver fibrosis when the insult is removed [Dufour et al. 1997]. Specifically for collagen synthesis, there exists a regulatory propeptide-mediated feedback on procollagen synthesis in human lung fibroblast cultures [Aycock et al. 1986, Wu et al. 1991], although it remains unknown if the decrease in collagen I expression observed is part of a negative feedback loop due to excessive collagen deposition on the ECM and not the

reversibility of phenotype. In the dermal wound healing model, the highest amount of active TGFβ1 release is between days 5-7 post-wounding, with a subsequent decrease thereafter [Yang et al. 1999], similar to the results shown in Figure 18.

An additional pulse administered 24h later potentiated myofibroblast maintenance (Figure 20), and we suggest that this models a non-physiological *in vivo* wound healing situation. Pathological fibrotic conditions are characterized by the overproduction (and reduced remodeling) of ECM components and persistence of the myofibroblasts. Similarly, the multiple pulses model was characterized by elevated collagen I production and α-SMA expression 14 days post-pulse. However, it remains unknown if the myofibroblast markers revert to baseline levels after the assessed 14 days period.
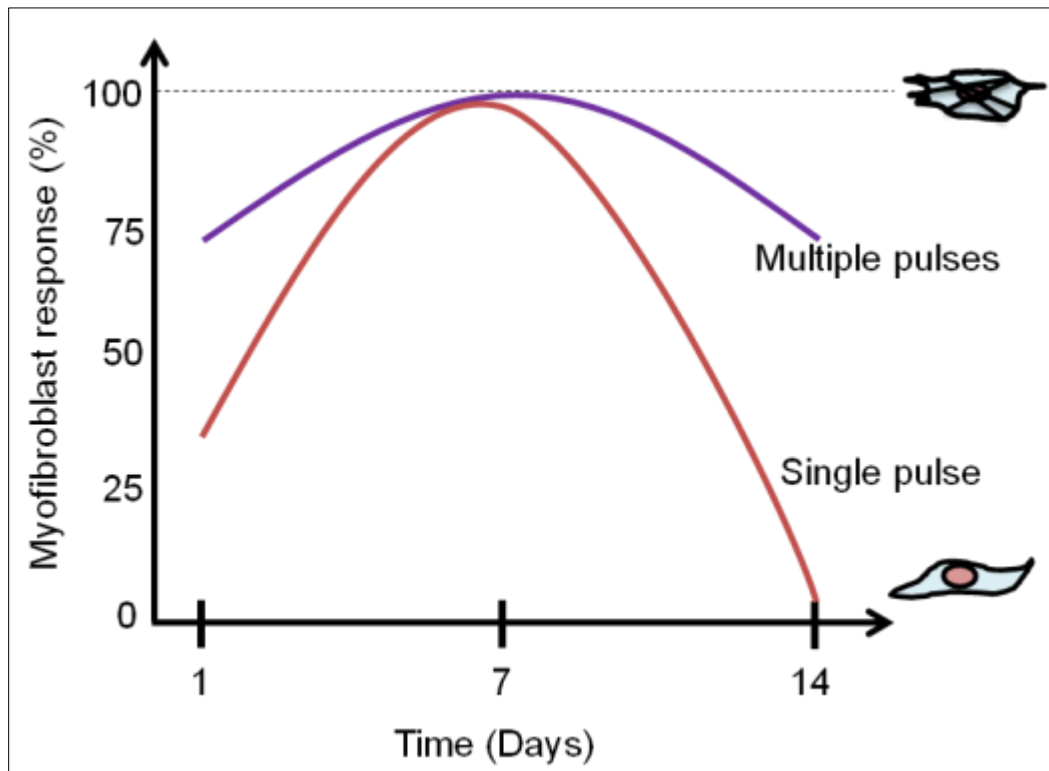
Figure 44. Theoretical myofibroblast response to single and multiple TGFβ1 pulse(s). A single pulse of TGFβ1 modeled physiological wound repair, with myofibroblastic response increasing initially and decreasing after 7 days. Double TGFβ1 pulses extended this effect.

Comparing the newly developed *in vitro* models to traditional 4 days TGFβ1 treatment (Figure 17), we demonstrated that the double pulses model (fibrotic condition) parallels the traditional 4 days TGFβ1 treatment. This suggests that the current *in vitro* model, besides being a poor reflection of *in vivo* cytokine regulation, is insufficient as an *in vitro* model for physiological wound healing, but suffices as a platform for fibrotic pathologies.

Pulsatile impact of cytokines (or TGFβ1) on target cells is not well studied, but it is conceivable that it offers advantages over continuous exposure. It avoids down-regulation of receptors on target cells as a possible response to signal bombardment [Hsieh et al. 1998]. While this keeps cells continuously responsive, it also reduces inertia in a feedback system. In contrast to hormones, growth factors work locally in a diffusion perimeter around releasing cells and can be stored and moved around in the ECM [Duchesne et al. 2012]. Release of TGFβ1 can be due to direct secretion (for example by inflammatory) cells or by proteolytic or mechanical release from matrix storage points, but it is not known whether these modes generate a continuous or a pulsatile-like scenario. In line with our findings, Webber et al. demonstrated that 72h treatment of TGFβ1 and removal thereafter induced a stable myofibroblast phenotype, mediated through SMAD3 phosphorylation, for up to 5 days in lung fibroblasts [Webber et al. 2009]. However, we establish that a short (0.5h) TGFβ1 pulse was sufficient for myofibroblast induction and maintenance, suggesting signal retention. TGFβ1 – TβRI/II interaction leads to phosphorylation of receptor activated SMADs (R-SMAD) SMAD2/3 and subsequent transcriptional regulation [Shi et al. 2003]. In a similar study focusing on TGFβ1/SMAD signaling dynamics, it was reported that cells have differing SMAD2-phosphoylation responses towards continuous and pulsatile TGFβ1 stimulation [Zi et al. 2011]. Further, we present novel evidence that trypsin passaging of myofibroblasts affected their phenotype (Figure 24). Trypsin, a serine protease, catalyzes the hydrolysis of peptide bonds [Rawlings et al. 1994], thereby releasing adherent cells off its surface, making it a useful tool in cellular sub-culture. Transformed cells are more

sensitive to trypsin [Brugmans et al. 1978], which provide an explanation as to why trypsin altered phenotypic properties in myofibroblasts but not fibroblasts. Trypsin also preferentially hydrolyses the main components of histone proteins (lysine and arginine residues), and trypsinzation of calf thymus cells was observed to release and hydrolyse histones, thereby compromising and disrupting nuclei structural integrity [Allfrey et al. 1962]. This suggests that trypsin passaging possibly altered histone properties in the passaged myofibroblasts.

The mRNA expression levels of selected fibrotic genes (from microarray) were quantified (Figure 19, Figure 21) and results summarized in Table 8.

Model	Single Pulse – 0.5h, 4h			Multiple Pulse – 2 x 0.5h, 2 x 4h		
Gene/Day	1	7	14	1	7	14
ACTA2 (α-SMA)	↑↑	=	=	↑↑	↑	=
FZD8	↑↑	↑	=	↑↑	↑	=
NOX4	↑↑	=	=	↑↑	↑	=
TSPAN2	↑↑	↑	=	↑↑	↑	↑

Table 8. Gene expression levels of selected fibrotic genes in the single versus double pulse(s) model. *Legend: ↑↑ indicates a marked elevation in mRNA expression and ↑ slightly elevated w.r.t untreated controls.*

ACTA2 (α-SMA): A single TGFβ1 pulse increased ACTA2 mRNA levels 24h post treatment, indicating elevated transcriptional activity, and post-translational conversion within a window of 7 days to the protein form. Multiple pulses extended this effect. ACTA2 expression reverted to baseline levels despite the persistence of protein expression, highlighting the variation between mRNA and actual protein levels, which casts light on mRNA levels solely taken as functional markers in experimental studies.

FZD8: We firstly demonstrate that FZD8 was elevated 1 and 7 (slight) days post TGFβ1 pulses. Cultures were washed with HBSS to remove traces of exogenous TGFβ1, suggesting that there was an ongoing TGFβ1 loop as a reactive response to the pulse(s). TGFβ1 – TβRI/II interaction triggers a cascade of events which activates the canonical Wnt/β-catenin pathway required for

96

TGFβ1-mediated fibrogenesis *in vitro* and *vivo* [Akhmetshina et al. 2012]. In the mouse model, Wnt/β-catenin signaling promoteed increased synthesis of FN [Surendran et al. 2005], the progression of chronic renal injury [Surendran et al. 2005] and renal interstitial fibrosis [He et al. 2009].

NOX4: *In vivo* studies showed that NOX4 inhibition exhibited curative effects [Laleu et al. 2010]. Also, knockdown of NOX4 in the bleomycin mouse model abrogated lung fibrosis [Hecker et al. 2010]. NOX4 was expressed in thickened pulmonary arteries of IPF patients [Pache et al. 2011] and was observed to be responsible for generation of ROS in injured cardiac tissue [Kuroda et al. 2010], thereby correlating its relationship in both cardiac and pulmonary fibrosis. NOX4 was also a mediator in hepatic fibrosis [Paik et al. 2011]. In the model, increased NOX4 expression suggests the probable production of ROS as part of a first-phase response to TGFβ1 pulse(s). Downregulation at days 7 and 14 post-pulse suggest that ROS was no longer present after a single TGFβ1 pulse. We propose that an additional TGFβ1 pulse prolonged ROS production.

TSPAN2: Presenting a general overview, in airway diseases (such as CF), TSPAN24/CD151 was observed to be an identification marker indicating the capacity of human adult basal cells for restoration of functional airway epithelial [Hajj et al. 2007]. TSPAN26/CD37 induced inflammation and knockdown of TSPAN26 attenuated glomerular IgA nephropathy [Rops et al. 2010]. TSPAN2 has not been implicated in fibrosis and we show for the first time, elevated TSPAN2 mRNA levels, concomitant to increased collagen I production, in response to TGFβ1 pulse(s).

5.2   *Investigating the memorized effects of TGFβ1 pulses*

In this section, we investigated three mechanisms – autocrine TGFβ1 production, epigenetic changes and cell – ECM influence to explain the memorized effects of TGFβ1 pulses. Firstly investigating autocrine TGFβ1 production, we noticed with great interest that a single pulse of

exogenous TGFβ1 led to the subsequent release of endogenous active TGFβ1 and therefore to an autocrine stimulation that was dampened during the first 24 hours (Figure 22a – b). Although we observe elevated latent TGFβ1 production after TGFβ1 pulses (Figure 22c – d), it remains unclear if the cells activate latent TGFβ1 storage. Wipff et al. demonstrated that latent TGFβ1 was stored in the ECM and myofibroblasts deposited and activated latent TGFβ1 stores in a contractile dependent manner [Wipff et al. 2008], and we propose that a latent TGFβ1 activation loop, mediated by myofibroblast contraction may contribute to the maintenance of phenotype after TGFβ1 pulse(s).

SAHA hyperacetylated histone-3 [Wang et al. 2009] leading to the speculation that acetylation changes mediated gene transcription after TGFβ1 treatment. Therefore, at the next level of intracellular changes that transiently stabilise the myofibroblast phenotype after a single TGFβ1 pulse; we considered epigenetic modifications affecting histone acetylation and DNA methylation. We could not establish significant changes of histone acetylation (Figure 23), and a CpG methylation scan of the proximal promoter regions of selected TGFβ1-responsive genes (ACTA and COL1A1, Table 7) was inconclusive, likely because these genes are downstream effector genes of TGFβ1 treatment. While this does not rule out methylation changes in other genes and regions under TGFβ1, this appears to fit the transient nature of the phenotypic change we have observed.

As the next option, we considered microenvironmental changes based on the notion of matrix reciprocity [Bisell et al. 1982, Sage et al. 1982]. We observed that the memorized TGFβ1 effects were a result of ECM influences (Figure 26). SDS-PAGE analysis of collagen deposition on decellularised ECM revealed minimal collagen I deposition (Figure 25c – d), likely due to the short culture period. However, ICC results suggested that the amount of collagen I deposited sufficed as a platform to assess the ECM's influence on untreated fibroblasts. TGFβ1 pulses elevated collagen I and FN deposition (Figure 25e – f), and of strong relevance to our

observations, the FN ED-A (splice variant) domain was observed to be crucial for TGFβ1 dependent myofibroblast induction in primary fibroblasts [Serini et al. 1998]. FN also colocalized with integrins, a mediator of contraction in fibrosis [Schultz et al. 2011, Wipff et al. 2008]. Taken together, the collagen I and FN network may functionally mediate phenotype changes in the untreated fibroblasts, probably through an array of bio- and/or mechanochemical stimulus [Rieder et al. 2007, Kis et al. 2011]. We observed with great interest that the M1 ECM (compared to M7) was better able to induce myofibroblast differentiation. We propose that this could be attributed to a variety of reasons: **a)** elevated LTBP-1 expression in M1 ECM (Figure 27a, discussed below); **b)** ECM remodeling, mediated by MMPs and proteases over the 7 day period, thereby reducing 'myofibroblast inductive' molecules required for differentiation; **3)** production of other profibrogenic cytokines (e.g. CTGF, PDGF) [Widgerow et al. 2011]; and **4)** the rapid kinetics of SMAD assembly, nuclear accumulation and subsequent activation of transcription of fibrogenic genes. TGFβ1 – TβRI/II leads to SMAD signaling processes and the formation of heteromeric complex SMAD2/3 – 4 which is translocated to the nucleus [Heldin et al. 1997]. Recently, it had been shown that the formation of heteromeric complex and nuclear translocation of SMAD2/3 – 4 takes place within 20 mins [Zieba et al. 2012]. An additional TGFβ1 pulse was observed to increase the expression of classic myofibroblast markers. Increasing TGFβ1 concentrations has been shown to be directly proportional to SMAD phosphorylation [Webber et al. 2009, Zi et al. 2011], and we suggest that this was a result of elevated on-going TGFβ1 signaling and transcriptional processes. The ECM control was observed to exhibit reduced α-SMA and collagen I expression as compared to TCP control and this may be attributed to a collagen I feedback mechanism which acts to downregulate and/or suppress basal collagen I through propeptide-mediated feedback regulatory role on procollagen synthesis and α-SMA expression in the re-seeded fibroblasts [Aycock et al. 1986, Wu et al. 1991]. In line with our findings, studies by other groups have reported ECM-dependent myofibroblast differentiation. Vitronectin mediated corneal myofibroblast differentiation [Wang et

al. 2012], collagen type VI induced myofibroblast differentiation in cardiac fibroblasts [Naugle et al. 2006] and ECM accumulation increased the development of dermal fibroblasts [Distler et al 2007].

LTBP-1 interacted directly with TGFβ1 [Saharinen et al. 2000] and was elevated in M1 ECM (Figure 27a), suggesting LTBP-1-mediated myofibroblast activation. In relation to our findings, LTBP-1 was observed to modulate the bioactivity of TGFβ1 [Mangasser-Stephan et al. 2001], and was upregulated in IPFs [Khalil et al. 2001]. *In vivo*, LTBP-1 knockout mice displayed increased resistance to hepatic fibrogenesis [Drews et al. 2008], suggesting that LTBP-1 direct association with TGFβ1 bioactivity. Double immunofluorescence staining reported the co-localization of LTBP-1 with FN and collagen I [Mangasser-Stephan et al. 2001]. It is not known whether LTBP-1 co-localizes with collagen I and FN our system, but the coincidental elevated collagen I, FN and LTBP-1 deposition observed suggests that collagen I and FN have in part, a role to play in the LTBP-1 regulation of the myofibroblast phenotype. A schematic depicting the proposed ECM-dependent latent TGFβ1 release and activation is illustrated in Figure 27b. It has been previously shown that the myofibroblast ECM contained self-generated TGFβ1 stores and activated latent TGFβ1 storage in a contractile dependent manner [Wipff et al. 2007, 2008]. Similarly, we propose that the release of latent TGFβ1 was mediated by contractile myofibroblasts which were more efficient in utilizing the self-generated TGFβ1 stores available on the M1 TGFβ1-pulsed ECM.

In a crossover experiment, we show that the normal fibroblast ECM reduced myofibroblast marker expression in normal and pathological myofibroblasts. Normal fibroblast ECM reduced to or reduced below fibroblast levels, collagen I production in re-seeded WI-38 (Figure 31) and HSF (Figure 32) myofibroblasts respectively, suggesting that the ECM contained soluble factors which regulated collagen production – a classic case where cues from the ECM modulated cell phenotype [Bisell et al. 1982, Widgerow et al. 2010, Schultz et al. 2011]. We suggest that

integrin-mediated cell attachment to collagens mediated increased MMP production [Steffensen et al. 2001] and ECM degradation, mechanisms which interfered with collagen suppression. Also, feedback from ECM components (e.g. collagen IV, proteoglycans) may act in synergy to blunt collagen production. In relation to our findings, the myofibroblast phenotype was reversed when myofibroblasts were cultured on Matrigel [Sohara et al. 2002] and cyropreserved amniotic membrane stromal surfaces [Li et al. 2008]. α-SMA expression however, remained unchanged in comparison to myofibroblasts, suggesting that ECM factors were unable to fully reverse the myofibroblast phenotype. Xie et al. demonstrated that HSFs exhibited higher endogenous SMAD2, along with lower inhibitory SMAD7 levels [Xie et al 2008], increased sensitivity to TGFβ1 [Chen et al. 2002] and produced CTGF [Colwell et al. 2005], suggesting that an on-going TGFβ1 – SMAD2/3 signaling loop probably perpetuated the maintenance of α-SMA expression. Also, we propose that fibroblast ECM components (collagen I and FN) maintained α-SMA expression in the re-seeded myofibroblasts. Substantiating our proposition, collagen I [Li et al. 2008] and FN ED-A [Serini et al. 1998] mediated myofibroblast maintenance. HSFs also exhibited increased FN deposition [Kischer et al. 1983] suggesting that FN (ED-A domain) plays a role in myofibroblast maintenance. Myofibroblast contraction may also activate basal latent TGFβ1 stores [Wipff et al. 2008], contributing to phenotypic maintenance. The normal fibroblast ECM however, appeared to have no effect on IPFs (Figure 33). IPFs endogenously expressed high levels of COL1A1 and TGFβ1 mRNA [Ramos et al. 2001] and NOX4 [Amara et al. 2010]; NOX4 being a crucial factor in TGFβ1-induced myofibroblast activation and fibrogenic response [Amara et al. 2010, Hecker et al. 2009, Bocchino M et al. 2010], suggesting that elevated endogenous NOX4 and TGFβ1 levels contributed to phenotypic maintenance. There has been limited reports of SMAD regulation in IPFs but we cannot rule out that TGFβ1 stimulation may have resulted in an NOX4 mediated autocrine positive loop of TGFβ1 signaling and production. Also IPF myofibroblasts could possibly remodel the ECM, contributing to phenotypic maintenance. Reduced α-SMA expression in the ECM negative control was observed, similar to

101

the ECM control in Figure 26, suggesting that this was a result of the fibroblast ECM feedback mechanism interfering with α-SMA transcriptional regulation. HSF myofibroblasts cultured on ECM and further stimulated with TGFβ1 (ECM positive control in Figure 32) expressed reduced collagen I production suggesting that exogenous TGFβ1 was not able to over-ride signals from the ECM. It is not known if collagen I feedback from the ECM may play a regulatory role on procollagen synthesis in the re-seeded myofibroblasts [Aycock et al. 1986, Wu et al. 1991].

Taken together, it appears that without appropriate cues from the ECM, myofibroblasts aim to remodel a normal ECM, making it fibrotic in nature (e.g. IPFs). With the HSF and WI-38 myofibroblasts however, the normal fibroblast ECM-mediated cues blunted collagen production, leading to reduced ECM accumulation.

5.3 *Revisiting SAHA's anti-fibrotic potential*

SAHA was non-toxic to fibroblasts, consistent with the findings of other groups [Wang et al. 2009, Cho et al. 2012]. The effector caspase-3/7 plays an essential role in the signal transduction of apoptotic cues and was elevated 1 day post-SAHA treatment (Figure 35), suggesting that SAHA increased caspase-dependent sensitivity of myofibroblasts to apoptotic signals. In agreement with our findings, HDACi TSA induced apoptosis in pathological keloid fibroblasts [Diao et al. 2011]. Caspase activity is an early marker along the apoptotic pathway and the decreased caspase-3/7 activity observed at days 2 – 3 after SAHA treatment does not rule out other mechanistic events along the apoptotic pathway (e.g. DNA fragmentation) which could be taking place concurrently.

Revisiting SAHA's effects in conjunction with TGFβ1 pulse(s), SAHA anti-fibrotic effects were determined and are summarized in Table 9.

Model	4h TGFβ1 pulse				2 x 4h TGFβ1 pulse			
Day	Day 1		Day 7		Day 1		Day 7	
Marker	Col I	α-SMA	Col I	α-SMA	Col I	α-SMA	Col I	α-SMA
Pre-treat	=	=	—	—	—	—	—	—
Post-treat	=	↓	↓	—	↓	↓	↓	—
Pre- & post-treat	=	↓	=	↓	=	↓	↓	—

Table 9. Summary of SAHA treatment versus TGFβ1 pulse(s). Pre- and post- SAHA treatment exhibied the most significant effects in reducing collagen I production and α-SMA expression. *Legend: ↓ indicates a reduction in marker expression; — indicates no effect; and = represents normalization of expression w.r.t TGFβ1 positive myofibroblast control.*

When administered in conjunction with TGFβ1 pulses, SAHA possessed anti-fibrotic potential. SAHA exhibited the highest anti-fibrotic potential 1 day post-SAHA treatment and it appeared that the duration of SAHA treatment correlated to anti-fibrotic effects, suggesting: **1)** SAHA's reversible effects; and **2)** the interference of SAHA with TGFβ1 signaling.

1) <u>SAHA's effects were reversible</u>

We demonstrated SAHA's reversible effects (Figure 45), suggesting that SAHA was no longer able to exert anti-fibrotic effects when removed from culture media. Confirming our findings, the reversible effects of HDACi LBH589 action was previously reported [Beckers et al. 2007]. SAHA's reversibility also suggests that the use of SAHA minimizes spill-over effects after therapy. Also, one should be able to tailor SAHA treatment in the specific window to modulate desired modification(s).
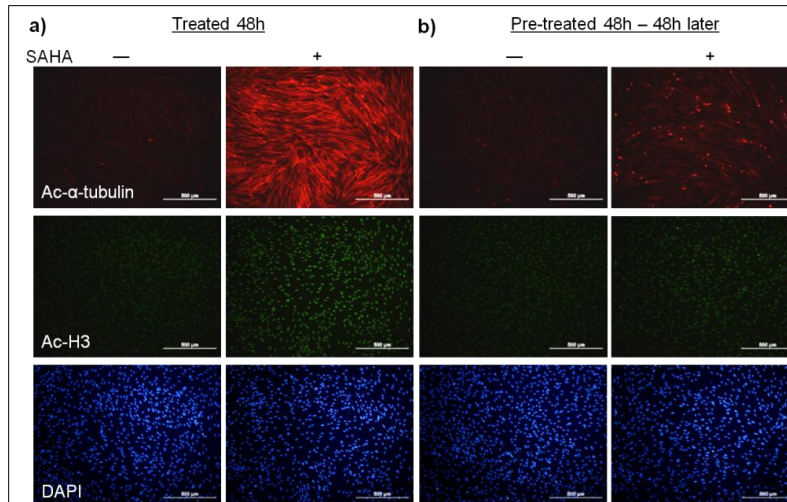
Figure 45. Reversible effects of SAHA-induced hyperacetylation on α-tubulin and histone 3. Fibroblasts were treated with and without SAHA for 48h. Cultures were assessed (a) immediately; and (b) 48h post-SAHA removal. Fibroblasts were maintained in 0.5% FBS DMEM post-SAHA removal.

2) Interference of SAHA with TGFβ1 signaling: SMAD-dependent and independent mechanisms

We propose that SAHA interfered with the TGFβ1 signaling process by: **1)** competing or interfering with SMAD regulation and activation; **2)** stabilizing SMAD7 inhibitory action; and **3)** interfering through 5'-TG-3'-interacting factor (TGIF) homeoproteins. Supporting our proposition, the literature has demonstrated the relationship between HDAC and SMADs. **1)** HDACi TSA inhibited nuclear translocation and DNA binding of SMAD3/4 complex in SSc fibroblasts [Huber et al. 2007]; and inhibited TGFβ1-induced SMAD2/3 [Cho et al. 2012]. **2)** TSA rescued TGFβ1-suppressed SMAD7 signaling [Cho et al. 2012]. Authors also reported that HDAC1-mediates SMAD7 deacetylation and decreased its stability [Simonsson et al. 2005]. Therefore, SAHA may hyperacetylate and stabilize SMAD7, but further work is required to elucidate this. **3)** TGIF-1 and -2 are two endogenous repressors of the TGFβ1 signaling pathway. siRNA specific downregulation of HDAC4 stimulated the expression of TGIFs [Glenisson et al. 2007], demonstrating the relationship between HDACs and TGIFs. Also, TSA affected TGFβ1-mediated SMAD signaling and strongly induced the expression of TGIFs [Rombouts et al. 2004].

HDACi also has been shown to interfere with transcriptional regulation in a SMAD-independent manner. TSA neither altered SMAD expression nor activation, but instead suppressed TGFβ1-induced expression of Sp1, an essential transcription factor for SMAD-dependent collagen synthesis [Ghosh et al. 2007]. In the presence of TGFβ1, TSA abrogated the induction of cell-cell and cell-ECM modulators, disintegrin and metalloproteinase 12 (ADAM12) and TIMP1 genes, without affecting SMAD phosphorylation [Barter et al. 2010]. Taken together, independent studies suggested that SAHA may affect TGFβ1-induced myofibroblast differentiation in a SMAD-dependent and -independent manner.

Our results are also aligned with current literature of HDACi and collagen production. Valproic acid decreased collagen-induced arthritis disease severity by decreasing collagen production [Saouaf et al. 2009]. HDACi sodium valproate and phenylbutyrate inhibited collagen I mRNA and protein expression in HSCs [Rishikof et al. 2004, Wantanabe et al. 2011]. TSA normalized TGFβ1-induced collagen synthesis in skin [Ghosh et al. 2007], keloid [Diao et al. 2011] and SSc fibroblasts [Wang et al. 2006]. Therefore, we speculate that SAHA treatment in conjunction with TGFβ1 pulse(s) interfered with downstream mediators of the collagen I biosynthesis pathway. In summary, the current literature supports the hypothesis that HDACi SAHA reduced myofibroblast marker expression by: **1)** competing or interfering with SMAD regulation and activation, **2)** functioning as a transcriptional co-repressor in the TGFβ1 transcriptional axis and **3)** increasing the stability of inhibitory SMAD7.

Exploring another facet of myofibroblast locomotion, we have demonstrated that SAHA compromised myofibroblast migration (Figure 42), suggesting the inhibition of HDAC6 (Class IIb), an essential HDAC required for cellular motility [Tran et al. 2007]. Also, it has been previously established that the presence of α-SMA was a signal for retardation of migratory behavior in myofibroblasts [Rønnov-Jessen et al. 1996]. SAHA reduced or normalised α-SMA expression in comparison to the myofibroblast controls, and this could explain migratory

retardation in SAHA-treated myofibroblasts. SAHA however, had no effect on myofibroblast contractility (Figure 43). Interestingly, it was recently shown that HDAC8 (Class I) associated with α-SMA to regulate cell contractility [Waltregny et al. 2005]. Our findings suggest the preferential inhibition of HDAC6. Indeed, SAHA, a non-selective HDACi for Class I/II HDACs, exhibited higher binding affinity to HDAC6 [Estiu e al. 2008, Wang et al. 2011], and significantly weaker (≈100x less) inhibition of HDAC8 [Estiu et al. 2008, Khan et al. 2008], a result of evolutionary divergence and differential structural characteristics between HDAC6 and HDAC8 [Estiu et al. 2008, KrennHrubec et al. 2007].

Chapter 6

Conclusions and Future Work

This chapter presents the overall conclusions of the project and discusses future work options for scientific advancement in the field of peri-implant fibrosis.

6.1 Conclusion

Fibroproliferative diseases and fibrosis around organs and implants continue to pose a substantial disease burden today and a therapeutic solution is keenly sought. Central to the progression of fibrosis are the myofibroblasts. There remains an unmet need for an effective anti-fibrotic therapeutic agent that can reverse or blunt the progression of fibrosis. In an indication discovery approach, our group has previously established the anti-fibrotic potential of FDA-approved HDACi, SAHA [Wang et al. 2009]. However, SAHA was unable to abrogate TGFβ1-effects if cultures were exposed to TGFβ1 treatment 24h before SAHA treatment.

1) To better assess the anti-fibrotic potential of SAHA, we developed a patho-physiologically relevant model to recapitulate pulsatile *in vivo* cytokine regulation on an *in vitro* platform. We demonstrated that a single 0.5h TGFβ1 pulse had long-term effects on the myofibroblast phenotype, and that this effect can be potentiated by a second pulse one day later. Further, we described the regulation and trend of selected fibrogenic genes in response to TGFβ1 pulse(s). We believe that our current model is a more realistic reflection of *in vitro* wound healing. It will form the basis for future anti-fibrotic therapy screening, and should contribute to the current knowledge of TGFβ1 and the understanding of myofibroblast induction and maintenance.

2) Intrigued by the long-lasting changes observed with a TGFβ1 pulse(s), we assessed mechanistic events which may contribute towards the myofibroblast phenotype maintenance. Although we did not observe epigenetic changes, we observed that the memorized effects of TGFβ1 were based on cell-matrix reciprocity: the microenvironment appears to retain a memory of TGFβ1 insults in the form of biochemical cues, including higher levels of endogenous LTBP-1 deposition on the ECM. This suggests that a positive feed-back loop was established and should in turn, lead to the perpetuation of the myofibroblast phenotype after limited TGFβ1 treatment. However, this was not the case and we observed instead the dampening and erasure of myofibroblast induction signals possibly due to matrix turnover and remodeling. In the crossover experiment, we demonstrated that the normal fibroblast ECM was able to normalize or reduce to fibroblast levels, collagen I production in WI-38 and HSF myofibroblasts, but not IPF fibroblasts. This suggests that biochemical cues from normal fibroblast ECM were able to remove cues for elevated collagen I production in the myofibroblasts. Together, the study on cell-ECM reciprocity has bearing for the development of antifibrotic therapy and points to future research avenues to study fibrotic processes.

3) Revisiting SAHA's effects in conjunction with TGFβ1 pulse(s), we demonstrated the reduction of classic myofibroblast markers in comparison with the myofibroblasts controls. This study provided valuable insight by reconfirming SAHA's anti-fibrotic potential in a physiologically relevant setting. Targeting another dimension of anti-fibrotic therapy, we presented evidence of compromised myofibroblast motility but not contractility.

Our findings contribute towards the understanding of TGFβ1-mediated myofibroblast induction and maintenance and the use of SAHA to curb fibrosis. SAHA is currently in clinical use for T-cell lymphoma treatment and data derived from this study, and subsequent *in vivo* studies can be faster translated towards clinical treatment of peri-implant fibrosis.

6.2 Future Work

a) The fibroblast ECM mode of action is still unknown and mass spectrometry analysis of soluble fractions in the ECM may unravel certain targets which may form or assist in anti-fibrotic therapy. The ECM can further be used as a platform to assess the anti-fibrotic potential in other cell lines. Incorporation of the decellularized ECM with anti-fibrotic agents and employed as a platform to assess drug efficacy in a native system will also serve as a feasible option for future exploration.

b) SAHA's mode of action in anti-fibrosis still continues to elude us and it would be interesting to single out independent or group of enzymes which are responsible for SAHA's effects, and the point at which SAHA interferes with TGFβ1 signaling. Also, SAHA could be incorporated into decellularized fibroblasts ECM and this study will potentially lay foundation for drug-mediated ECM treatment.

c) This thesis provides further promising evidence of SAHA's anti-fibrotic effects, and the next stage would be to move into studying SAHA's effects in a preclinical animal model. We have designed a peri-implant model which will involve a pilot and exploratory study. Briefly, commercial 0.22µM filtered ovalbumin (Sigma-Aldrich, St. Louis, MO) and/or drug of interest, SAHA will be loaded into the ALZET® (Durect Corporations, Cupertino, CA) osmotic pump. The pump will be subcutaneously implanted on the dorsal surface of the mouse.

Pilot study: The ALZET® pump will provide continuous infusion of commercial grade ovalbumin to site of interest. Animals will be sacrificed every fortnight, with the last experimental endpoint 2 months post-implant to study onset of fibrosis. Histopathological studies (staining of collagen I and α-SMA) will be performed on excised implant and surrounding tissue.

<u>Exploratory Study</u>: To assess SAHA efficacy in preventing the occurrence of peri-implant fibrosis, the ALZET® pump will provide continuous infusion of ovalbumin and SAHA to the targeted region. After 3 – 4 weeks post-implant (using onset of fibrosis data obtained from pilot study), the animals will be sacrificed. To assess the efficacy of SAHA in curbing or reducing fibrosis after it has been established, the animals will first undergo a surgery for ovalbumin infusion. Upon the onset of fibrosis, the ovalbumin-filled pump will be removed and a new SAHA-filled pump will be implanted in place of the old pump. Histopathological studies, biochemical assays and histochemistry will be performed on extracted tissue.

Bibliography

1.   Abe R, Donnelly SC, Peng T, Bucala R, Metz CN. Peripheral blood fibrocytes: differentiation pathway and migration to wound sites. *J Immunol.* 2001

2.   Aiken SP, Brown WM. Treatment of epilepsy: existing therapies and future developments. *Front Biosci.* 2000

3.   Akhmetshina A, Palumbo K, Dees C, Bergmann C, Venalis P, Zerr P, Horn A, Kireva T, Beyer C, Zwerina J, Schneider H, Sadowski A, Riener MO, MacDougald OA, Distler O, Schett G, Distler JH. Activation of canonical Wnt signalling is required for TGF-β-mediated fibrosis. *Nat Commun.* 2012

4.   Allfrey VG, Faulkner R, Mirsky AE. Acetylation and methylation of histones and their possible role in the regulation of RNA synthesis. *Proc Natl Acad Sci USA* 1964

5.   Allfrey BVG, Littau VC, Mirsky AE. On the role of histones in regulating ribonucleic acid synthesis in the cell nucleus. *Biochemistry.* 1962

6.   Alvarez-Breckinridge CA. The HDAC inhibitor valproic acid lessens NK cell action against oncolytic virus-infected glioblastoma cells with inhibition of STAT5/T-BET signaling and IFNγ generation. *J. Virology.* 2012

7.   Amara N, Goven D, Prost F, Muloway R, Crestani B, Boczkowski J. NOX4/NADPH oxidase expression is increased in pulmonary fibroblasts from patients with idiopathic pulmonary fibrosis and mediates TGFβ1-induced fibroblast differentiation into myofibroblasts. *Thorax.* 2010

8.   Anderson JM, Rodriguez A, Chang DT. Foreign body reaction to biomaterials. *Semin Immunol.* 2008

9.   Annes JP, Munger JS, Rifkin DB. Making sense of latent TGFβ1 activation. *J Cell Sci.* 2003

10.   Asano Y, Czuwara J, Trojanowska M. Transforming growth factor-β regulates DNA binding activity of transcription factor Fli1 by p300/CREB-binding protein-associated factor-dependent acetylation. *J Biol Chem.* 2007.

11.   Askari JA, Buckley PA, Mould AP, Humphries MJ. Linking integrin conformation to function. *J Cell Sci.* 2009

12.   Atadja P. Development of the pan-DAC inhibitor panobinostat (LBH589): successes and challenges. *Cancer Lett.* 2009

13.   Aumailley M., Gayraud B. Structure and biological activity of the extracellular ECM. *J. Mol. Med.* 1998

14.   Aycock R.S., Raghow R., Stricklin G.P, Seyer J.M, Kang A.H. Post-transcriptional Inhibition of Collagen and Fibronectin Synthesis by a Synthetic Homolog of a Portion of the Carboxyl-terminal Propeptide of Human Type I Collagen. *J. Biol Chem.* 1986

15.   van Amerongen MJ et al. Macrophage depletion impairs wound healing and increases left ventricular remodeling after myocardial injury in mice. *Am J Pathol* 2007

16.   Bartsich S, Ascherman JA, Whittier S, Yao CA, Rohde C. The breast: a clean-contaminated surgical site. *Aesthetic surgery journal.* 2011

17.   Barter MJ, Pybus L, Litherland GJ, Rowan AD, Clark IM, Edwards DR, Cawston TE, Young DA. HDAC-mediated control of ERK- and PI3K-dependent TGF-β-induced extracellular ECM-regulating genes. *ECM Biol.* 2010

18.   Barcellos-Hoff MH, Derynck R, Tsang ML, Weatherbee JA. Transforming growth factor-β activation in irradiated murine mammary gland. *J Clin Invest.* 1994

19.   Beidler SK, Douillet CD, Berndt DF, Keagy BA, Rich PB, Marston WA. Multiplexed analysis of ECM metalloproteinases in leg ulcer tissue of patients with chronic venous insufficiency before and after compression therapy. *Wound Repair Regen* 2008

20.   Beckers T, Burkhardt C, Wieland H, Gimmnich P, Ciossek T, Maier T, Sanders K. Distinct pharmacological properties of second generation HDAC inhibitors with the benzamide or hydroxamate head group. *Int J Cancer.* 2007

21.   Bechtel W, McGoohan S, Zeisberg EM, Müller GA, Kalbacher H, Salant DJ, Müller CA, Kalluri R, Zeisberg M. Methylation determines fibroblast activation and fibrogenesis in the kidney. *Nat Med.* 2010

22.   Bhattacharyya S, Wei J, Melichian DS, Milbrandt J, Takehara K, Varga J. The transcriptional cofactor nab2 is induced by TGFβ1 and suppresses fibroblast activation: physiological roles and impaired expression in scleroderma. *PLoS One.* 2009.

23.   Bissell MJ. The differentiated state of normal and malignant cells or how to define a "normal" cell in culture. *Int. Rev. Cytol.* 1981.

24.   Biernacka A, Dobaczewski M, Frangogiannis NG. TGF-β signaling in fibrosis. *Growth Factors.* 2011.

25.   Blantz RC, Munger K. Role of nitric oxide in inflammatory conditions. *Nephron.* 2002

26.   Bocchino M, Agnese S, Fagone E, Svegliati S, Grieco D, Vancheri C, Gabrielli A, Sanduzzi A, Avvedimento EV. Reactive oxygen species are required for maintenance and differentiation of primary lung fibroblasts in idiopathic pulmonary fibrosis. *PLoS One.* 2010

27.   Bornstein P, Sage EH. Matricellular proteins: extracellular modulators of cell function. *Curr Opin Cell Biol.* 2002

28.   Brahimi-Horn MC, Bellot G, Pouysségur J. Hypoxia and energetic tumor metabolism. *Curr Opin Genet Dev.* 2011

29.   Brem H, Tomic-Canic M. Cellular and molecular basis of wound healing in diabetes. *J Clin Invest* 2007

30.   Brugmans M, Cassiman JJ, Van Den Berghe H. Selective adhesion and impaired adhesive properties of transformed cells. *J Cell Sci.* 1978

31.   van den Berg B, Wain R, Dobson CM, Ellis RJ. Macromolecular crowding perturbs protein refolding kinetics: implications for folding inside the cell. *EMBO J.* 2000

32.   Chan E.C., F. Jiang, H.M. Peshavariya, G.J. Dusting. Regulation of cell proliferation by NADPH oxidase-mediated signaling: potential roles in tissue repair, regenerative medicine and tissue engineering. *Pharmacol Ther*, 2009

33.   Chang CC, Lieberman SM, Moghe PV. Leukocyte spreading behavior on vascular biomaterial surfaces: consequences of chemoattractant stimulation. *Biomaterials.* 1999

34.   Chen CZ, Raghunath M. Focus on collagen: in vitro systems to study fibrogenesis and antifibrosis state of the art. *Fibrogenesis Tissue Repair*. 2009

35.   Chen CZC, Peng YX, Wang ZB, Fish PV, Kaar JL, Koepsel RR, et al. The Scar-in-a-Jar: studying potential antifibrotic compounds from the epigenetic to extracellular level in a single well. *Br J Pharmacol* 2009

36.   Chen C, Loe F, Blocki A, Peng Y, Raghunath M. Applying macromolecular crowding to enhance extracellular ECM deposition and its remodeling in vitro for tissue engineering and cell-based therapies. *Adv Drug Deliv Rev*. 2011

37.   Chen W, Fu X, Sun T, Sun X, Zhao Z, Sheng Z. Change of gene expression of transforming growth factor-β1, Smad 2 and Smad 3 in hypertrophic scars skins. *Zhonghua Wai Ke Za Zhi*. 2002

38.   Chen P, Parks WC. Role of ECM metalloproteinases in epithelial migration. *J Cell Biochem*. 2009

39.   Cho JS, Moon YM, Park IH, Um JY, Moon JH, Park SJ, Lee SH, Kang HJ, Lee HM. Epigenetic regulation of myofibroblast differentiation and extracellular ECM production in nasal polyp-derived fibroblasts. *Clin Exp Allergy*. 2012

40.   Cicha I, Rüffer A, Cesnjevar R, Glöckler M, Agaimy A, Daniel WG, et al. Early obstruction of decellularized xenogenic valves in pediatric patients: involvement of inflammatory and fibroproliferative processes. *Cardiovasc Pathol*. 2011

41.   Clark RA, Ashcroft GS, Spencer MJ, Larjava H, Ferguson MW. Re-epithelialization of normal human excisional wounds is associated with a switch from αvβ 5 to αvβ 6 integrins. *Br J Dermatol*. 1996

42.   Coward WR, Watts K, Feghali-Bostwick CA, Knox A, Pang L. Defective histone acetylation is responsible for the diminished expression of COX2 in idiopathic pulmonary fibrosis. *Mol Cell Biol*. 2009.

43.   Coolen MW, Statham AL, Gardiner-Garden M, Clark SJ. Genomic profiling of CpG methylation and allelic specificity using quantitative high-throughput mass spectrometry: critical evaluation and improvements. *Nucleic Acids Res*. 2007

44.   Coward WR, Watts K, Feghali-Bostwick CA, Knox A, Pang L. Defective histone acetylation is responsible for the diminished expression of COX2 in idiopathic pulmonary fibrosis. *Mol Cell Biol*. 2009

45.   Colwell AS, Phan TT, Kong W, Longaker MT, Lorenz PH. Hypertrophic scar fibroblasts have increased connective tissue growth factor expression after TGF-β stimulation. *Plast Reconstr Surg*. 2005

46.   Crestani B, Besnard V, Boczkowski J. Signaling pathways from NADPH oxidase-4 to idiopathic pulmonary fibrosis. *Int J Biochem Cell Biol*. 2011

47.   Daley WP, Peters SB, Larsen M. Extracellular ECM dynamics in development and regenerative medicine. *J Cell Sci*. 2008

48.   Deckert J, Struhl K. Histone acetylation at promoters is differentially affected by specific activators and repressors. *Mol Cell Biol.* 2001

49.   DeMali, K. A., Wennerberg, K. and Burridge, K. Integrin signaling to the actin cytoskeleton. *Curr. Opin. Cell Biol*. 2003

50.   Desmoulière A, Geinoz A, Gabbiani F, Gabbiani G. Transforming growth factor-beta 1 induces alpha-smooth muscle actin expression in granulation tissue myofibroblasts and in quiescent and growing cultured fibroblasts. *J Cell Biol.* 1993

51.   Desmoulière A. Factors influencing myofibroblast differentiation during wound healing and fibrosis. *Cell Biol Int.* 1995

52.   Distler JH, Jüngel A, Huber LC, Schulze-Horsel U, Zwerina J, Gay RE, Michel BA, Hauser T, Schett G, Gay S, Distler O. Imatinib mesylate reduces production of extracellular ECM and prevents development of experimental dermal fibrosis. *Arthritis Rheum.* 2007

53.   Diao JS, Xia WS, Yi CG, Wang YM, Li B, Xia W, Liu B, Guo SZ, Sun XD. Trichostatin A inhibits collagen synthesis and induces apoptosis in keloid fibroblasts. *Arch Dermatol Res.* 2011

54.   Dolce CJ, Stefanidis D, Keller JE, Walters KC, Newcomb WL, Heath JJ, Norton HJ, Lincourt AE, Kercher KW, Heniford BT. Pushing the envelope in biomaterial research: initial results of prosthetic coating with stem cells in a rat model. *Surg Endosc* 2010

55.   Dovey OM, Foster CT, Cowley SM. HDAC1 but not HDAC2, controls embryonic stem cell differentiation. *Proc Natl Acad Sci USA.* 2010

56.   Draoui N, Feron O. Lactate shuttles at a glance: from physiological paradigms to anti-cancer treatments. *Dis Model Mech.* 2011

57.   Drews F, Knöbel S, Moser M, Muhlack KG, Mohren S, Stoll C, Bosio A, Gressner AM, Weiskirchen R. Disruption of the LTBP-1 gene causes alteration in facial structure and influences TGF-β bioavailability. *Biochim Biophys Acta.* 2008

58.   Dufour J.F, DeLellis, R, Kaplan M, Reversibility of hepatic fibrosis in autoimmune hepatitis. *J Ann Intern Med.* 1997

59.   Duchesne L, Octeau V, Bearon RN, Beckett A, Prior IA, Lounis B, Fernig DG: Transport of fibroblast growth factor 2 in the pericellular matrix is controlled by the spatial distribution of its binding sites in heparan sulfate. *PLoS Biol.* 2012

60.   Dvorak H.F, Brown L.F., Detmar M., Dvorak A.M. Vascular permeability factor/vascular endothelial growth factor, microvascular hyperpermeability, and angiogenesis. *Am. J. Pathol.* 1995

61.   Eberharter A, Becker PB. Histone acetylation: a switch between repressive and permissive chromatin. Second in review series on chromatin dynamics. *EMBO Reports* 2002

62.   Ekert JE, Murray LA, Das AM, Sheng H, Giles-Komar J, Rycyzyn MA. Chemokine (C-C motif) ligand 2 mediates direct and indirect fibrotic responses in human and murine cultured fibrocytes. *Fibrogenesis Tissue Repair.* 2011

63.   Ellmers LJ, Scott NJ, Piuhola J, Maeda N, Smithies O, Frampton CM, Richards AM, Cameron VA. Npr1-regulated gene pathways contributing to cardiac hypertrophy and fibrosis. *J Mol Endocrinol. 2007*

64.   El Bialy SA, El Kader KF, El-Ashmawy MB. Current Progress in Antifibrotics. *Curr Med Chem.* 2011

65.   Estiu G, Greenberg E, Harrison CB, Kwiatkowski NP, Mazitschek R, Bradner JE, Wiest O. Structural origin of selectivity in class II-selective HDAC inhibitors. *J Med Chem*. 2008

66.   Felsenfeld G, Groudine M. Controlling the double helix. *Nature.* 2003

67.   Ferguson MW, Whitby DJ, Shah M, Armstrong J, Siebert JW, Longaker MT. Scar formation: the spectral nature of fetal and adult wound repair. *Plast Reconstr Surg*. 1996

68.   FibroGen, Inc. FibroGen Reports that FG-4539, HIF-PH Inhibitor, is Renoprotective and Improves Renal Function in Preclinical Models of Acute Kidney Injury (*press release*). *San Diego, CA*. 2006

69.   Firth JD, Uitto VJ, Putnins EE. Mechanical induction of an epithelial cell chymase associated with wound edge migration. *J Biol Chem* 2008

70.   Finnin MS, Donigian JR, Cohen A, Richon VM, Rifkind RA, Marks PA, Breslow R, Pavletich NP. Structures of a HDAC homologue bound to the TSA and SAHA inhibitors. *Nature* 1999

71.   Flanagan CA, Millar RP, Illing N. Advances in understanding gonadotrophin-releasing hormone receptor structure and ligand interactions. *Rev. Reprod.* 1998

72.   Frank S., Hubner G., Breier G., Longaker M.T., Greenhalgh D.G., Werner S. Regulation of vascular endothelial growth factor expression in cultured keratinocytes. Implications for normal and impaired wound healing. *J. Biol. Chem*. 1995

73.   Fragiadaki M, Mason RM. EMT in renal fibrosis - evidence for and against. *Int J Exp Pathol*. 2011

74.   Fries KM, Blieden T, Looney RJ, Sempowski GD, Silvera MR, Willis RA, Phipps RP. Evidence of fibroblast heterogeneity and the role of fibroblast subpopulations in fibrosis. *Clin Immunol Immunopathol*. 1994

75.   Fulton AB. How crowded is the cytoplasm? *Cell*. 1982

76.   Furst DE, Fernandes AW, Iorga SR, Greth W, Bancroft T. Epidemiology of Systemic Sclerosis in a Large US Managed Care Population. *J Rheumatol* 2012

77.   Gan Q, Yoshida T, Li J, Owens GK. Smooth muscle cells and myofibroblasts use distinct transcriptional mechanisms for SMA-α expression. *Circ Res* 2007

78.   Gemmell CH, Black JP, Yeo EL, Sefton MV. Material induced up-regulation of leukocyte CD11b during whole blood contact: material differences and a role for complement. *J Biomed Mater Res*. 1996

79.   Gelse K et al. Collagens – structure, function and biosynthesis, *ADDR Rev.* 2003

80.   Ghosh AK, Vaughan DE. PAI-1 in tissue fibrosis. *J Cell Physiol*. 2012

81.   Ghosh AK, Varga J. The transcriptional coactivator and acetyltransferase p300 in fibroblast biology and fibrosis. *J Cell Physiol*. 2007

82.   Ghosh K, Ingber DE. Micromechanical control of cell and tissue development: implications for tissue engineering. *Adv Drug Deliv Rev* 2007

83.   Ghosh AK, Mori Y, Dowling E, Varga J. Trichostatin A blocks TGF-β-induced collagen gene expression in skin fibroblasts: involvement of Sp1. *Biochem Biophys Res Commun*. 2007

84.   Glozak MA, Sengupta N, Zhang X, Seto E. Acetylation and deacetylation of non-histone proteins. *Gene*. 2005

85.   Glenisson W, Castronovo V, Waltregny D. HDAC4 is required for TGFβ1-induced myofibroblastic differentiation. *Biochim Biophys Acta.* 2007

86.   Grieb G, Steffens G, Pallua N, Bernhagen J, Bucala R. Circulating fibrocytes: biology and mechanisms in wound healing and scar formation. *Int Rev Cell Mol Biol.* 2011

87.   Guo W, Shan B, Klingsberg RC, Qin X, Lasky JA. Abrogation of TGF-β1-induced fibroblast-myofibroblast differentiation by HDAC inhibition. *Am J Physiol.* 2009

88.   Harrell AG, Novitsky YW, Peindl RD, Cobb WS, Austin CE, Cristiano JA, Norton JH, Kercher KW, Heniford BT. Prospective evaluation of adhesion formation and shrinkage of intra-abdominal prosthetics in a rabbit model. *Am Surg.* 2006

89.   Hahnen E, Hauke J, Tränkle C, Eyüpoglu IY, Wirth B, Blümcke I. HDAC inhibitors: possible implications for neurodegenerative disorders. *Expert Opin Investig Drugs.* 2008

90.   Harrison CA, Gossiel F, Layton CM, Bullock AJ, Johnson T, Blumsohn A and MacNeil S. Use of an *in vitro* model tissue-engineered human skin to investigate the mechanism of skin graft contraction. *Tissue Eng.* 2006

91.   Hecker L, Vittal R, Jones T, Jagirdar R, Luckhardt TR, Horowitz JC, Pennathur S, Martinez FJ, Thannickal VJ. NADPH oxidase-4 mediates myofibroblast activation and fibrogenic responses to lung injury. *Nat Med.* 2009

92.   Hertig A, Flier SN, Kalluri R. Contribution of epithelial plasticity to renal transplantation-associated fibrosis. *Transplant Proc.* 2010

93.   Henninger N, Woderer S, Kloetzer HM, Staib A, Gillen R, Li L, et al. Tissue response to subcutaneous implantation of glucose-oxidase-based glucose sensors in rats. *Biosens Bioelectron.* 2007

94.   Heldin, C., Miyazono, K., & Dijke, P. TGF-b signalling from cell membrane to nucleus through SMAD proteins. *Nature.* 1997

95.   He Chen, Wei-Wei Yang, Qiu-Ting Wen, Li Xu, Ming Chen. TGF-β induces FAP expression. *Experimental and Molecular Pathology* 2009

96.   Hemmann S, Graf J, Roderfeld M, Roeb E. Expression of MMPs and TIMPs in liver fibrosis - a systematic review with special emphasis on anti-fibrotic strategies. *J Hepatol.* 2007

97.   He W, Dai C, Li Y, Zeng G, Monga SP, Liu Y. Wnt/β-catenin signaling promotes renal interstitial fibrosis. *J Am Soc Nephrol.* 2009

98.   Hemmatazad H, Rodrigues HM, Maurer B, Brentano F, Pileckyte M, Distler JH, Gay RE, Michel BA, Gay S, Huber LC, Distler O, Jüngel A. HDAC7, a potential target for the antifibrotic treatment of systemic sclerosis. *Arthritis Rheum.* 2009

99.   Hinz B, Mastrangelo D, Iselin CE, Chaponnier C, Gabbiani G. Mechanical tension controls granulation tissue contractile activity and myofibroblast differentiation. *Am J Pathol.* 2001

100.   Hsieh SC, Graves DT: Pulse application of platelet-derived growth factor enhances formation of a mineralizing matrix while continuous application is inhibitory. *J Cell Biochem.* 1998

101.   Huber P.E., Bickelhaupt S., Peschke P., Tietz A., Wirkner U., Lipson K.E., Heidelberg D.E. Reversal of Established Fibrosis by Treatment with the Anti-CTGF

Monoclonal Antibody FG-3019 in a Murine Model of Radiation-Induced Pulmonary Fibrosis. *Am J Respir Crit Care Med*. 2010

102.   Hubbert C, Guardiola A, Shao R, Kawaguchi Y, Ito A, Nixon A, Yoshida M, Wang XF, Yao TP., Huang L, Pardee AB. Suberoylanilide hydroxamic acid as a potential therapeutic agent for human breast cancer treatment. *Mol Med*. 2000

103.   Huang SK, Fisher AS, Scruggs AM, White ES, Hogaboam CM, Richardson BC, Peters-Golden M. Hypermethylation of PTGER2 confers prostaglandin E2 resistance in fibrotic fibroblasts from humans and mice. *Am J Pathol*. 2010

104.   Hu B, Gharaee-Kermani M, Wu Z, Phan SH. Essential role of MeCP2 in the regulation of myofibroblast differentiation during pulmonary fibrosis. *Am J Pathol*. 2011

105.   Hu B, Gharaee-Kermani M, Wu Z, Phan SH. Epigenetic regulation of myofibroblast differentiation by DNA methylation. *Am J Pathol*. 2010

106.   Huber LC, Distler JH, Moritz F, Hemmatazad H, Hauser T, Michel BA, Gay RE, Matucci-Cerinic M, Gay S, Distler O, Jüngel A. Trichostatin A prevents the accumulation of extracellular ECM in a mouse model of bleomycin-induced skin fibrosis. *Arthritis Rheum*. 2007

107.   Hutt DM, Olsen CA, Vickers CJ, Herman D, Chalfant M, Montero A, Leman LJ, Burkle R, Maryanoff BE, Balch WE, Ghadiri MR. Potential Agents for Treating Cystic Fibrosis: Cyclic Tetrapeptides that Restore Trafficking and Activity of ΔF508-CFTR. *ACS Med Chem Lett*. 2011

108.   Hurwitz JL, Stasik I, Kerr EM, Holohan C, Redmond KM, McLaughlin KM, Busacca S, Barbone D, Broaddus VC, Gray SG, O'Byrne KJ, Johnston PG, Fennell DA, Longley DB. Vorinostat/SAHA-induced apoptosis in malignant mesothelioma is FLIP/caspase 8-dependent and HR23B-independent. *Eur J Cancer*. 2012

109.   Ignotz RA, Massague J. TGFβ1 stimulates the expression of fibronectin and collagen and their incorporation into the extracellular ECM. *J Biol Chem*. 1986

110.   Ingber DE. Cellular tensegrity: defining new rules of biological design that govern the cytoskeleton. *J Cell Sci*. 1993

111.   Ito K, Caramori G, Lim S, Oates T, Chung KF, Barnes PJ, Adcock IM. Expression and activity of HDACs in human asthmatic airways. *Am J Respir Crit Care Med*. 2002

112.   Jozsef Dudas, Tümen Mansuroglu, Danko Batusic, Bernhard Saile and Giuliano Ramadori. Thy-1 is an in vivo and in vitro marker of liver myofibroblasts. *Cell and Tissue Research*. 2007

113.   Kaartinen V, Voncken J, Shuler C, Warburton D, Bu D, Heisterkamp N, Groffen J. Abnormal lung development and cleft palate in mice lacking TGFβ3 indicates defects of epithelial-mesenchymal interaction. *Nat Genet* 11 (4): 415–21. 1995

114.   Kee HJ, Kook H. Krüppel-like factor 4 mediates HDAC inhibitor-induced prevention of cardiac hypertrophy. *J Mol Cell Cardiol*. 2009

115.   Keeley EC, Mehrad B, Strieter RM. Fibrocytes: bringing new insights into mechanisms of inflammation and fibrosis*. Int J Biochem*, 2010

116.   Kent WJ, Sugnet CW, Furey TS, Roskin KM, Pringle TH, Zahler AM, et al. The Human Genome Browser at UCSC. *Genome Res*. 2002

117.   Khalil N. TGFβ1: from latent to active. *Microbes Infect*. 1999

118. Khalil N, Parekh TV, O'Connor R, Antman N, Kepron W, Yehaulaeshet T, Xu YD, Gold LI. Regulation of the effects of TGF-β 1 by activation of latent TGF-β 1 and differential expression of TGF-β receptors (T β R-I and T β R-II) in idiopathic pulmonary fibrosis. *Thorax.* 2001

119. Khan N, Jeffers M, Kumar S, Hackett C, Boldog F, Khramtsov N, Qian X, Mills E, Berghs SC, Carey N, Finn PW, Collins LS, Tumber A, Ritchie JW, Jensen PB, Lichenstein HS, Sehested M. Determination of the class and isoform selectivity of small-molecule HDAC inhibitors. *Biochem J.* 2008

120. Kischer CW, Hendrix MJ. Fibronectin in hypertrophic scars and keloids. *Cell Tissue Res.* 1983

121. Kis K, Liu X, Hagood JS. Myofibroblast differentiation and survival in fibrotic disease. *Expert Rev Mol Med.* 2011

122. Kleinman HK, McGarvey ML, Liotta LA, Robey PG, Tryggvason K, Martin GR. Isolation and characterization of type IV procollagen, laminin, and heparan sulfate proteoglycan from the EHS sarcoma. *Biochemistry* 1982

123. Knutson SK, Chyla BJ, Amann JM, Bhaskara S, Huppert SS, Hiebert SW. Liver-specific deletion of HDAC 3 disrupts metabolic transcriptional networks. *EMBO J.* 2008.

124. Komura E, Tonetti C, Penard-Lacronique V, Chagraoui H, Lacout C, Lecouédic JP, Rameau P, Debili N, Vainchenker W, Giraudier S. Role for the NF-kappaB pathway in TGFβ1 production in idiopathic myelofibrosis. *Cancer Res.* 2005.

125. Kohama K, Nonaka K, Hosokawa R, Shum L, Ohishi M. TGFβ3 promotes scarless repair of cleft lip in mouse fetuses. *J Dent Res.* 2002

126. Komatsu Y., Waku T, Iwasaki N, Ono W, Yamaguchi C., Yanagisawa J. Global analysis of DNA methylation in early-stage liver fibrosis. *BMC Medical Genomics* 2012

127. Krennhrubec K, Marshall BL, Hedglin M, Verdin E, Ulrich SM. Design and evaluation of 'Linkerless' hydroxamic acids as selective HDAC8 inhibitors. *Bioorg Med Chem Lett.* 2007

128. Kuroda J, Ago T, Matsushima S, Zhai P, Schneider MD, Sadoshima J. NOX4 is a major source of oxidative stress in the failing heart. *Proc Natl Acad Sci USA.* 2010

129. Kottler Ulrike B. Comparative effects of TGFβ1, -2 on extracellular ECM production, proliferation, migration and collagen contraction of human Tenon's capsule fibroblasts in pseudoexfoliation and primary open-angle glaucoma. *Exp Eye Res.* 2004

130. Kubo M, Van de Water L, Plantefaber LC, Mosesson MW, Simon M, Tonnesen MG, Taichman L, Clark RA. Fibrinogen and fibrin are anti-adhesive for keratinocytes: a mechanism for fibrin eschar slough during wound repair. *J Invest Dermatol.* 2001

131. Langsetmo I, Jacob C, Ho W, Stephenson R, Sirenko O, Sidhu P, Flippin L, Seeley T, Klaus S, Lin A, Liu D. Inhibition of HIF-Prolyl Hydroxylases with FG-4539 is Neuroprotective in a Mouse Model of Permanent Focal Ischemia. *International Stroke Conference*, Kissimmee, Florida Presentation #427. 2006

132. Laleu B, Gaggini F, Orchard M, Fioraso-Cartier L, Cagnon L, Houngninou-Molango S, Gradia A, Duboux G, Merlot C, Heitz F, Szyndralewiez C, Page P. First in class, potent, and orally bioavailable NOX4 inhibitors for the treatment of idiopathic pulmonary fibrosis. *J Med Chem.* 2010.

133.   Lareu RR, Subramhanya KH, Peng Y, Benny P, Chen C, Wang Z, Rajagopalan R, Raghunath M. Collagen ECM deposition is dramatically enhanced in vitro when crowded with charged macromolecules: the biological relevance of the excluded volume effect. *FEBS Lett*. 2007

134.   Lareu RR, Harve KS, Raghunath M. Emulating a crowded intracellular environment in vitro dramatically improves RT-PCR performance. *Biochem Biophys Res Commun*. 2007

135.   Lafleur MA, Handsley MM, Edwards DR. Metalloproteinases and their inhibitors in angiogenesis. *Expert Rev Mol Med*. 2003

136.   Larjava H, Salo T, Haapasalmi K, Kramer RH, Heino J. Expression of integrins and basement membrane components by wound keratinocytes. *J Clin Invest*. 1993

137.   Lafarga V, Aymerich I, Tapia O, Mayor F Jr, Penela P. A novel GRK2/HDAC6 interaction modulates cell spreading and motility. *EMBO J*. 2011

138.   Lindstedt E and Sandblom P. Wound healing in man: tensile strength of healing wounds in some patient groups. *Ann Surg.* 1975.

139.   Liu X, Bai C, Gong D, Yuan Y, Han L, Lu F, Han Q, Tang H, Huang S, Xu Z. Pleiotropic effects of TGFβ1 on pericardial interstitial cells. *J Am Coll Cardiol*. 2011

140.   Li LC, Dahiya R. MethPrimer: designing primers for methylation PCRs. *Bioinformatics*. 2002

141.   Li H, Fu X, Ouyang Y, Cai C, Wang J, Sun T. Adult bone-marrow-derived mesenchymal stem cells contribute to wound healing of skin appendages. *Cell Tissue Res*. 2006

142.   Lukas J. A. C. Hawinkels, Peter ten Dijke. Exploring anti-TGFβ1 therapies in cancer and fibrosis. *Growth Factors.* 2011

143.   Lyons RM, Keski-Oja J, Moses HL. Proteolytic activation of latent TGFβ1 from fibroblast-conditioned medium. *J Cell Biol*. 1988

144.   Liu Y, Min D, Bolton T, Nubé V, Twigg SM, Yue DK, McLennan SV. Increased ECM MMP9 predicts poor wound healing in diabetic foot ulcers. *Diabetes Care*. 2009

145.   Ludwig TE, Bergendahl V, Levenstein ME, Yu J, Probasco MD, Thomson JA. Feeder-independent culture of human embryonic stem cells. *Nat Methods*. 2006

146.   Li W, He H, Chen YT, Hayashida Y, Tseng SC. Reversal of myofibroblasts by amniotic membrane stromal extract. *J Cell Physiol*. 2008

147.   Liu F, Levin MD, Petrenko NB, Lu MM, Wang T, Yuan LJ, Stout AL, Epstein JA, Patel VV. Histone-deacetylase inhibition reverses atrial arrhythmia inducibility and fibrosis in cardiac hypertrophy independent of angiotensin. *J Mol Cell Cardiol*. 2008.

148.   Mason. Pharmacological therapy for IPF. *NHLBI Workshop*. 1998

149.   Mahdavian-Delavary B, van der Veer WM, van Egmond M, Niessen FB, Beelen RH., Macrophages in skin injury and repair. *Immunobiology*, 2011

150.   Martin Joseph B. and William J. Millard. Brain regulation of GH secretion. *Am Soc of Animal Science*. 1986

151.   Martinez-Ferrer M, Afshar-Sherif AR, Uwamariya C, de Crombrugghe B, Davidson JM, Bhowmick NA. Dermal TGF-β responsiveness mediates wound contraction and epithelial closure. *Am J Pathol* 2010

152.   Mangasser-Stephan K, Gartung C, Lahme B, Gressner AM. Expression of isoforms and splice variants of the LTBPs in cultured human liver myofibroblasts. *Liver*. 2000

153.   Marks PA, Xu WS. HDAC Inhibitors: Potential in Cancer Therapy. *J. Cell. Biochem*. 2009

154.   Matsuyama A, Shimazu T, Sumida Y, Saito A, Yoshimatsu Y, Seigneurin-Berny D, Osada H, Komatsu Y, Nishino N, Khochbin S, Horinouchi S, Yoshida M. In vivo destabilization of dynamic microtubules by HDAC6-mediated deacetylation. *EMBO J*. 2002

155.   Marks PA, Breslow R. Dimethyl sulfoxide to vorinostat: development of this HDAC inhibitor as an anticancer drug. *Nat Biotechnol*. 2007

156.   McDonald JA, Kelley DG, Broekelmann TJ. Role of fibronectin in collagen deposition: Fab' to the gelatin-binding domain of fibronectin inhibits both fibronectin and collagen organization in fibroblast extracellular ECM. *J Cell Biol*. 1982

157.   Meltzer EB, Noble PW. Idiopathic pulmonary fibrosis. *Orphanet J Rare Dis*. 2008

158.   Mintz B, Illmensee K. Normal genetically mosaic mice produced from malignant teratocarcinoma cells. *Proc. Natl. Acad. Sci*. 1975

159.   Montgomery RL, Davis CA, Potthoff MJ, Haberland M, Fielitz J, Qi X, Hill JA, Richardson JA, Olson EN. HDACs 1 and 2 redundantly regulate cardiac morphogenesis, growth, and contractility. *Genes Dev*. 2007

160.   Murahidy A, Ito M, Adcock IM, Barnes PJ, Ito K. Reduction of HDAC expression and activity in smoking asthmatics. *Am J Respir Crit Care Med*. 2005

161.   Mutsaers SE, Bishop JE, McGrouther G, Laurent GJ. Mechanisms of tissue repair: from wound healing to fibrosis. *Int J Biochem Cell Biol*. 1997

162.   Mwaura B, Mahendran B, Hynes N, Defreitas D, Avalos G, Adegbola T, Adham M, Connolly CE, Sultan S. The impact of differential expression of extracellular ECM metalloproteinase inducer, MMP-2, TIMP-2 and PDGF-AA on the chronicity of venous leg ulcers. *Eur J Vasc Endovasc Surg*. 2006

163.   Nam JS, Turcotte TJ, Smith PF, Choi S, Yoon JK. Mouse cristin/R-spondin family proteins are novel ligands for the FZD8 and LRP6 receptors and activate β-catenin-dependent gene expression. *J Biol Chem.* 2006.

164.   Naugle JE, Olson ER, Zhang X, Mase SE, Pilati CF, Maron MB, Folkesson HG, Horne WI, Doane KJ, Meszaros JG. Type VI collagen induces cardiac myofibroblast differentiation: implications for postinfarction remodeling. *Am J Physiol Heart Circ Physiol*. 2006

165.   Nalabothula N, Carrier F. Cancer cells' epigenetic composition and predisposition to HDAC inhibitor sensitization. *Epigenomics.* 2011

166.   Nelson CM, Bissell MJ. Of extracellular ECM, scaffolds, and signaling: tissue architecture regulates development, homeostasis, and cancer. *Annu Rev Cell Dev Biol*. 2006

167.   Nguyen DT, Orgill DP. Murphy G.F. The pathophysiologic basis for wound healing and cutaneous regeneration. *Biomaterials For Treating Skin Loss.* 2009

168.   Norris MG, Malys N. What is the true enzyme kinetics in the biological system? An investigation of macromolecular crowding effect upon enzyme kinetics of glucose-6-phosphate dehydrogenase. *Biochem. Biophys. Res. Commun.* 2011

169.   Noh H, Oh EY, Seo JY, Yu MR, Kim YO, Ha H, Lee HB. HDAC2 is a key regulator of diabetes- and TGFβ1-induced renal injury. *Am J Physiol Renal Physiol.* 2009

170.   Nurden AT. Platelets, inflammation and tissue regeneration. *Thromb Haemost*, 2011

171.   Nwogu JI, Geenen D, Bean M, Brenner MC, Huang X, Buttrick PM. Inhibition of collagen synthesis with prolyl 4-hydroxylase inhibitor improves left ventricular function and alters the pattern of left ventricular dilatation after myocardial infarction. *Circulation.* 2001

172.   Ogawa M, LaRue AC, Drake CJ. Hematopoietic origin of fibroblasts/myofibroblasts: Its pathophysiologic implications. *Blood.* 2006

173.   O'Keefe KL, Cohle SD, McNamara JE, Hooker RL. Early catastrophic stentless valve failure secondary to possible immune reaction. *Ann Thorac Surg.* 2011

174.   Okuda S, Languino LR, Ruoslahti E, Border WA. Elevated expression of TGF-β and proteoglycan production in experimental glomerulonephritis. *J Clin Invest.* 1990

175.   O'Toole EA, Marinkovich MP, Peavey CL, Amieva MR, Furthmayr H, Mustoe TA, Woodley DT. Hypoxia increases human keratinocyte motility on connective tissue. *J Clin Invest* 1997.

176.   Pache JC, Carnesecchi S, Deffert C, Donati Y, Herrmann FR, Barazzone-Argiroffo C, Krause KH. NOX-4 is expressed in thickened pulmonary arteries in idiopathic pulmonary fibrosis. Nat Med. 2011

177.   Pang M, Zhuang S. HDAC: a potential therapeutic target for fibrotic disorders. *J Pharmacol Exp Ther.* 2010

178.   Pankov R, Yamada KM. Fibronectin at a glance. *J Cell Science.* 2002

179.   Paik YH, Brenner DA. NADPH oxidase mediated oxidative stress in hepatic fibrogenesis. *Korean J Hepatol.* 2011

180.   Parker KK, Brock AL, Brangwynne C, Mannix RJ, Wang N, Ostuni E, Geisse NA, Adams JC, Whitesides GM, Ingber DE. Directional control of lamellipodia extension by constraining cell shape and orienting cell tractional forces. *FASEB J.* 2002

181.   Page-McCaw A, Ewald AJ, Werb Z. MMPs and the regulation of tissue remodelling. *Nat Rev Mol Cell Biol.* 2007

182.   Pelton RW, Saxena B, Jones M, Moses HL, Gold LI. Immunohistochemical localization of TGFβ1 1, TGFβ2, and TGFβ3 in the mouse embryo. *J Cell Biol.* 1991

183.   Perucca E. Pharmacological and therapeutic properties of valproate. *CNS Drugs.* 2002

184.   Pol S, Vallet-Pichard A, Corouge M, Mallet VO. Hepatitis C: epidemiology, diagnosis, natural history and therapy. *Contrib Nephrol.* 2012

185.   Preissner KT, Seiffert D. Role of vitronectin and its receptors in haemostasis and vascular remodeling. *Thromb. Res.* 1998

186.   Ratner B.D. Reducing capsular thickness and enhancing angiogenesis around implant drug release systems. *J Control Release.* 2002

187.   Raghunath M, Steinmann B, Delozier-Blanchet C, Extermann P, Superti-Furga A. Prenatal diagnosis of collagen disorders by direct biochemical analysis of chorionic villus biopsies. *Pediatr Res.* 1994

188.   Ranganathan P, Agrawal, A., Bhushan, R., Chavalmane, A., Kalathur, R., Takahashi, T. Expression profiling of genes regulated by TGF-β: Differential regulation in normal and tumor cells. *BMC Genomics.* 2007

189.   Rayment EA, Upton Z, Shooter GK. Increased MMP-9 activity observed in chronic wound fluid is related to the clinical severity of the ulcer. *Br J Dermatol.* 2008

190.   Rawlings ND, Barrett AJ. Families of serine peptidases. *Meth. Enzymol.* 1994

191.   Ramos C, Montaño M, García-Alvarez J, Ruiz V, Uhal BD, Selman M, Pardo A. Fibroblasts from idiopathic pulmonary fibrosis and normal lungs differ in growth rate, apoptosis, and tissue inhibitor of metalloproteinases expression. *Am J Respir Cell Mol Biol.* 2001

192.   Revill P, Mealy N, Serradell N, Bolos J, Rosa E. Panobinostat. *Drugs of the Future.* 2007

193.   de Ruijter AJ, van Gennip AH, Caron HN, Kemp S, van Kuilenburg AB. HDACs: characterization of the classical HDAC family. *Biochem J.* 2003

194.   Rishikof DC, Ricupero DA, Liu H, Goldstein RH. Phenylbutyrate decreases type I collagen production in human lung fibroblasts. *J Cell Biochem.* 2004

195.   Rieder F, Brenmoehl J, Leeb S, Schölmerich J, Rogler G. Wound healing and fibrosis in intestinal disease. *Gut.* 2007

196.   Rosenson-Schloss RS, Chang CC, Constantinides A, Moghe PV. Alteration of leukocyte motility on plasma-conditioned prosthetic biomaterial, ePTFE, via a flow-responsive cell adhesion molecule, cd43. *J Biomed Mater Res.* 2002

197.   Roberts AB, Sporn MB. Differential expression of the TGFβ1 isoforms in embryogenesis suggests specific roles in developing and adult tissues. *Mol Reprod Dev.* 1992

198.   Roberts AB, Heine UI, Flanders KC, Sporn MB. TGF-β. Major role in regulation of extracellular ECM. *Ann N Y Acad Sci.* 1990

199.   Rombouts K, Niki T, Greenwel P, Vandermonde A, Wielant A, Hellemans K, De Bleser P, Yoshida M, Schuppan D, Rojkind M, Geerts A. Trichostatin A, a HDAC inhibitor, suppresses collagen synthesis and prevents TGFβ1-induced fibrogenesis in skin fibroblasts. *Exp Cell Res.* 2002

200.   Rønnov-Jessen L, Petersen OW. A function for filamentous alpha-smooth muscle actin: retardation of motility in fibroblasts. *J Cell Biol.* 1996

201.   Ruszczak Z. Effect of collagen ECM on dermal wound healing. *ADDR Rev.* 2003

202.   Ruscetti F, Varesio L, Ochoa A, Ortaldo J. Pleiotropic effects of TGF-β on cells of the immune system. *Ann N Y Acad Sci.* 1993.

203.   Rubenstein RC, Zeitlin PL. Sodium 4-phenylbutyrate downregulates Hsc70: implications for intracellular trafficking of ΔF508-CFTR. *Am J Physiol Cell Physiol.* 2000

204.   Sakurai E, Anand A, Ambati BK, van Rooijen N, Ambati J. Macrophage depletion inhibits experimental choroidal neovascularization, *Invest Ophthalmol Vis Sci.* 2003

205.   Sato M, Suzuki S, Senoo H. Hepatic stellate cells: unique characteristics in cell biology and phenotype. *Cell Struct Funct.* 2003

206.   Sato Y, Murase K, Kato J, Kobune M, Sato T, Kawano Y, et al. Resolution of liver cirrhosis using vitamin A-coupled liposomes to deliver siRNA against a collagen-specific chaperone. *Nat Biotechnol.* 2008

207.   Sanders YY, Tollefsbol TO, Varisco BM, Hagood JS. Epigenetic regulation of thy-1 by HDAC inhibitor in rat lung fibroblasts. *Am J Respir Cell Mol Biol.* 2011

208.   Saharinen, J, Keski-Oja J. Specific sequence motif of 8-Cys repeats of TGF-β binding proteins, LTBPs, creates a hydrophobic interaction surface for binding of small latent TGF-β. *Mol. Biol. Cell.* 2000

209.   Sarcar B, Kahali S, Chinnaiyan P. Vorinostat enhances the cytotoxic effects of the topoisomerase I inhibitor SN38 in glioblastoma cell lines. *J Neurooncol.* 2010

210.   Saouaf SJ, Li B, Zhang G, Shen Y, Furuuchi N, Hancock WW, Greene MI. Deacetylase inhibition increases regulatory T cell function and decreases incidence and severity of collagen-induced arthritis. *Exp Mol Pathol.* 2009

211.   Sage H, Bornstein P. Endothelial cells from umbilical vein and a hemangioendothelioma secrete basement membrane largely to the exclusion of interstitial procollagens. *Arteriosclerosis.* 1982

212.   Schmidt M, Sun G, Stacey MA, Mori L, Mattoli S. Identification of circulating fibrocytes as precursors of bronchial myofibroblasts in asthma. *J Immunol.* 2003

213.   Schultz GS, Davidson JM, Kirsner RS, Bornstein P, Herman IM. Dynamic reciprocity in the wound microenvironment. *Wound Repair Regen.* 2011

214.   Schmudde M, Braun A, Pende D, Sonnemann J, Klier U, Beck JF, Moretta L, Bröker BM. HDAC inhibitors sensitize tumor cells for cytotoxic effects of natural killer cells. *Cancer Lett.* 2008

215.   Serini G, Bochaton-Piallat ML, Ropraz P, Geinoz A, Borsi L, Zardi L, Gabbiani G. The fibronectin domain ED-A is crucial for myofibroblastic phenotype induction by TGFβ1. *J Cell Biol.* 1998

216.   Shah M., Foreman D.M. and Ferguson, M.W.J. Neutralising antibody to TGFβ1,2 or exogenous addition of TGFβ3 to cutaneous rat wounds reduces scarring. *J Cell Sci.* 1994

217.   Shi Y, Massagué J. Mechanisms of TGFβ1 signaling from cell membrane to the nucleus. *Cell* 2003

218.   Sivakumar P, Das A.M., Fibrosis, chronic inflammation and new pathways for drug discovery. *Inflamm Res.* 2008

219.   Silverstein RL, Leung LL, Harpel PC, Nachman RL. Complex formation of platelet thrombospondin with plasminogen. *J Clin Invest.* 1984

220.   Simonsson M, Heldin CH, Ericsson J, Grönroos E. The balance between acetylation and deacetylation controls Smad7 stability. *J Biol Chem.* 2005

221.   Simkovic D. Contribution to the method of cultivation of cells on a transparent collagen gel. *Exp Cell Res.* 1959

222.   Somalinga B., Roy R. Volume exclusion effect as a driving force for reverse proteolysis. *J Biol Chem.* 2002

223.   Sohara N, Znoyko I, Levy MT, Trojanowska M, Reuben A. Reversal of activation of human myofibroblast-like cells by culture on a basement membrane-like substrate. *J Hepatol.* 2002

224.	Sonnemann J, Dreyer L, Hartwig M, Palani CD, Hong le TT, Klier U, Bröker B, Völker U, Beck JF. HDAC inhibitors induce cell death and enhance the apoptosis-inducing activity of TRAIL in Ewing's sarcoma cells. *J Cancer Res Clin Oncol.* 2007

225.	Stadelmann, WK. Digenis, AG. Tobin, GR. Physiology and healing dynamics of chronic cutaneous wounds. *American journal of surgery.* 1998

226.	Strahl BD, Allis CD. The language of covalent histone modifications. *Nature.* 2000

227.	Steffensen B, Häkkinen L, Larjava H. Proteolytic events of wound-healing: coordinated interactions among MMPs, integrins, and extracellular ECM molecules. *Crit Rev Oral Biol Med.* 2001

228.	Surendran K, Schiavi S, Hruska KA. Wnt-dependent β-catenin signaling is activated after unilateral ureteral obstruction, and recombinant secreted frizzled-related protein 4 alters the progression of renal fibrosis. *J Am Soc Nephrol.* 2005.

229.	Sweetwyne MT, Murphy-Ullrich JE. Thrombospondin1 in tissue repair and fibrosis: TGF-β-dependent and independent mechanisms. *ECM Biol.* 2012

230.	Tan J, Saltzman WM. Topographical control of human neutrophil motility on micropatterned materials with various surface chemistry. *Biomaterials.* 2002

231.	Tang L, Eaton JW. Inflammatory responses to biomaterials. *Am J Clin Pathol.* 1995

232.	Tie J, Desai J. Antiangiogenic therapies targeting the vascular endothelia growth factor signaling system. *Crit Rev Oncog.* 2012

233.	Todorovic V, Jurukovski V, Chen Y, Fontana L, Dabovic B, Rifkin DB. Latent TGF-β binding proteins. *Int J Biochem Cell Biol.* 2005

234.	To Y, Elliott WM, Ito M, Hayashi S, Adcock IM, Hogg JC, Barnes PJ, Ito K. Total HDAC activity decreases with increasing clinical stage of COPD. *Am J Respir Crit Care Med.* 2004

235.	Truong H, Danen EH. Integrin switching modulates adhesion dynamics and cell migration. *Cell Adh Migr.* 2009

236.	Tran AD, Marmo TP, Salam AA, Che S, Finkelstein E, Kabarriti R, Xenias HS, Mazitschek R, Hubbert C, Kawaguchi Y, Sheetz MP, Yao TP, Bulinski JC. HDAC6 deacetylation of tubulin modulates dynamics of cellular adhesions. *J Cell Sci* 2007

237.	Tschank G, Raghunath M, Günzler V, Hanauske-Abel HM. Pyridinedicarboxylates, the first mechanism-derived inhibitors for prolyl-4-hydroxylase, selectively suppress cellular hydroxyprolyl biosynthesis. Decrease in interstitial collagen and Clq secretion in cell culture. *J Biochem.* 1987

238.	Turtle E.D, Ho W.B. Inhibition of procollagen C-proteinase: fibrosis and beyond. *Expert Opinion on Therapeutic Patents.* 2004

239.	Wang Z, Chen C, Finger SN, Kwajah S, Jung M, Schwarz H, Swanson N, Lareu FF, Raghunath M. Suberoylanilide hydroxamic acid: a potential epigenetic therapeutic agent for lung fibrosis? *Eur Respir J.* 2009

240.	Wang C, Henkes LM, Doughty LB, He M, Wang D, Meyer-Almes FJ, Cheng YQ. Thailandepsins: bacterial products with potent HDAC inhibitory activities and broad-spectrum antiproliferative activities. *J Nat Prod.* 2011

241. Wang Y, Fan PS, Kahaleh B. Association between enhanced type I collagen expression and epigenetic repression of the FLI1 gene in scleroderma fibroblasts. *Arthritis Rheum*. 2006

242. Wang L, Ly CM, Ko CY, Meyers EE, Lawrence DA, Bernstein AM. uPA binding to PAI-1 induces corneal myofibroblast differentiation on vitronectin. *Invest Ophthalmol Vis Sci*. 2012

243. Wang JC, Chen C, Dumlao T, Naik S, Chang T, Xiao YY, Sominsky I, Burton J. Enhanced HDAC enzyme activity in primary myelofibrosis. *Leuk Lymphoma*. 2008

244. Wanczyk M, Roszczenko K, Marcinkiewicz K, Bojarczuk K, Kowara M, Winiarska M. HDACi-going through the mechanisms. *Front Biosci*. 2011

245. Watanabe T, Tajima H, Hironori H, Nakagawara H, Ohnishi I, Takamura H, Ninomiya I, Kitagawa H, Fushida S, Tani T, Fujimura T, Ota T, Wakayama T, Iseki S, Harada S. Sodium valproate blocks the TGFβ1 autocrine loop and attenuates the TGFβ1-induced collagen synthesis in a human hepatic stellate cell line. *Int J Mol Med*. 2011

246. Waltregny D, Glénisson W, Tran SL, North BJ, Verdin E, Colige A, Castronovo V. HDAC8 associates with smooth muscle HDAC-actin and is essential for smooth muscle cell contractility. *FASEB J.* 2005

247. Watterson KR, Lanning DA, Diegelmann RF, Spiegel S. Regulation of fibroblast functions by lysophospholipid mediators: potential roles in wound healing. *Wound Repair Regen*. 2007

248. Webber J, Meran S, Steadman R, Phillips A. Hyaluronan orchestrates TGFβ1-dependent maintenance of myofibroblast phenotype. *J Biol Chem*. 2009

249. Wells A. EGF receptor. *Int J Biochem Cell Biol*. 1999

250. WHO. The Global Burden of Disease, Geneva, Switzerland. *WHO press*. 2004

251. Witte MB, Barbul A. Role of nitric oxide in wound repair, *Am J Surg*, 2002

252. Wipff PJ, Rifkin DB, Meister JJ, Hinz B. Myofibroblast contraction activates latent TGF-β1 from the extracellular ECM. *J Cell Biol*. 2007

253. Wipff PJ, Hinz B. Integrins and the activation of latent TGFβ1 – an intimate relationship. *Eur J Cell Biol*. 2008

254. Widgerow AD. Current concepts in scar evolution and control. *Aesthetic Plast Surg*. 2011

255. Wu Catherine H., Walton Cherie M., Wu George Y. Propeptide-mediated regulation of Procollagen Synthesis in IMR-90 Human Lung Fibroblast Cell Cultures. *J. Biol Chem*. 1991

256. Varga J, Pasche B. AntiTGF-β therapy in fibrosis: recent progress and implications for systemic sclerosis. *Curr Opin Rheumatol* 2008

257. Veldhuis J.D. Pulsatile Hormone Secretion (Chapter 10): Mechanisms, Significance and Evaluation. Ultradian Rhythms from Molecules to Mind (Book). 2008

258. Xie JL, Qi SH, Pan S, Xu YB, Li TZ, Liu XS, Liu P. Expression of Smad protein by normal skin fibroblasts and hypertrophic scar fibroblasts in response to TGF β1. *Dermatol Surg*. 2008

259. Yang Liju, Cindy X. Qiu, Anna Ludlow, Mark W. J. Ferguson, Georg Brunner. Active TGFβ1 in Wound Repair. *American Journal of Pathology*. 1999

260.   Yamaguchi Y, Mann DM, Ruoslahti E. Negative regulation of TGF-β by the proteoglycan decorin. *Nature*. 1990

261.   Yoshikawa M, Hishikawa K, Marumo T, Fujita T. Inhibition of HDAC activity suppresses EMT induced by TGF-β1 in human renal epithelial cells. *J Am Soc Nephrol*. 2007

262.   Yu J, Wu C.W, Chu E.S.H, Hui A.Y, Cheng A.S.L, Go MYY, Ching AKK, Chui UL, Chan HLY, Sung JJY. Elucidation of the role of COX-II in liver fibrogenesis using transgenic mice. *Biochem Biophys Res Comm*. 2008

263.   Zafiropoulos A, Fthenou E, Chatzinikolaou G, Tzanakakis GN. Glycosaminoglycans and PDGF signaling in mesenchymal cells. *Connect Tissue Res*. 2008

264.   Zeiger AS, Loe FC, Li R, Raghunath M, Van Vliet KJ. Macromolecular crowding directs extracellular ECM organization and mesenchymal stem cell behavior. *PLoS One*. 2012

265.   Zeplin PH, Larena-Avellaneda A, Jordan M, Laske M, Schmidt K. Phosphorylcholine-coated silicone implants: effect on inflammatory response and fibrous capsule formation. *Ann Plast Surg*. 2010

266.   Zhou Y, Hagood JS, Murphy-Ullrich JE. Thy-1 expression regulates the ability of rat lung fibroblasts to activate TGF-β in response to fibrogenic stimuli. *Am J Pathol*. 2004

267.   Zhong, C., Chrzanowska-Wodnicka, M., Brown, J., Shaub, A., Belkin, A. M. and Burridge, K. Rho-mediated contractility exposes a cryptic site in fibronectin and induces fibronectin ECM assembly. *J. Cell Biol*. 1998

268.   Zieba A, Pardali K, Soderberg O, Lindbom L, Nystrom E, Moustakas A, Heldin CH, Landegren U. Intercellular variation in signaling through the TGF-β pathway and its relation to cell density and cell cycle phase. *Mol Cell Proteomics*. 2012

269.   Zimmerman SB. MMC effects on macromolecular interactions: some implications for genome structure and function. *Biochim. Biophys. Acta*. 1993

270.   Zimmerman SB, Harrison B. MMC increases binding of DNA polymerase to DNA: an adaptive effect. *Proc. Natl. Acad. Sci. USA.* 1987

271.   Zi Z, Feng Z, Chapnick DA, Dahl M, Deng D, Klipp E, Moustakas A, Liu X. Quantitative analysis of transient and sustained TGF-β signaling dynamics. *Mol Syst Biol*. 2011

Appendix I

Appendix I.A   Conferences

TERMIS, Asia-Pacific Chapter, Singapore: Poster Presentation (2011)

Biomedical Engineering Society: Oral Presentation (2010)

TERMIS, Europe Chapter, Ireland: Poster Presentation (2009)

East-Asian Pacific Student Workshop: Oral Presentation (2009)

Appendix I.B   Awards

TERMIS, Asia-Pacific Chapter: SYIS Young Investigator Best Poster Presentation Award, 1st Runner-Up (2011)

Biomedical Engineering Society, 5th Meeting: Best Oral Presenter Award, 1st Runner-Up (2010)

East-Asian Pacific Student Workshop, 3rd Meeting: Top 10 Best Oral Presenter Award (2009)